Investigating Hulls From The Loewner Equation

A Dissertation Presented for the

Doctor of Philosophy

Degree

The University of Tennessee, Knoxville

Andrew Charles Starnes

May 2018

© by Andrew Charles Starnes, 2018
All Rights Reserved.

To all of the mathematicians studying the Loewner equation after me and, most importantly, to the reader.

Acknowledgments

First and foremost, I would like to thank my advisor, Joan Lind, for all of her support and encouragement. I appreciate all of the opportunities that you have given me, as well as the countless hours that you have spent discussing mathematics, pedagogy, and professionalism. Your willingness to serve so selflessly inspires me.

I am extremely grateful to Kei Kobayashi for introducing me to the random world of probability, for his work towards this dissertation, and for all of the advice about the academic job hunt. I thank my grandfather, Charles Kee, for his coding expertise which saved me weeks of simulation time. I also would like to thank Pam Armentrout who has always been there when I needed her. For the time change project, Kei, Joan, and I would like to thank Krzysztof Burdzy for pointing out some useful references.

On a personal note, I would like to thank my family for believing in me and my friends, especially Darrin, for providing me with welcomed distractions. Last, but not least, I would like to thank Sara for going on this long journey with me.

Abstract

The Loewner equation gives a correspondence between real functions and sets in the upper half-plane called Loewner hulls. This dissertation has three major parts.

First, Kager, Nienhuis, and Kadanoff conjectured that the hull generated from the Loewner equation driven by two constant functions with constant weights could be generated by a single rapidly and randomly oscillating function. We prove their conjecture and generalize to multiple continuous driving functions. In the process, we generalize to multiple hulls a result of Roth and Schleissinger that says multiple slits can be generated by constant weight functions. The proof gives a simulation method for hulls generated by the multiple Loewner equation.

Second, we study the geometric effect on the Loewner hulls when the driving function is composed with a random time change, such as the inverse of an alpha-stable subordinator. In contrast to SLE, we show that for a large class of random time changes, the time-changed Brownian motion process does not generate a simple curve. Further we develop criteria which can be applied in many situations to determine whether the Loewner hull generated by a time-changed driving function is simple or non-simple.

Third, Lind proved that if the Lipschitz one-half norm of the driving function is less than 4, then the generated curve is simple. After this, Lind and Rohde showed that if a Lipshitz one-half driving function generates a spacefilling curve then the norm is greater than 4.0001. This bound is not optimal. We discuss our work towards finding the optimal lower bound on the Lipschitz one-half norm of driving functions that generate a spacefilling curve.

Table of Contents

List of Tables

List of Figures

List of Symbols

$\mathrm{B}(z,r)$	Ball of radius r centered at z
$\overline{\mathbb{H}}$	Closure of $\mathbb{H}$ in $\mathbb{C}$
∂_t	Derivative with respect to t
$\mathrm{diam}(A)$	Diameter of set A defined $\sup\{\lvert z-w\rvert : z,w\in A\}$
$\mathrm{hcap}(A)$	Half-plane capacity of $A\subseteq\mathbb{C}$
K_t	Hull generated by Loewner equation at time t
$\lvert\lvert\cdot\rvert\rvert_{\frac{1}{2}}$	Lipschitz-1/2 norm
$\mathscr{R}(A)$	Reflection of $A\subseteq\mathbb{C}$ across the imaginary axis $\{-x+iy : x+iy\in A\}$
$\mathrm{Lip}(\frac{1}{2})$	Set of Lipschitz-1/2 continuous functions
g_t	Solution to Loewner equation
$\mathrm{supp}(\mu)$	Support of measure μ
g_A	Unique conformal map from $\mathbb{H}\setminus A$ to $\mathbb{H}$
$g_{s,t}$	Unique conformal map from $\mathbb{H}\setminus g_s(K_t\setminus K_s)$ to $\mathbb{H}$ and $g_t = g_{s,t}\circ g_s$
$\mathbb{H}$	Upper half-plane $\{x+iy : x,y\in\mathbb{R}, y>0\}$

Chapter 1

Introduction

The Loewner equation has been used to connect the areas of conformal map theory, probability, and physics. It is the initial value problem given by

$$\frac{\partial}{\partial t} g_t(z) = \frac{2}{g_t(z) - \lambda(t)}, \quad g_0(z) = z \tag{1.1}$$

for z in the upper half-plane and $\lambda : [0,T] \to \mathbb{R}$. We call λ the driving function. In particular, the Loewner equation gives a one-to-one correspondence between real continuous functions and certain sets in the upper half plane called hulls. Originally discovered by Charles Loewner in 1923 ([29]), its modern day relevance was discovered by Oded Schramm in 2000 ([48]), when he showed that the Loewner equation driven by a Brownian motion could be used to analyze the scaling limits of the Uniform Spanning Tree and the Loop Erased Random Walk. The random family of curves that the Loewner equation generates when it is driven by Brownian motion is called the Schramm-Loewner evolution (SLE) in his honor. Fields medals were awarded to Werner in 2006 and Smirnov in 2010 for their work regarding SLE and its relationship to conformal field theory, critical percolation, and the Ising model. The Loewner equation also has connections to the Gaussian Free Field, Diffusion Limited Aggregation, and Liouville Quantum Gravity (see for example [2], [5], and [36]). The multiple Loewner equation, which is a weighted sum of Loewner equations driven by different driving functions, is of interest due to its generalization of the Schramm-Loewner evolution to the multiple Schramm-Loewner evolution (see for example [3]).

We will study the Loewner equation and multiple Loewner equation in what follows. This dissertation focuses on three separate projects with the following motivating questions:

- Given disjoint hulls, are there constant weights and continuous driving functions that can generate these hulls from the multiple Loewner equation?
- What happens when the driving function of the Loewner equation is time-changed by the inverse of an (α, κ)-tempered stable subordinator?
- What is the optimal lower bound on 1/2-Hölder continuous functions that generate spacefilling curves?

The first project deals with the hulls generated by the multiple Loewner equation. In [44], it was shown that multiple disjoint slits (simple curves starting on $\mathbb{R}$) can be generated by constant weights and continuous driving functions. We generalize from slits to hulls in Theorem 3.2 which gives the analogous result for hulls. This result was motivated by a conjecture in [19] which addresses one aspect of how the single Loewner equation relates to the multiple Loewner equation. We prove in Proposition 3.1 that union of multiple disjoint hulls can be generated from the single Loewner equation by using a sequence of rapidly and randomly oscillating driving functions. Simulation methods for the single Loewner equation are well understood and this result allows us to simulate the hulls of the multiple Loewner equation with the standard Loewner equation simulation methods. Chapter 3 begins with our generalization from [44] and then addresses the conjecture from [19]. This chapter concludes with a discussion of our simulation method.

The second project is joint work with Kei Kobayashi and Joan Lind where we investigate time-changing the driving function of the Loewner equation by an (α, κ)-tempered stable subordinator. One of our main focuses is how the hulls generated by Brownian motion are affected by the time-change. A key property of the Loewner equation is a Brownian motion type self-similarity. Motivated by [8], we show that the limit of the rescaled hulls of time-changed Brownian motion is a vertical line segment (Corollary 4.7). We further show in Theorem 4.1 that the time-changed Brownian motion does not generate a simple curve, which shows that the time-change fundamentally changes the structure of the hull. Other examples of how the time-change affects the hulls are also discussed. For example, we consider how the time-change affects the curve generated by the square root function in Example 4.14. Without the time change, the square root function generates a ray emanating from the origin that leaves at a prescribed angle. However, the time-change square root function generates a curve that leaves the real line tangentially. Further showing the extreme effects of the time-change, if $\alpha > 0.5$ then the generated hull is simple, whereas if $\alpha < 0.5$ then the generated hull is not simple. Chapter 4 begins with a background section covering the probability needed for the rest of the chapter. After this, we look at the limiting behavior of the rescaled hulls. Finally we look at how the time-change affects the simpleness of the curve with a few examples.

The final project is an attempt to find an optimal bound on when 1/2-Hölder continuous functions generate spacefilling curves. Note that 1/2-Hölder continuous functions are also called Lipschitz-1/2 functions. In [27], it was shown that if a 1/2-Hölder continuous function generates a spacefilling curve, then its Hölder-1/2 norm is at least 4.0001. The bound of 4.0001 is not optimal, that is there are no Lipschitz-1/2 functions with norm 4.0001 that generate a spacefilling curve. In this project, we construct a family of driving functions with controllable Lipschitz-1/2 norm by reverse engineering the potentially spacefilling curves that we want them to have. The spacefilling curve candidates are constructed similarly to the typical spacefilling curve construction. We attempted to prove that the curves are spacefilling originally using conformal map theory, but these methods failed to lead to a proof. We turned to numerically investigating the hulls generated by this family by constructing new families of driving functions that bound our original driving functions and lend themselves to numerical simulation. Chapter 5 begins by examining simulations of our candidate spacefilling curves. After this we discuss properties of Lipschitz-1/2 functions and then construct our candidate driving function family and the bounding families. Next we provide our numerical evidence given by our bounding families. Once this is done, we discuss the future of our spacefilling project.

In order to orient the reader, we discuss the order of the dissertation. We begin with a chapter on background information on the Loewner equation that includes standard results from Loewner equation theory and then moves to discussion of hulls, Loewner hulls, and multiple Loewner hulls. This chapter ends with the standard method used to simulate the Loewner equation. After this, we present our projects on the multiple Loewner equation, time-changing the driving function, and our spacefilling work. The appendix includes the Mathematica [17] code needed for our simulations in this dissertation.

Chapter 2

Introduction to Loewner Theory

This chapter is dedicated to results and information about the Loewner equation and its corresponding hulls that relate to more than just one of our three projects. In particular, we define the Loewner equation and give a few known results. After this we discuss hulls and Loewner hulls (that is, hulls that can be generated from the Loewner equation by a continuous function). We then look at multiple Loewner hulls (hulls that can be generated by the multiple Loewner equation by continuous driving functions). This chapter concludes with the standard simulation method for the Loewner equation.

2.1 Loewner Equation

Let $\mathbb{H} = \{x + iy \in \mathbb{C} : y > 0\}$ denote the upper halfplane. Let $\lambda : [0, T] \to \mathbb{R}$ be continuous. For $z \in \mathbb{H}$, the (single, chordal) Loewner equation is the initial value problem

$$\frac{\partial}{\partial t} g_t(z) = \frac{2}{g_t(z) - \lambda(t)}, \quad g_0(z) = z. \tag{2.1}$$

A solution to the Loewner equation exists on some time interval, where the only issue stopping existence is when $g_t(z) = \lambda(t)$. We denote K_t as the points of $\mathbb{H}$ when the solution has failed to exist at some time up to time t, that is,

$$K_t = \{z \in \mathbb{H} : g_s(z) = \lambda(s) \text{ for some } s \in [0, t]\}. \tag{2.2}$$

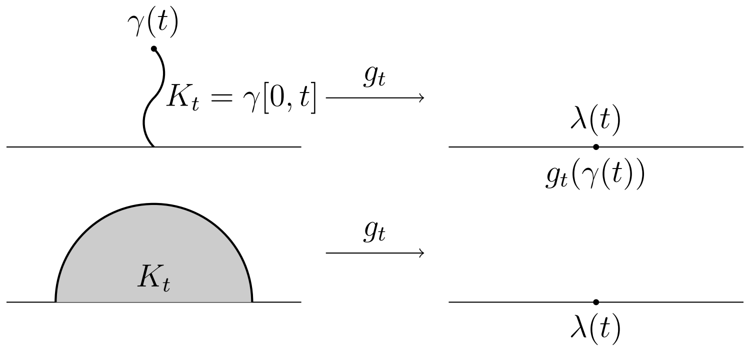

Figure 2.1: Example of $g_t : \mathbb{H} \setminus K_t \to \mathbb{H}$

The function λ is called the driving function and $(g_t)_{t\in[0,T]}$ is called a Loewner chain. For $t \in [0,T]$, we call K_t a Loewner hull and we call the family $(K_t)_{t\in[0,T]}$ a Loewner family (see Section 2.3). We introduce the Loewner hull moniker to distinguish hulls that can be generated by a single, continuous driving function from hulls that cannot. For example, using $\lambda(t) = c$, we can grow a vertical line starting at c (see Figure 2.2). However, two vertical lines at c_1 and c_2 (with $c_1 \neq c_2$) cannot be generated from a single continuous driving function. We discuss this further in Section 2.3. The solution $g_t(z)$ is the conformal map from $\mathbb{H} \setminus K_t$ onto $\mathbb{H}$ (see Figure 2.1) that satisfies

$$g_t(z) = z + \frac{2t}{z} + O\left(\frac{1}{z^2}\right) \tag{2.3}$$

near infinity. We define the half-plane capacity of K_t, $\mathrm{hcap}(K_t)$, to be $2t$ (see Section 2.2). This quantity is useful as it tells us about the size of the hull as viewed from infinity. It has the following probabilistic interpretation:

$$\mathrm{hcap}(K_t) = \frac{1}{2} \lim_{y\to\infty} y\, \mathbb{E}^{iy} \mathrm{Im}(B_\tau),$$

where B_t is a Brownian motion started at iy and stopped at $\tau = \inf\{s : B_s \in \mathbb{R} \cup K_t\}$ (see Proposition 3.41 in [24]). When the limit exists, define

$$\gamma(t) = \lim_{y\downarrow 0} g_t^{-1}(\lambda(t) + iy). \tag{2.4}$$

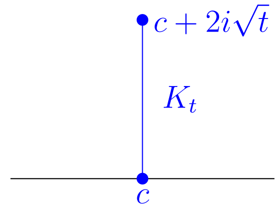

Figure 2.2: Hull driven by $\lambda(t) \equiv c$.

If $\gamma(t)$ exists and is continuous for every $t \in [0, T]$, we call $\gamma(t)$ the trace of K_T. For $t \in [0, T]$, K_t is the closure in $\overline{\mathbb{H}}$ of the complement of the unbounded component of $\mathbb{H} \setminus \gamma[0, t]$. Intuitively, this means that the boundary of K_t is governed by $\gamma(t)$.

On the flipside, if we were to start with a family of continuously growing hulls K_t ($K_t \subset \overline{\mathbb{H}}$, $K_t = \overline{\mathbb{H}} \cap \overline{K_t}$, $\mathbb{H} \setminus K_t$ simply connected, K_t right-continuous, K_t continuously increasing), after possibly reparameterizing we can find a conformal map $g_t : \mathbb{H} \setminus K_t \to \mathbb{H}$ and a continuous function $\lambda : [0, T] \to \mathbb{R}$ satisfying (2.1) and (2.3). This gives a one-to-one correspondence between families of hulls and real-valued continuous functions. For more details, see Section 4.1 in [24] (particularly Lemma 4.2, Theorem 4.6, and the discussion following Example 4.12).

For a basic example, let $\lambda(t) \equiv c \in \mathbb{R}$. Then $g_t(z) = \sqrt{(z-c)^2 + 4t} + c$ and $K_t = \gamma[0, t]$, where $\gamma(t) = c + 2i\sqrt{t}$ is the vertical slit from c to $c + 2i\sqrt{t}$ (see Figure 2.2). This also shows that $\text{hcap}([c, c + 2i\sqrt{t}]) = t$. On the other hand, for a non-constant $\lambda(t)$ we see a non-vertical hull growth that is not as tall as the hull of the constant driving function.

We mention four important properties of the Loewner equation:

Theorem 2.1. Let $\lambda : [0, T] \to \mathbb{R}$ generate $g_t(z)$ with hull K_t.

- (Scaling) For $r > 0$, $\frac{1}{r}\lambda(r^2 t)$ generates the Loewner chain $\frac{1}{r} g_{r^2 t}(rz)$ and the scaled hull rK_{t/r^2}.

- (Shifting) For $x \in \mathbb{R}$, $\lambda(t) + x$ generates the Loewner chain $g_t(z - x) + x$ and the shifted hull $K_t + x$.

- (Concatenation) Let $s \in (0, T)$ and define $\hat{\lambda}$ on $[s, T]$ to be the restricted function $\lambda|_{[s,T]}$, and let $\hat{K}$ be the final hull generated by $\hat{\lambda}$. Then $K_T = K_s \cup g_s^{-1}(\hat{K})$.

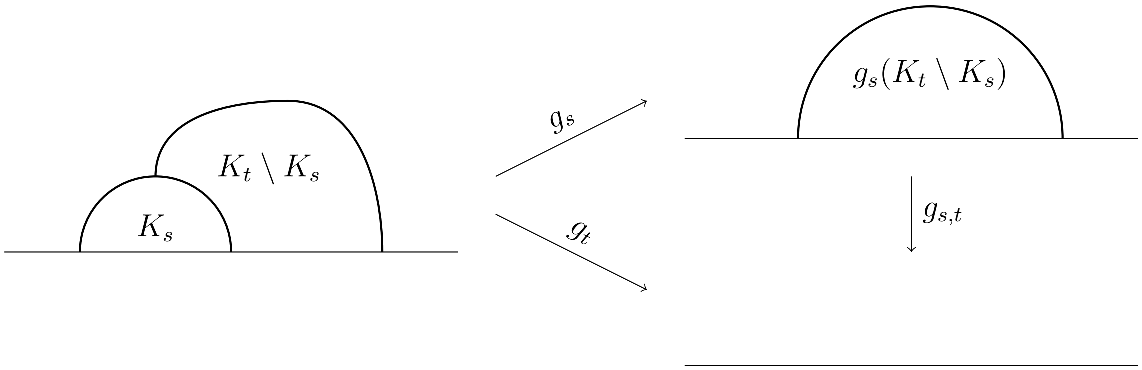

Figure 2.3: Concatenation as a picture

- (Reflection) Also, $-\lambda(t)$ generates the reflected hull $\mathscr{R}(K_t) = \{-x + iy : x + iy \in K_t\}$.

This gives us the following correspondence for $r > 0$ and $x \in \mathbb{R}$:

$$\frac{1}{r}\lambda(r^2 t) + x \quad \longleftrightarrow \quad \frac{1}{r} g_{r^2 t}(r(z-x)) + x \quad \longleftrightarrow \quad \frac{1}{r} K_{r^2 t} + x \tag{2.5}$$

Often concatenation is used to map down part of a hull. For example, if $\lambda : [0,T] \to \mathbb{R}$ drives g_t with hull K_t and $s < t$, then the hull generated by $\lambda|_{[s,t]}$ is $g_s(K_t \setminus K_s)$ as shown in Figure 2.3.

When $\lambda(t) = \sqrt{\kappa} B_t$ where B_t is a Brownian motion starting at 0 and $\kappa > 0$, a random family of curves is generated via the Loewner equation, and we call them the *Schramm–Loewner Evolution* (SLE$_\kappa$). For SLE$_\kappa$, it is well-known that almost surely the trace $\gamma(t)$ exists [42]. Note that the self-similarity of the Brownian motion (i.e. $(rB_t)_{t \geq 0} \stackrel{\mathrm{d}}{=} (B_{r^2 t})_{t \geq 0}$ for each $r > 0$, where $\stackrel{\mathrm{d}}{=}$ means equality in distribution) is the same as the scaling of the Loewner equation, which gives the same self-similarity of the hulls and traces (i.e. $(rK_t)_{t \geq 0} \stackrel{\mathrm{d}}{=} (K_{r^2 t})_{t \geq 0}$ and $(r\gamma(t))_{t \geq 0} \stackrel{\mathrm{d}}{=} (\gamma(r^2 t))_{t \geq 0}$). This self-similarity means that SLE$_\kappa$ is invariant under scaling by a real constant, which allows for different geometric behavior for different values of κ. Rohde and Schramm [42] proved that SLE$_\kappa$ exhibits phase transitions based on κ as follows (see Figure 2.4)

- $\kappa \in [0,4]$: $\gamma(t)$ is a.s. a simple path in $\mathbb{H} \cup \{0\}$
- $\kappa \in (4,8)$: $\gamma(t)$ is a.s. a non-simple path
- $\kappa \in [8,\infty)$: $\gamma(t)$ is a.s. a spacefilling curve

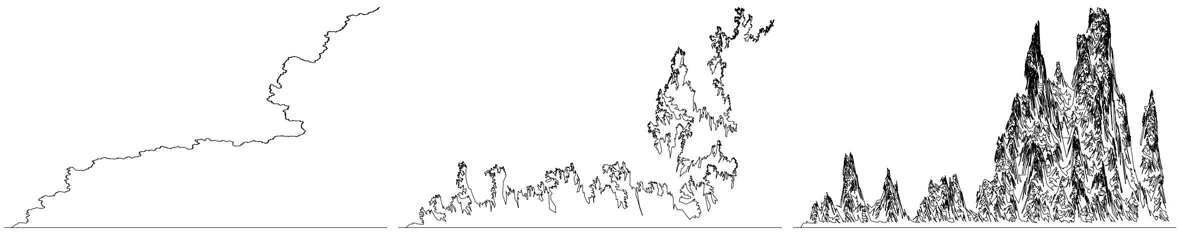

Figure 2.4: Plots of SLE_1, SLE_6, and SLE_{36}

In the deterministic setting, a natural class of functions to consider is the Lipschitz-1/2 continuous functions (i.e. Hölder continuous functions of exponent $\frac{1}{2}$), which is denoted as $\mathrm{Lip}(\frac{1}{2})$. This is the set of functions such that $|\lambda(s) - \lambda(t)| \leq c\sqrt{|t-s|}$, and the norm, denoted $\|\lambda\|_{1/2}$, is the smallest such c. Note that for $r > 0$, $r\|\lambda\|_{1/2} = \|\lambda(r^2 t)\|_{1/2}$, which is the scaling of the Loewner equation. The phase transitions in this setting are different from SLE_κ and slightly more complicated since for any $c > 0$ we can find $\lambda \in \mathrm{Lip}(\frac{1}{2})$ so that $\|\lambda\|_{1/2} = c$ and λ generates a simple curve. Nevertheless, the following two theorems and the example discussed afterwards show that a deterministic phase transition occurs when $\|\lambda\|_{1/2} = 4$.

Theorem 2.2 ([28])**.** If $\lambda \in \mathrm{Lip}(\frac{1}{2})$ with $\|\lambda\|_{1/2} < 4$, then the domains $\mathbb{H} \setminus K_t$ generated by λ are quasi-slit halfplanes. In particular, K_t is a simple curve in $\mathbb{H}$.

Theorem 2.3 ([27])**.** Suppose λ is a $\mathrm{Lip}(\frac{1}{2})$ driving function that generates a curve with non-empty interior. Then $\|\lambda\|_{\frac{1}{2}} \geq 4.0001$.

When considering phase transitions, the key deterministic example is $\lambda(t) = c\sqrt{1-t}$. For $c < 4$, the hulls are simple curves, whereas if $c \geq 4$, then the hulls are not simple. For more details, see [19]. The behavior of this family for $c \geq 4$ was leveraged in [26] to show that the scaled Weierstrass function generates a non-simple hull for a large enough scale. (See Section 4.2 for a further discussion of the Weierstrass example.) We state their technique in the following theorem, which we will use in proving Theorem 4.9.

Theorem 2.4 ([26])**.** Let $\lambda(t)$ be a continuous function. If $|\lambda(T) - \lambda(t)| \geq 4\sqrt{T-t}$ on $[T-\epsilon, T]$ for some $\epsilon > 0$, then the hull generated by λ at time $t = T$ is non-simple.

Let $\lambda_1, ..., \lambda_n : [0,T] \to \mathbb{R}$ be continuous and $w_1, ..., w_n \in L^1[0,T]$ with $\sum_{k=1}^{\infty} w_k(t) \equiv 1$. For $z \in \mathbb{H}$, the multiple Loewner equation is the initial value problem

$$\frac{\partial}{\partial t} g_t(z) = \sum_{k=1}^{n} \frac{2w_k(t)}{g_t(z) - \lambda_k(t)} \text{ a.e. } t \in [0,T], \quad g_0(z) = z. \tag{2.6}$$

This is the sum of weighted Loewner equations, which allows growth of multiple Loewner hulls simultaneously. Note that (2.6) holds a.e. $t \in [0,T]$ whereas (2.1) holds for all $t \in [0,T]$.

Both the single, chordal Loewner equation and the multiple Loewner equation come from a more general, measure defined, Loewner equation. For $z \in \mathbb{H}$, the generalized Loewner equation is the initial value problem

$$\frac{\partial}{\partial t} g_t(z) = \int_{\mathbb{R}} \frac{d\mu_t(u)}{g_t(z) - u}, \quad g_0(z) = z, \tag{2.7}$$

where μ_t is a nonnegative Borel measure on $\mathbb{R}$ $(t \geq 0)$, $\int_{\mathbb{R}} f d\mu_s \to \int_{\mathbb{R}} f d\mu_t$ as $s \to t$ for f bounded and continuous and for each t there exists $M_t < \infty$ such that

- $\sup\{\mu_s(\mathbb{R}) : 0 \leq s \leq t\} < M_t$ and
- $\operatorname{supp}\mu_s \subseteq [-M_t, M_t]$, $s \leq t$.

If μ_t is the Dirac measure (i.e. point mass measure) concentrated on $\lambda(t)$, then we get the single, chordal Loewner equation. When μ_t is a weighted sum of Dirac measures concentrated on $\lambda_i(t)$, then we get the multiple Loewner equation.

There are other versions of the Loewner equation for the disc, the whole complex plane, multiply connected domains, and higher dimensions. However, all of the work included here is on the upper half plane, so we only work the the single and multiple chordal Loewner equation.

2.2 Hulls

Definition 2.5. A bounded set $K \subseteq \mathbb{H}$ is a hull if $\mathbb{H} \setminus K$ is simply connected.

For any hull K, there is a unique conformal map $g_K : \mathbb{H} \setminus K \to \mathbb{H}$ with $\lim_{z\to\infty}(g_K(z) - z) = 0$, by Riemann mapping theorem (see Proposition 3.36 in [24]). The inverse of g_K satisfies the

Nevanlinna representation formula

$$g_K^{-1}(z) = z + \int_{\mathbb{R}} \frac{d\mu_K(t)}{t-z} \tag{2.8}$$

for some finite, nonnegative Borel measure on $\mathbb{R}$ (see Section 3.1 in [47]). We now state a very useful result from [44].

Lemma 2.6 (3.4 [44])**.** Let A be a hull.

(a) If $\overline{A} \cap \mathbb{R}$ is contained in the closed interval $[a,b]$, then $g_A(\alpha) \leq \alpha$ for every $\alpha \in \mathbb{R}$ with $\alpha < a$ and $g_A(\beta) \geq \beta$ for every $b \in \mathbb{R}$ with $\beta > b$.

(b) If the open interval (a,b) is contained in $\mathbb{R} \setminus \overline{A}$, then $|g_A(\beta) - g_A(\alpha)| \leq |\beta - \alpha|$ for all $\alpha, \beta \in (a,b)$.

Definition 2.7. Let K be a hull. The half-plane capacity of K is defined as

$$\mathrm{hcap}(K) = \lim_{z\to\infty} z(g_K(z) - z). \tag{2.9}$$

Half-plane capacity is a real value relating g_K and K. Part of the importance of the half-plane capacity is captured in the following lemma from [44].

Lemma 2.8 (3.1 [44])**.** Let A, A_1, A_2 be hulls.

(a) If $A_1 \cup A_2$ and $A_1 \cap A_2$ are hulls, then

$$\mathrm{hcap}(A_1) + \mathrm{hcap}(A_2) \geq \mathrm{hcap}(A_1 \cup A_2) + \mathrm{hcap}(A_1 \cap A_2) \tag{2.10}$$

(b) If $A_1 \subset A_2$, then $\mathrm{hcap}(A_2) = \mathrm{hcap}(A_1) + \mathrm{hcap}(g_{A_1}(A_2 \setminus A_1)) \geq \mathrm{hcap}(A_1)$.

(c) If $A_1 \cup A_2$ is a hull and $A_1 \cap A_2 = \emptyset$, then $\mathrm{hcap}(g_{A_1}(A_2)) \leq \mathrm{hcap}(A_2)$.

(d) If $c > 0$, then $\mathrm{hcap}(cA) = c^2\mathrm{hcap}(A)$ and $\mathrm{hcap}(A \pm c) = \mathrm{hcap}(A)$.

Remark 3.50 in [24] gives that there exists $M > 0$ so that for any hull K,

$$\mathrm{diam}(g_K(K)) < M\mathrm{diam}(K). \tag{2.11}$$

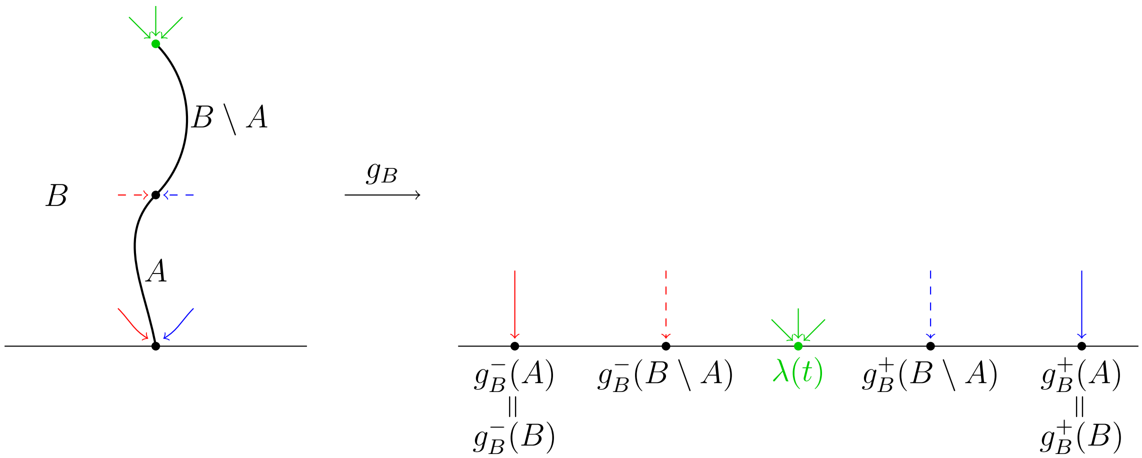

Figure 2.5: Graph of $g_B^-(A)$ and $g_B^+(A)$

In order to further discuss diam$g_K(K)$, we introduce some notation.

Definition 2.9. Let A and B be hulls or a finite union of hulls. Let $g_B : \mathbb{H} \setminus B \to \mathbb{H}$ be the hydrodynamically normalized conformal map. Define $g_B^+(A) = 0$ if $A \subseteq \text{int}(B)$ and otherwise

$$g_B^+(A) = \max\left\{\lim_{n\to\infty} g_B(z_n) : (z_n)_{n=1}^\infty \subseteq \mathbb{H} \setminus B, z_n \to z \in A, g_B(z_n) \to x \in \mathbb{R}\right\}. \tag{2.12}$$

Similarly, define $g_B^-(A) = 0$ if $A \subseteq \text{int}(B)$ and otherwise

$$g_B^-(A) = \min\left\{\lim_{n\to\infty} g_B(z_n) : (z_n)_{n=1}^\infty \subseteq \mathbb{H} \setminus B, z_n \to z \in A, g_B(z_n) \to x \in \mathbb{R}\right\}. \tag{2.13}$$

See Figure 2.5 for an example graph of this definition.

This means

$$g_K^+(K) - g_K^-(K) = \text{diam}(g_K(K)) \leq M\text{diam}(K) \tag{2.14}$$

2.3 Loewner Hulls

As previously mentioned, not all hulls can be grown from the Loewner equation driven by a continuous function, for instance a tree or a disconnected set. We will call these special hulls Loewner hulls.

Definition 2.10. We say that a family of hulls, $(K_t)_{t\in[0,T]}$ is a Loewner family if for all $t \in [0,T]$, $\text{hcap}(K_t) = 2t$, $K_s \subset K_t$ for $s < t$, and for all $\epsilon > 0$ there exists $\delta > 0$ so that for $t \in [0, T-\delta]$ there is a bounded, connected set $S \subset \mathbb{H} \setminus K_t$ with $\text{diam}(S) < \epsilon$ where S disconnects $K_{t+\delta} \setminus K_t$ from infinity in $\mathbb{H} \setminus K_t$.

The above definition is motivated by Theorem 2.6 of [25] which states that $(K_t)_{t\in[0,T]}$ is a Loewner family if and only if there exists $\lambda : [0,T] \to \mathbb{R}$ continuous so that $(K_t)_{t\in[0,T]}$ is driven by λ. Furthermore, $\lambda(t)$ is the point in $\bigcap_{\epsilon>0} g_t(K_{t+\epsilon} \setminus K_t)$. We will say that two Loewner families $(K_t)_{t\in[0,T]}$ and $(L_s)_{s\in[0,S]}$ are disjoint if $\overline{K_T} \cap \overline{L_S} = \emptyset$, where the closure is taken in $\overline{\mathbb{H}}$. Similarly, if A and B are hulls, we say they are disjoint if $\overline{A} \cap \overline{B} = \emptyset$. When there is no risk of confusion, we denote Loewner families simply by K_t, dropping the index on t.

Definition 2.11. We say that the hull K with $\text{hcap}(K) = 2T$ is a Loewner hull if there is a Loewner family K_t with $K_T = K$.

The relationship between a Loewner family and its driving function is very deep. We exemplify this relationship by stating a few results that will prove useful.

Lemma 2.12 (3.3 (a) [8])**.** Let K_t be a Loewner family driven by λ. If $\lambda(t) \in [a,b]$ for all $t \in [0,T]$, then $\overline{K_T} \subset [a,b] \times \mathbb{R}$.

Lemma 2.13 (4.13 [24])**.** Let K_t be a Loewner family generated by λ with Loewner chain g_t. Define $R_t = \max\{\sqrt{t}, \sup\{|\lambda(s)| : 0 \le s \le t\}\}$. Then $\sup\{|z| : z \in K_t\} \le 4R_t$. In fact, if $|z| > 4R_t$, then $|g_s(z) - z| \le R_t$ for $0 \le s \le t$.

Beyond the driving function, Loewner families can only grow in particular ways.

Definition 2.14 ([24])**.** Let K_t be a Loewner family. We call z a t-accessible point if $z \in K_t \setminus \cup_{s<t} K_s$ and there exists a continuous curve $\gamma : [0,1] \to \mathbb{C}$ with $\gamma(0) = z$ and $\gamma(0,1] \subseteq \mathbb{H} \setminus K_t$.

Proposition 2.15 (4.26 [24])**.** If $t > 0$ and z is a t-accessible point, then there is a strictly increasing sequence $s_j \uparrow t$ and a sequence of s_j-accessible points z_j with $z_j \to z$.

Proposition 2.16 (4.27 [24])**.** For each $t > 0$, there is at most one t-accessible point. Also, the boundary of the time t hull is contained in the closure of the set of s-accessible points for $s \le t$.

The restriction on the number of t-accessible points also shows that the boundary of a hull always intersects the boundary of previous hulls.

Lemma 2.17. Let K_t be a Loewner family generated by λ. Fix $0 < t \le T$. Then there exists $0 < s < t$ so that $\partial_{\mathbb{H}} K_t \cap K_s \neq \emptyset$. Moreover, $\partial_{\mathbb{H}} K_t \cap \partial K_r \neq \emptyset$ for $s \le r \le t$.

Note that here we use $\partial_{\mathbb{H}}$ to indicate the boundary with respect to $\mathbb{H}$. Explicitly, for $A \subseteq \mathbb{H}$,

$$\partial_{\mathbb{H}} A = \{z \in \mathbb{C} : \text{ exists } (z_n)_{n=1}^{\infty} \subseteq \mathbb{H} \setminus A \text{ with } z_n \to z\} \tag{2.15}$$

Proof. Suppose not - that is, for some fixed $t \in (0, T]$, $\partial_{\mathbb{H}} K_t \cap K_s = \emptyset$ for all $0 < s < t$. Since $0 < t$, we have that $\partial_{\mathbb{H}} K_t$ is larger than a singleton set. Let $z_1, z_2 \in \partial_{\mathbb{H}} K_t$ with $|z_1 - z_2| = \delta > 0$. Then there are $w_1, w_2 \in \mathbb{H} \setminus K_t$ with $|z_i - w_i| < \frac{\delta}{3}$ for $i = 1, 2$. Let $\gamma_i : [0, 1] \to \mathbb{H}$ be the straight line segment starting at w_i and ending at z_i for $i = 1, 2$. Let $t_i \in (0, 1]$ be the first time that γ_i intersects K_t and $z_i' = \gamma_i(t_i)$. Two important facts follow. First, since $z_i' \in \partial_{\mathbb{H}} K_t \subseteq K_t \setminus \bigcup_{s<t} K_s$ for $i = 1, 2$, z_1' and z_2' are t-accessible. Second, by construction $|z_1' - z_2'| > \frac{\delta}{3}$, so $z_1' \neq z_2'$. This shows that there is more than one t-accessible point, a contradiction to Proposition 2.16. So, for all $t \in (0, T]$ there is $0 < s < t$ with $\partial_{\mathbb{H}} K_t \cap K_s \neq \emptyset$.

The moreover statement follows immediately using the fact that $s \le r \le t$ gives $K_s \subseteq K_r \subseteq K_t$. □

Often we will be considering the family $(g_L(K_t))_{t \in [0,T]}$ where L is a hull disjoint from K_T. The next lemma investigates what happens when a Loewner family is conformally transformed.

Lemma 2.18 (2.8 [25])**.** Let $(K_t)_{t \in [0,T]}$ be a Loewner family driven by λ. Let D be a relatively open subset of $\overline{\mathbb{H}}$ which contains $\overline{K_T}$, and set $D_{\mathbb{R}} := D \cap \mathbb{R}$. Let $G : D \to \overline{\mathbb{H}}$ be conformal in $D \setminus D_{\mathbb{R}}$ and continuous in D, and suppose that $G(D_{\mathbb{R}}) \subset \mathbb{R}$. Then $(G(K_t))_{t \in [0,T]}$ is a Loewner family. Moreover, $\partial_t[\text{hcap}(G(K_t))] = G'(\lambda(0))^2 \partial_t \text{hcap}(K_t)$ at $t = 0$.

The next two results will be used in our discussion of driving functions that generate spacefilling curves. These results deal with two driving functions U and V where $U(t) \leq V(t)$. The first results says, under some necessary assumptions, that if $x > V(0)$, then the image of x under the Loewner chain driven by V is always bigger than the image of x under the Loewner chain driven by U. The second result says, under some necessary assumptions, that if x is not in V's hull, then it is not in U's hull either.

Proposition 2.19. Let $U, V : [0,T] \to \mathbb{R}$ with $U(t) \leq V(t)$ for $t \in [0,t]$. Let g_t^U and g_t^V be the Loewner chains generated by U and V with hulls K_t^U and K_t^V, respectively. Let $x > V(0)$ and

$$\sigma = \inf\{t \in [0,T] : x \in K_t^U \cup K_t^V\}. \tag{2.16}$$

Suppose for all $t < \sigma$, we have that $g_t^V(x) > V(t)$. Then for all $t < \sigma$, $g_t^U(x) \leq g_t^V(x)$.

Note that we assume that $g_t^V(x) > V(t)$, so that even if V is discontinuous the result holds.

Proof. Let $U, V, g_t^U, g_t^V, K_t^U, K_t^V, x$, and σ be as in the statement. Since $x > V(0) \geq U(0)$, $\sigma > 0$. Let $t_0 \in [0, \sigma)$ so that $g_{t_0}^U(x) = g_{t_0}^V(x)$. Then

$$\left.\frac{\partial}{\partial t} g_t^U(x)\right|_{t=t_0} = \frac{2}{g_{t_0}^U(x) - U(t_0)} \tag{2.17}$$

$$= \frac{2}{g_{t_0}^V(x) - U(t_0)} \tag{2.18}$$

$$\leq \frac{2}{g_{t_0}^V(x) - V(t_0)} \tag{2.19}$$

$$= \left.\frac{\partial}{\partial t} g_t^V(x)\right|_{t=t_0}. \tag{2.20}$$

This means if $g_t^U(x) = g_t^V(x)$, then $g_t^V(x)$ is increasing faster than $g_t^U(x)$. Hence $g_t^U(x) \leq g_t^V(x)$ for $t \in [0, \sigma]$. $\square$

Corollary 2.20. Let $U, V : [0,T] \to \mathbb{R}$ with $U(t) \leq V(t)$ for $t \in [0,t]$. Let g_t^U and g_t^V be the Loewner chains generated by U and V with hulls K_t^U and K_t^V, respectively. Let $x > V(0)$, $x \notin K_t^V$, and $g_t^V(x) > V(t)$ for $t \in [0,T]$. Let

$$\sigma = \inf\{t \in [0,T] : g_t^u(x) = V(t)\}. \tag{2.21}$$

Then for $t < \sigma$, $g_t^U(x) \le g_t^V(x)$ and $x \notin K_t^U$.

Proof. By the previous proposition, if $x \notin K_t^U \cup K_t^V$ for $t < \sigma$, then $g_t^U(x) \le g_t^V(x)$. Since $x \notin K_t^V$ for $t \in [0, T]$, it suffices to show that $x \notin K_t^U$ for $t < \sigma$. Note that since

$$g_0^U(x) = x > V(0) \ge U(0), \tag{2.22}$$

we have $\sigma > 0$ and $g_t^U(x) > V(t)$ for $t < \sigma$. So,

$$0 < g_t^U(x) - V(t) \le g_t^U(x) - U(t). \tag{2.23}$$

This means $x \notin K_t^U$ for $t < \sigma$ and we have the result. $\square$

2.4 Multiple Loewner Hulls

2.4.1 Prime Ends

In order to generalize the results of [44], we need to generalize the tip of a curve into the setting of hulls. This is done with prime ends, which are equivalence classes of crosscuts. We give only a brief introduction, for more details see [41].

Definition 2.21 ([41])**.** Let $\Omega \subseteq \mathbb{H}$ be a simply connected domain containing ∞. Let C be a crosscut of Ω (that is, a Jordan arc in Ω with endpoints in $\partial\Omega$) and Ω_C the component of $\Omega \setminus C$ not containing ∞. A prime end of Ω is represented by a sequence of pairwise disjoint crosscuts $(C_n)_{n=1}^\infty$ with $\operatorname{diam}(C_n) \to 0$ as $n \to \infty$ and $C_{n+1} \subseteq \overline{\Omega_{C_n}}$. Two sequences, $(C_n)_{n=1}^\infty$ and $(\widetilde{C}_n)_{n=1}^\infty$, represent the same prime end if for each n there is a $J_n \in \mathbb{N}$ so that $\widetilde{C}_j \subseteq \Omega_{C_n}$ for $j \ge J_n$ and vice versa.

Definition 2.22. Let p be a prime end represented by the sequence of crosscuts $(C_n)_{n=1}^\infty$. The impression of p is defined as $I(p) = \bigcap_{n=1}^\infty \overline{\Omega_{C_n}}$. Since $(\overline{\Omega_{C_n}})_{n=1}^\infty$ is a decreasing sequence of nonempty, compact, and connected sets, the impression of p is nonempty. Moreover, the impression of p is independent of its representation.

Lemma 2.23. Let K_t be a Loewner family generated by λ. Fix $0 < t \leq T$. If there exists $0 < s < t$ such that $\lambda(s) < \lambda(r)$ or $\lambda(s) > \lambda(r)$ for $r \in (s,t)$, then $\overline{K_s} \cap \partial_{\mathbb{H}} K_t \neq \emptyset$.

Proof. Suppose $\lambda(s) < \lambda(r)$ (resp. $\lambda(s) > \lambda(r)$) for $s < r < t$. Then Lemma 2.12 shows that $\lambda(s) \leq \min\{\overline{g_{K_s}(K_t \setminus K_s)} \cap \mathbb{R}\}$ ($\geq$ max resp.). As $\lambda(s) \in \overline{g_{K_s}(K_t \setminus K_s)}$, $\lambda(s) \in \partial \overline{g_{K_s}(K_t \setminus K_s)}$. Now, there exists $(w_n)_{n=1}^{\infty} \subset \mathbb{H} \setminus \overline{g_{K_s}(K_t \setminus K_s)}$ with $w_n \to \lambda(s)$. So, there exists a corresponding sequence $(z_n)_{n=1}^{\infty} \subset \mathbb{H} \setminus K_t$ so that $g_{K_s}(z_n) = w_n$. Furthermore, there is a subsequence of $(z_n)_{n=1}^{\infty}$ that converges to a point in $\overline{K_s}$ as there is at least one point in the impression of the prime end corresponding to $\lambda(s)$. This shows that $\overline{K_s} \cap \partial_{\mathbb{H}} K_t \neq \emptyset$. $\square$

Definition 2.24. Let $\Omega \subseteq \mathbb{H}$ be a simply connected domain containing ∞. Let $P(\Omega)$ denote the set of prime ends of Ω and $\widehat{\Omega} := \Omega \cup P(\Omega)$ denote the Carathéodory compactification of Ω. We can define a topology on $\widehat{\Omega}$ by making the following equivalent:

- $(z_j)_{j=1}^{\infty} \subseteq \Omega$ converges to $p \in P(\Omega)$
- for any $(C_n)_{n=1}^{\infty} \in p \in P(\Omega)$ there exists $J \in \mathbb{N}$ so that $(z_j)_{j=J}^{\infty} \subseteq \Omega_{C_n}$

Under this topology, if $g : \Omega \to \mathbb{H}$ is conformal, then g extends to a homeomorphism $\widehat{g} : \widehat{\Omega} \to \overline{\mathbb{H}}$. We can identify prime ends of Ω with boundary points of Ω as follows:

$$(z_j)_{j=1}^{\infty} \subseteq \Omega \text{ with } z_j \to z \in \partial\Omega \text{ if and only if } (z_j)_{j=1}^{\infty} \subseteq \Omega \text{ with } z_j \to p \in P(\Omega) \tag{2.24}$$

If $z \in \partial\Omega$ and $p \in P(\Omega)$ are identified, we do not distinguish the point z and the prime end p.

Since the identity map on $\mathbb{H}$ is conformal, $\overline{H}$ and $\widehat{H}$ are homeomorphic and we can think of boundary points (i.e. real points) as prime ends and the other way around.

Definition 2.25. Let K_t be a Loewner family driven by λ with Loewner chain g_t. Let p be a prime end of $\mathbb{H} \setminus K_t$. We say that "p corresponds to $\lambda(t)$" or "p is the (generalized) tip of K_t" if $\widehat{g}_t(p) = \lambda(t)$.

This gives us a family of prime ends $(p_t)_{t\in[0,T]}$ each corresponding to $\lambda(t)$ which generates K_t. More specifically, $\widehat{g}_t(p_t) = \lambda(t)$ where g_t is the Loewner chain corresponding to K_t and λ is its driving function.

In the situation of a curve γ with Loewner chain g_t, since $g_t(\gamma(t)) = \lambda(t)$, the tip at time t, $\gamma(t)$, is the prime end corresponding to $\lambda(t)$. This is the reason that we use prime ends to generalize tips.

We now will revisit the definitions of $g_B^+(A)$ and $g_B^-(A)$ and relate them to prime ends. If $A \not\subseteq \mathrm{int}(B)$,

$$g_B^+(A) = \sup\{g_B(p) \in \mathbb{R} : p \in P(\mathbb{H} \setminus A), I(p) \cap \overline{A} \neq \emptyset\} \tag{2.25}$$

and

$$g_B^-(A) = \inf\{g_B(p) \in \mathbb{R} : p \in P(\mathbb{H} \setminus A), I(p) \cap \overline{A} \neq \emptyset\}. \tag{2.26}$$

This follows from g_B extending to $\widehat{\mathbb{H} \setminus B}$. Note that from now on, we will assume g_B is its extension $\widehat{g}_B$.

2.4.2 Estimates for Multiple Loewner Hulls

We now switch to the setting of our main result: multiple, disjoint Loewner families. Let K and L be disjoint hulls. There are many ways that $K \cup L$ can be mapped down to the real line. Two basic ways are mapping down one hull and then mapping down the image other hull, see Figure 2.6. By uniqueness we have

$$g_{g_K(L)} \circ g_K = g_{K\cup L} = g_{g_L(K)} \circ g_L. \tag{2.27}$$

This gives a significant amount of flexibility in our maps.

We now state a few preliminary results on what happens when another hull is added.

Lemma 2.26. Let K_t be a Loewner family and L a hull disjoint from K_T. If $K_s \cap \partial_{\mathbb{H}} K_t \neq \emptyset$, then for $s \leq r \leq t$,

$$g^-_{K_t\cup L}(K_t \setminus K_s) \leq g^-_{K_t\cup L}(K_t \setminus K_r) \leq g^+_{K_t\cup L}(K_t \setminus K_r) \leq g^+_{K_t\cup L}(K_t \setminus K_s) \tag{2.28}$$

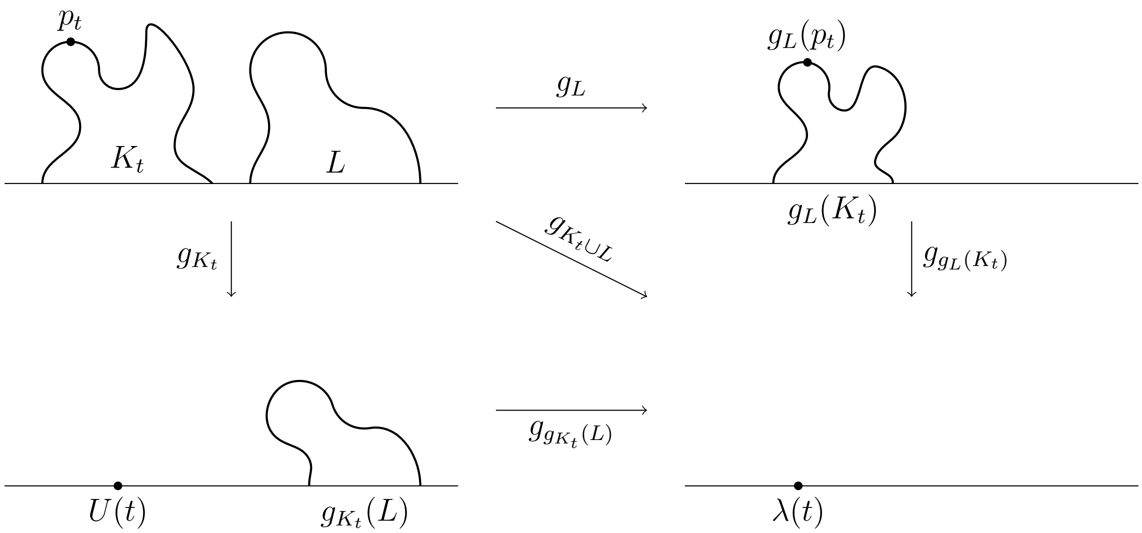

Figure 2.6: Mapping Down Hulls in Different Orders

Proof. The middle inequality follows from the definitions of $g^-_{K_t \cup L}$ and $g^+_{K_t \cup L}$.

For the first inequality, let $(z_n)_{n=1}^{\infty} \subseteq \mathbb{H} \setminus (K_t \cup L)$ with $z_n \to z \in K_t \setminus K_r$ and $g_{K_t \cup L} \to x \in \mathbb{R}$. Then as $K_s \subseteq K_r$, $z \in K_t \setminus K_s$. So, $g_{K_t \cup L}(K_t \setminus K_s) \le x$. This holds for any such sequence, so the first inequality is proven.

The third inequality follows in the same manner. $\square$

Let K_t be a Loewner family driven by $U : [0, T] \to \mathbb{R}$ and L be a hull disjoint from K_T. What happens to U if we map down L and then map down $g_L(K_t)$? What happens to U if we do the opposite and map down K_t then L? The answer is actually given using (2.27) and $g_{K_t}(p_t) = U(t)$ for the corresponding family of prime ends p_t. Observe:

$$g_{g_{K_t}(L)}(U(t)) = g_{g_{K_t}(L)}(g_{K_t}(p_t)) = g_{g_L(K_t)}(g_L(p_t)). \tag{2.29}$$

If we define $\lambda(t) = g_{g_{K_t}(L)}(U(t))$, then, as $g_L(p_t)$ is the (generalized) tip of $g_L(K_t)$, λ drives $g_L(K_t)$. Moreover, by (2.29), $\lambda(t) = g_{K_t \cup L}(p_t)$ (see Figure 2.6). Since p_t is the (generalized) tip of K_t in the hull $K_t \cup L$, we get the usual relationship between tips and driving functions. This gives us a concrete way of defining the driving function in the multiple hull setting.

Lemma 2.27. Let K_t be a Loewner family driven by $U : [0, T] \to \mathbb{R}$. Let L be a hull disjoint from K_T. Let $\lambda(t) = g_{g_{K_t}(L)}(U(t))$. Fix $0 \le s < t \le T$ so that $K_s \cap \partial_{\mathbb{H}} K_t \ne \emptyset$. Then for

$s \le r \le t$

$$g^{-}_{K_t \cup L}(K_t \setminus K_s) \le \lambda(r) \le g^{+}_{K_t \cup L}(K_t \setminus K_s). \tag{2.30}$$

Proof. Let $0 \le s < t \le T$, $K_s \cap \partial K_t \neq \emptyset$, and $A_r = g_{K_r \cup L}(K_t \setminus K_r)$ for $s \le r \le t$. Then $\lambda(r) \in \mathbb{R} \cap \overline{g_{K_r \cup L}(K_t \setminus K_r)} = \mathbb{R} \cap \overline{A_r}$. Since $g_{K_t \cup L} = g_{A_r} \circ g_{K_r \cup L}$, by Lemma 2.6, $\lambda(r) \in \mathbb{R} \cap \overline{g_{K_t \cup L}(K_t \setminus K_r)}$. So, $g^{-}_{K_t \cup L}(K_t \setminus K_r) \le \lambda(r) \le g^{+}_{K_t \cup L}(K_t \setminus K_r)$ for $s \le r \le t$.

Let $s < r < t$. Then as $K_s \subset K_r$ and $K_s \cap \partial_{\mathbb{H}} K_t \neq \emptyset$, we have $K_r \cap \partial_{\mathbb{H}} K_t \neq \emptyset$. Using Lemma 2.26,

$$g^{-}_{K_t \cup L}(K_t \setminus K_s) \le g^{-}_{K_t \cup L}(K_t \setminus K_r) \le \lambda(r) \le g^{+}_{K_t \cup L}(K_t \setminus K_r) \le g^{+}_{K_t \cup L}(K_t \setminus K_s) \tag{2.31}$$

Lastly, let $r_n \uparrow t$ with $s \le r_n$. Then for all $n \in \mathbb{N}$

$$g^{-}_{K_t \cup L}(K_t \setminus K_s) \le \lambda(r_n) \le g^{+}_{K_t \cup L}(K_t \setminus K_s) \tag{2.32}$$

As λ is continuous, the result holds for t. $\square$

Corollary 2.28. Let K_t be a Loewner family driven by $U : [0,T] \to \mathbb{R}$. Let L be a hull disjoint from K_T. Let $\lambda(t) = g_{g_{K_t}(L)}(U(t))$. If $|\lambda(t) - \lambda(s)| > |\lambda(t) - \lambda(r)|$ for $s < r < t$, then $K_s \cap \partial_{\mathbb{H}} K_t \neq \emptyset$.

Proof. Since $L \cap K_T = \emptyset$, $g_L(K_t)$ is a Loewner family and furthermore is driven by λ. If $|\lambda(t) - \lambda(s)| > |\lambda(t) - \lambda(r)|$ for $s < r < t$, then clearly $\lambda(s) \neq \lambda(r)$ for $s < r < t$. Since λ is continuous either $\lambda(s) > \lambda(r)$ for all $s < r < t$ or $\lambda(s) < \lambda(r)$ for all $s < r < t$. By Lemma 2.23, $\partial_{\mathbb{H}} g_L(K_t) \cap g_L(K_s) \neq \emptyset$. By the disjointness of K_T and L, $\partial_{\mathbb{H}} K_t \cap K_s \neq \emptyset$ as well. $\square$

Whenever we use the families K_t and L_s, we will assume that K_T is on the left side of L_S. We note that the next lemma is a generalization of Lemma 3.5 from [44]. The proof of part (a) uses the key ideas brought up in the corresponding proof in [44], but the proof of part (b) is fundamentally different.

Lemma 2.29. Let $(K_t)_{t \in [0,T]}$ and $(L_v)_{v \in [0,S]}$ be two disjoint Loewner families. Then, for any $t \in [0,T]$ and $s \in [0,S]$,

(a) $g^{-}_{K_T \cup L_S}(K_T) \le g^{-}_{K_t \cup L_s}(K_T) < g^{+}_{K_t \cup L_s}(L_S) \le g^{+}_{K_T \cup L_S}(L_S)$

(b) $g^-_{K_t\cup L_s}(L_S) - g^+_{K_t\cup L_s}(K_T) \geq g^-_{K_T\cup L_S}(L_S) - g^+_{K_T\cup L_S}(K_T)$.

Proof of (a). First, the middle inequality is immediate since $\overline{K_T} \cap \overline{L_S} = \emptyset$.

Second, we will prove the first inequality. Let $t \in [0,T]$ and $s \in [0,S]$. Define

$$A_1 = \overline{g_{K_t\cup L_s}(K_T \setminus K_t)} \text{ and } A_2 = \overline{g_{K_t\cup L_s}(L_S \setminus L_s)}. \tag{2.33}$$

Then $A_1 \cap \mathbb{H}$ and $A_2 \cap \mathbb{H}$ are disjoint hulls. Let $a = g^-_{K_t\cup L_s}(K_T \setminus K_t)$ and $b = g^+_{K_t\cup L_s}(L_S \setminus L_s)$. Since $K_T \setminus K_t \subseteq K_T$, $g^-_{K_t\cup L_s}(K_T) \leq a$. Define $A = A_1 \cup A_2$ which is a hull with $\overline{A} \cap \mathbb{R} \subseteq [a,b]$.

If $g^-_{K_t\cup L_s}(K_T) < a$, then by Lemma 2.6 (a),

$$g^-_{K_T\cup L_S}(K_T) = g_A(g^-_{K_t\cup L_s}(K_T)) \leq g^-_{K_t\cup L_s}(K_T). \tag{2.34}$$

If $g^-_{K_t\cup L_s}(K_T) = a$, then as $g_A \circ g_{K_t\cup L_s} = g_{K_T\cup L_S}$,

$$g^-_{K_T\cup L_S}(K_T) = g^-_A(g_{K_t\cup L_s}(K_T)) \leq g^-_{K_t\cup L_s}(K_T). \tag{2.35}$$

In both cases, $g^-_{K_T\cup L_S}(K_T) \leq g^-_{K_t\cup L_s}(K_T)$.

Lastly, the other inequality follows in the same manner. □

Proof of (b). Let $A = \overline{g_{K_t\cup L_s}((K_T \setminus K_t) \cup (L_S \setminus L_s))}$. Then $A \cap \mathbb{H}$ is a hull with

$$A \cap \mathbb{R} = [g^-_{K_t\cup L_s}(K_T \setminus K_t), g^+_{K_t\cup L_s}(K_T \setminus K_t)] \cup [g^-_{K_t\cup L_s}(L_S \setminus L_s), g^+_{K_t\cup L_s}(L_S \setminus L_s)] \tag{2.36}$$

Let $(x_n)_{n=1}^\infty, (y_n)_{n=1}^\infty \subset \mathbb{R}$ so that $x_n \downarrow g^+_{K_t\cup L_s}(K_T)$, $y_n \uparrow g^-_{K_t\cup L_s}(L_S)$, and

$$g^+_{K_t\cup L_s}(K_T) < x_n < \frac{g^+_{K_t\cup L_s}(K_T) + g^-_{K_t\cup L_s}(L_S)}{2} < y_n < g^-_{K_t\cup L_s}(L_S) \tag{2.37}$$

Then for every n, $0 < g_A(y_n) - g_A(x_n) \leq y_n - x_n$ by Lemma 2.6 (b) as $(x_n, y_n) \subseteq \mathbb{R} \setminus A$. Since $g_A \circ g_{K_t\cup L_s} = g_{K_T\cup L_s}$,

$$g^-_{K_t\cup L_s}(L_S) - g^+_{K_t\cup L_s}(K_T) \geq g^-_A(g_{K_t\cup L_s}(L_S)) - g^+_A(g_{K_t\cup L_s}(K_T)) = g^-_{K_T\cup L_S}(L_S) - g^+_{K_T\cup L_S}(K_T). \tag{2.38}$$

$\square$

We will now generalize the notion of Loewner families to the multiple hull setting.

Definition 2.30. Let $K_1, ..., K_n$ be disjoint Loewner hulls and $\text{hcap}(K_1 \cup \cdots \cup K_n) = 2T$. For $j = 1, ..., n$ let K_t^j be an increasing family of hulls so that

- $t \mapsto \text{hcap}(K_t^j)$ is nondecreasing
- $\text{hcap}(K_t^1 \cup \cdots \cup K_t^n) = 2t$ for $t \in [0, T]$
- $K_T^j = K_j$

We call $K_t = (K_t^1, ..., K_t^n)$ a Loewner parameterization for the hull $K_1 \cup \cdots \cup K_n$.

We say that g_t^n converges to g_t in the Carathéodory sense, denoted $g_t^n \xrightarrow{Cara} g_t$, if for each $\epsilon > 0$ g_t^n converges to g_t uniformly on the set

$$[0, T] \times \{z \in \mathbb{H} : \text{dist}(z, K_t) \geq \epsilon\}. \tag{2.39}$$

This form of convergence allows for convergence of functions when their domains are changing.

Theorem 2.31 (2.4 [44])**.** For $j \in \{1, 2\}$ let $w_j^n, w_j \in L^1[0, 1]$ be weight functions and let $\lambda_j^n, \lambda_j \in C[0, 1]$ be driving functions with associated Loewner chains g_t^n, g_t. If λ_j^n converges to λ_j uniformly on $[0, 1]$ and if w_j^n converges weakly in $L^1[0, 1]$ to w_j for $j = 1, 2$, then g_t^n converges in the Carathéodory sense to the chain g_t.

2.5 Simulating the Chordal Loewner Equation

The Loewner equation yields a conformal map that takes sets in the upper half-plane and maps them down to the real line and for this reason is sometimes referred to as the downward Loewner equation. For a map that does the opposite, we can consider the initial value problem

$$\partial_t f_t(z) = \frac{-2}{f_t(z) - \xi(t)}, \quad f_0(z) = z. \tag{2.40}$$

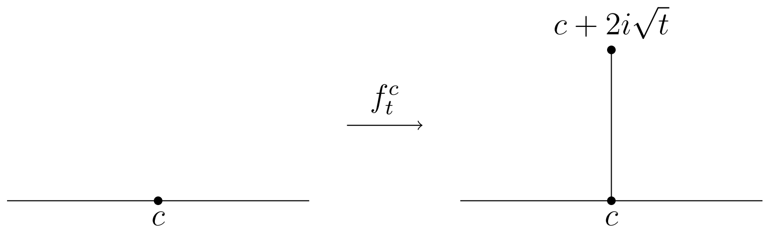

Figure 2.7: Mapping Up Hull Corresponding to f_t^c

We call this the upward Loewner equation and the conformal maps f_t grow sets in the upper half-plane. There is a relationship between the downward and upward Loewner equations. If g_t is the map given by the downward Loewner equation driven by $\lambda : [0, T] \to \mathbb{R}$ and f_t is the map given by the upward Loewner equation driven by $\xi(t) = \lambda(T - t)$, then $f_T = g_T^{-1}$.

The idea of the standard algorithm to simulate the hulls from the Loewner equation uses the upward Loewner equation driven by constant functions (see for instance [4], [20], [21], or [31]). For a constant driving function $\xi(t) = c$, the solution to the upward Loewner equation is

$$f_t^c(z) = \sqrt{(z - c)^2 - 4t} + c. \tag{2.41}$$

The algorithm for simulating the hull driven by $\lambda : [0, T] \to \mathbb{R}$ with $N + 1$ sample points is as follows:

0. Compute $\lambda(T)$ and add to hull
1. Apply (2.41) with $c = \lambda(T \cdot \frac{N-k}{N})$ to points in hull
2. Add $\lambda(T \cdot \frac{N-k}{N})$ to hull
3. Repeat steps 1-2 for $k \in \{1, ..., N\}$

Chapter 3

The Loewner Equation for Multiple Hulls

In [19], it was conjectured that the multiple Loewner equation driven by $\lambda_1 = -1$ and $\lambda_2 = 1$ with constant weights equal to $\frac{1}{2}$ could be realized by a single rapidly and randomly oscillating function driven by the Loewner equation. We prove this conjecture with the following more general result.

Proposition 3.1. Let $K = \bigcup_{i=1}^{n} K_i$, where $K_1, ..., K_n$ are disjoint hulls driven by continuous driving functions in the chordal sense. Then K is the limit of hulls generated by a sequence of randomly and rapidly oscillating functions.

This proposition inspires a simulation method for hulls from the multiple Loewner equation driven with constant weights. The idea is to use a single driving function that randomly and rapidly oscillates between the multiple driving functions, which generalizes the conjecture in [19]. We simulate the hull investigated in [19] and compare it to the actual hull in Section 3.3.

The proof of Proposition 3.1 result follows from a generalization of Theorem 1.1 in [44], which says that multiple slits can be generated through the multiple Loewner equation by continuous driving functions and constant weights. We generalize this to multiple hulls, as follows:

Theorem 3.2. Let $K^1, ..., K^n$ be disjoint Loewner hulls. Let $\text{hcap}(K^1 \cup \cdots \cup K^n) = 2T$. Then there exist constants $w_1, ..., w_n \in (0, 1)$ with $\sum_{k=1}^{n} w_k = 1$ and continuous driving functions $\lambda_1, ..., \lambda_n : [0, T] \to \mathbb{R}$ so that

$$\frac{\partial}{\partial t} g_t(z) = \sum_{k=1}^{n} \frac{2w_k}{g_t(z) - \lambda_k(t)}, \quad g_0(z) = z \tag{3.1}$$

satisfies $g_T = g_{K^1 \cup \cdots \cup K^n}$.

One significant difference between Theorem 1.1 in [44] and this result is the lack of uniqueness. This is due to the fact that we do not know the growth over time of the hulls in Theorem 3.2, we only know what the hull looks like at a particular time. This ambiguity allows the possibility that a hull can be driven by different driving functions, whereas any slit has a unique driving function. For example, if the hull is a semi-circle of radius 1 centered at 0, then two ways to generate this hull are by travelling the boundary clockwise or counterclockwise. This corresponds to scaling the driving function by -1. However, if we have K_t^j for each time and each $j \in \{1, ..., n\}$, then using the same proof of uniqueness for slits from [44], we would have uniqueness in the multiple hull setting as well.

3.1 Loewner Parameterization Precompactness

The generalization of Theorem 1.1 in [44], Theorem 3.2 here, follows with almost the same proof due to prime ends generalizing tips so appropriately. In [44] a few technical lemmas are shown, then Theorems 1.1 and 2.2 are proven. Since credit for the proofs goes to the authors of [44], we will state results where the proofs generalize quickly without proof and direct the reader to [44].

Lemma 3.3 (3.2 [44])**.** Let K_t be a Loewner family. Let L be a hull disjoint from K_T. Then there exists a constant $c > 0$ so that for all $0 \leq s < t \leq T$

$$c \leq \frac{\text{hcap}(K_t \cup L) - \text{hcap}(K_s \cup L)}{t - s} \tag{3.2}$$

Lemma 3.4 (3.3 [44]). Let $(K_t)_{t\in[0,T_1]}$ and $(L_t)_{t\in[0,T_2]}$ be two disjoint Loewner families. Then there is a constant $c > 0$ so that

$$c \leq \frac{\operatorname{hcap}(K_{t_1} \cup L_{t_2}) - \operatorname{hcap}(K_{s_1} \cup L_{s_2})}{t_j - s_j} \tag{3.3}$$

for all $0 \leq s_j < t_j \leq T_j$ and $j = 1, 2$.

Lemma 3.5 (3.6 [44]). Let $(K_t)_{t\in[0,T]}$ and $(L_v)_{v\in[0,S]}$ be two disjoint Loewner families. Then there exists a constant $M > 0$ so that

$$|g_{K_t\cup L_u}(p) - g_{K_t\cup L_v}(p)| \leq M|v - u| \tag{3.4}$$

for any $t \in [0, T]$ and $u, v \in [0, S]$ where p is the prime end corresponding to K_t.

The proof of Lemma 3.5 from [44], deals with images of base points of slits. We denote the base points of the two slits as p_1 and p_2, using the same notation as in [44] for convenience. In particular, the proof looks at the real points that correspond to the prime ends p_1 and p_2. This is equivalent to mapping down both slits and looking at the corresponding line segments. In order to prove this lemma, we replace p_1 by K_T and p_2 be L_S, which gives the analogue of mapping down both slits. The change from base points of a slit to entire hulls in the proof of Lemma 3.5 comes from the fact that for a slit, the two images of the base are the smallest and largest real points in the image of the mapped down slit, whereas with hulls, this corresponds to mapping down the entire hull.

Lemma 3.6 (3.7 [44]). Let K_t be a Loewner family driven by $U : [0, T] \to \mathbb{R}$. Let L be a hull disjoint from K_T. Let $\lambda(t) = g_{g_{K_t}(L)}(U(t))$. Then there exists $\omega : [0, T] \to [0, \infty)$ increasing with $\lim_{\delta\downarrow 0} \omega(\delta) = \omega(0) = 0$ such that

$$|g_{K_t\cup L}(p_t) - g_{K_s\cup L}(p_s)| \leq \omega(|t - s|) \tag{3.5}$$

for $s, t \in [0, T]$, where p_t and p_s are the prime ends corresponding to $\lambda(t)$ and $\lambda(s)$ respectively.

The proof of (3.5) in the setting of hulls requires more background work than in the setting of slits. The majority of the results in Section 2.4 are used to show that hulls grow similarly to slits. It is this subtle difference in growth that requires a different proof of (3.5) than in [44]. However, the proof that $\omega(\delta) \to 0$ as $\delta \to 0$ is the exact same as in [44], so we refer the reader there for the proof.

Proof. Let $\omega : [0, T] \to [0, \infty)$ be defined by $\omega(0) = 0$ and

$$\omega(\delta) = \sup\{g^+_{K_t}(K_t \setminus K_s) - g^-_{K_t}(K_t \setminus K_s) : 0 \le s < t \le T, t - s \le \delta\} \tag{3.6}$$

Clearly, $\omega(\delta)$ is increasing.

Next, we will prove the inequality in (3.5). Let $0 \le s' < t \le T$ and $\delta' = t - s'$. Lemma 2.17 and the corollary to Lemma 2.23 show that there exists $s' \le s < t$ with $K_s \cap \partial_{\mathbb{H}} K_t \neq \emptyset$ and

$$|g_{K_t \cup L}(p_t) - g_{K_{s'} \cup L}(p_{s'})| = |\lambda(t) - \lambda(s')| \le |\lambda(t) - \lambda(s)| = |g_{K_t \cup L}(p_t) - g_{K_s \cup L}(p_s)| \tag{3.7}$$

Let $\delta = t - s \le \delta'$, so $\omega(\delta) \le \omega(\delta')$. Since $K_s \cap \partial_{\mathbb{H}} K_t \neq \emptyset$, by Lemma 2.27 we have for $r \in [s, t]$

$$g^-_{K_t \cup L}(K_t \setminus K_s) \le \lambda(r) \le g^+_{K_t \cup L}(K_t \setminus K_s). \tag{3.8}$$

So,

$$|g_{K_t \cup L}(p_t) - g_{K_s \cup L}(p_s)| = |\lambda(t) - \lambda(s)| \le g^+_{K_t \cup L}(K_t \setminus K_s) - g^-_{K_t \cup L}(K_t \setminus K_s). \tag{3.9}$$

Since $g_{K_t \cup L} = g_{g_{K_t}(L)} \circ g_{K_t}$, Lemma 2.6 (b) shows

$$g^+_{K_t \cup L}(K_t \setminus K_s) - g^-_{K_t \cup L}(K_t \setminus K_s) \le g^+_{K_t}(K_t \setminus K_s) - g^-_{K_t}(K_t \setminus K_s) \le \omega(\delta). \tag{3.10}$$

Combining (3.7), (3.10), and $\omega(\delta) \le \omega(\delta')$ gives the result. $\square$

Lemma 3.7 (3.8 [44])**.** Let $(K_t)_{t\in[0,T]}$ and $(L_v)_{v\in[0,S]}$ be two disjoint Loewner families. Then there exists constants $c, M > 0$ and $\omega : [0, T] \to [0, \infty)$ increasing with $\lim_{\delta\downarrow 0} \omega(\delta) = \omega(0) = 0$

such that

$$|g_{K_t \cup L_v}(p_t) - g_{K_s \cup L_u}(p_s)| \le \omega\left(\frac{1}{c}|\mathrm{hcap}(K_t \cup L_v) - \mathrm{hcap}(K_s \cup L_u)|\right) \tag{3.11}$$

$$+ \frac{M}{c}|\mathrm{hcap}(K_t \cup L_v) - \mathrm{hcap}(K_s \cup L_u)| \tag{3.12}$$

for all $s, t \in [0, T]$ and $u, v \in [0, S]$, where p_t and p_s are the prime ends corresponding to $\lambda(t)$ and $\lambda(s)$, respectively.

Theorem 3.8 (2.2 [44])**.** Let A be a multi-Loewner hull with $\mathrm{hcap}(A) = 2T$. For any Loewner parameterization $K_t = (K_t^1, K_t^2)$ of A, let λ_K^j be the driving function of K_t^j for $j = 1, 2$. Then the sets

$$\{\lambda_K^j : [0, T] \to \mathbb{R} \mid K \text{ Loewner parameterization of } A\} \tag{3.13}$$

are precompact subsets of the Banach space $C([0, T], \mathbb{R})$ for $j = 1, 2$.

The first step in proving this theorem in [44] is to get a uniform bound (in time) on $\lambda_K^j(t)$ for $j = 1, 2$. This bound, in our case, is

$$g_A^-(A) = g_T^-(A) \le \lambda_K^j(t) \le g_T^+(A) = g_A^+(A). \tag{3.14}$$

The rest of the proof in [44] generalizes.

Theorem 3.2 (1.1 [44])**.** Let $K^1, ..., K^n$ be disjoint Loewner hulls. Let $\mathrm{hcap}(K^1 \cup \cdots \cup K^n) = 2T$. Then there exist constants $w_1, ..., w_n \in (0, 1)$ with $\sum_{k=1}^n w_k = 1$ and continuous driving functions $\lambda_1, ..., \lambda_n : [0, T] \to \mathbb{R}$ so that

$$\partial_t g_t(z) = \sum_{k=1}^{n} \frac{2w_k}{g_t(z) - \lambda_k(t)}, \quad g_0(z) = z \tag{3.15}$$

satisfies $g_T = g_{K^1 \cup \cdots \cup K^n}$.

The proof of this theorem is the proof in [44], but we include it so that the reader can see where the previously proven lemmas are used.

Proof. Let K^1, K^2 be disjoint Loewner hulls, $\text{hcap}(K^1 \cup K^2) = 2$, $c_j = \frac{1}{2}\text{hcap}(K_j)$.

Define $\alpha_{n,w} : [0,1] \to \{0,1\}$ for $(n,w) \in \mathbb{N} \times [0,1]$ as follows:

$$\alpha_{n,w}(t) = \begin{cases} 1 & t \in (\frac{k}{2^n}, \frac{k+w}{2^n}) \\ 0 & t \in (\frac{k+w}{2^n} \frac{k+1}{2^n}) \end{cases} \tag{3.16}$$

for $k \in \{0, ..., 2^n\}$. Let

$$\partial_t g_{t,n}(z) = \frac{2\alpha_{n,w}(t)}{g_{t,n}(z) - \lambda_{1,n}(t)} + \frac{2(1-\alpha_{n,w}(t))}{g_{t,n}(z) - \lambda_{2,n}(t)}, \qquad g_0(z) = z. \tag{3.17}$$

By the construction of $\alpha_{n,w}$ only one hull grows at a time. So, the Loewner equation (with a single driving function) gives that $\lambda_{1,n}(t)$ is defined on $\bigcup_{k=0}^{2^n-1}(\frac{k}{2^n}, \frac{k+w}{2^n})$ (similarly for $\lambda_{2,n}(t)$). The disjointness of the hulls gives that we can extend $\lambda_{j,n}$ to be the image of $\lambda_{j,n}(t)$ under the map corresponding to the other hull. So, $\lambda_{1,n}$ and $\lambda_{2,n}$ are continuous on $[0,1]$. For $t \in [0,1]$ the hull at time t is

$$H_{n,w,t} = K^1_{x_{n,w,t}} \cup K^2_{y_{n,w,t}} \tag{3.18}$$

where $x_{n,w,t} \in [0,1]$ depends continuously on w. For all $n \in \mathbb{N}$, $x_{n,0,1} = 0$ and $x_{n,1,1} = 1$ (as $w = 0$ and $w = 1$ correspond to single hull growth of K^1 and K^2 respectively). By the Intermediate Value Theorem, for each $n \in \mathbb{N}$ there exists w_n so that $x_{n,w_n,1} = c_1$. By Lemma 2.8 (b), $y_{n,w_n,1} = c_2$. So, $H_{n,w_n,1} = K^1 \cup K^2$. Which means that α_{n,w_n} is a sequence of weights and $\lambda_{j,n}$ are sequences of continuous driving function generating $K^1 \cup K^2$.

By Theorem 3.8, there is a subsequence of $\lambda_{1,n}$ converging to a function λ_1. Using Theorem 3.8 again on the corresponding subsequence of $\lambda_{2,n}$ we get that there is a further subsequence converging to a function λ_2. Furthermore, the corresponding subsequence of w_n has a convergent subsequence converging to $w \in [0,1]$. We will now reindex this sequence by $n \in \mathbb{N}$.

Let

$$\partial_t g_t(z) = \frac{2w}{g_{t,n}(z) - \lambda_{1,n}(t)} + \frac{2(1-w)}{g_{t,n}(z) - \lambda_{1,n}(t)}, \qquad g_0(z) = z. \tag{3.19}$$

Then it is easy to see that α_{n,w_n} converges weakly to w in $L^1([0,1])$ (similar to Lemma 3.9). Now, by Theorem 2.31, we have the result. $\square$

3.2 Convergence of Hulls Using Rapid and Random Oscillation

3.2.1 Introduction to Conjecture

In Section 6 of [19], Kager, Nienhuis, and Kadanoff investigate the multiple Loewner equation generated from constant driving functions, $\lambda_1 \equiv -1$ and $\lambda_2 \equiv 1$, and constant weights, $w_1 = w_2 = \frac{1}{2}$. They show that the hull is given by

$$K_t = \left\{ \sqrt{\frac{2\theta_t}{\sin(2\theta_t)}} (\pm \cos\theta_t + i \sin\theta_t) \right\} \tag{3.20}$$

where θ_t increases from 0 to $\frac{\pi}{2}$ as t increases. They make the conjecture that the same hull can be generated by a single driving function that "makes rapid (random) jumps between the values λ_j." In this section, we will say that a sequence of driving functions generate a hull if the corresponding conformal maps from the Loewner equation converge in the Carathéodory sense to the conformal map corresponding to the hull. We will prove their conjecture constructively. The key tool in the proof is to apply Theorem 2.31 due to Roth and Schleissinger from [44] which we use to relate the multiple Loewner equation and a single driving function.

The idea to constructing a randomly, rapidly oscillating driving function is to use the driving functions that generate the hull K_t from the multiple Loewner equation. We do this by dividing up the time interval into smaller intervals and then randomly pick which driving function to use on each small interval. This random picking is governed by the weights. Furthermore, this construction is not limited to the case described above that is considered in [19]. In fact, Proposition 3.1 is a more general answer to their conjecture.

3.2.2 Controlled Oscillation

Before we tackle the conjecture, we will do an example. In the situation of [19], let $\lambda_1 \equiv -1$, $\lambda_2 \equiv 1$, $w_1 = w_2 = \frac{1}{2}$, and K_t be as in (3.20). We will create a sequence of rapidly oscillating functions that generate K_t. The idea here is essentially the idea in the more general case: divide the interval into smaller pieces and decide whether the driving function is -1 or 1 on each piece. Here, since $w_1 = w_2 = \frac{1}{2}$, we will simply rotate between the driving functions -1 and 1. Let

$$\lambda^n(t) = \sum_{k=0}^{2^{n-2}} \chi_{[\frac{2k+1}{2^n}, \frac{2(k+1)}{2^n})} - \chi_{[\frac{2k}{2^n}, \frac{2k+1}{2^n})}(t). \tag{3.21}$$

So, we take $[0,1]$ and divide it into an even number of intervals of the from $[\frac{j}{2^n}, \frac{j+1}{2^n})$. When j is even $\lambda^n|_{[\frac{j}{2^n}, \frac{j+1}{2^n})} \equiv -1$ and when j is odd $\lambda^n|_{[\frac{j}{2^n}, \frac{j+1}{2^n})} \equiv 1$. This means for any $n \in \mathbb{N}$ $\lambda^n(t) = -1 = \lambda_1$ for half of the time and $\lambda^n(t) = 1 = \lambda_2$ for the other half of the time, corresponding to $w_1 = w_2 = \frac{1}{2}$. Now, we will show that K_t is generated by λ^n. The proof uses Theorem 2.31 to relate the multiple Loewner equation to a single driving function. We have already defined the driving function, so we will now set up the multiple Loewner equation situation. Define the weight functions

$$w_1^n(t) := \sum_{k=0}^{2^{n-1}-1} \chi_{[\frac{2k}{2^n}, \frac{2k+1}{2^n})}(t) \quad \text{and} \quad w_2^n(t) := \sum_{k=1}^{2^{n-1}} \chi_{[\frac{2k-1}{2^n}, \frac{2k}{2^n})}(t). \tag{3.22}$$

At any time, they sum to 1 and they are never 1 at the same time. We will show w_j^n converges to $\frac{1}{2}$ weakly. Since the conformal maps from the Loewner equation driven by λ^n and the conformal maps from the multiple Loewner equation driven by λ_1, λ_2, w_1^n, and w_2^n are the same, we will have that K_t is generated by $(\lambda^n)_{n=1}^{\infty}$.

Lemma 3.9. As $n \to \infty$, w_j^n converges weakly to $\frac{1}{2}$ for $j = 1, 2$ - that is, for each $h \in L^\infty[0,1]$

$$\int w_1^n h \to \int \frac{1}{2} h \text{ as } n \to \infty. \tag{3.23}$$

Proof. We will prove this for $j = 1$ first. Let $\epsilon > 0$ and $h \in L^\infty[0,1]$. By Lusin's Theorem there exists $E \in \mathscr{B}([0,1])$ (the Borel sets of $\mathbb{R}$) compact with $m([0,1] \setminus E) < \frac{\epsilon}{2||h||_\infty}$ (m

denotes Lebesgue measure) and h is continuous on E. So,

$$\left|\int_{[0,1]\setminus E} h\left(w_1^n - \frac{1}{2}\right)\right| < \frac{\epsilon}{2}. \tag{3.24}$$

Since E is compact, h is uniformly continuous on E. So there exists $\delta > 0$ such that for each $x, y \in E$ with $|x-y| < \delta$, we have that $|h(x) - h(y)| < \epsilon$. Also, there exists $N \in \mathbb{N}$ such that for all $n \geq N$, $\frac{1}{2^{n-1}} < \delta$. Let $n \geq N$. For $k \in \mathbb{N}$, define

$$I_k = \left[\frac{k}{2^n}, \frac{k+1}{2^n}\right) \cap E. \tag{3.25}$$

Then

$$\left|\int_E h \cdot \left(w_1^n - \frac{1}{2}\right)\right| = \left|\sum_{k=0}^{2^n-1} \int_{I_k} \frac{(-1)^k}{2} h\right| \leq \frac{1}{2} \sum_{k=0}^{2^{n-1}-1} \left|\int_{I_{2k}} h - \int_{I_{2k+1}} h\right|. \tag{3.26}$$

Since the length of $I_{2k} \cup I_{2k+1}$ is $\frac{1}{2^{n-1}} < \delta$, for all $x \in I_{2k} \cup I_{2k+1}$,

$$h\left(\frac{2k+1}{2^n}\right) - \epsilon \leq h(x) \leq h\left(\frac{2k+1}{2^n}\right) + \epsilon. \tag{3.27}$$

So,

$$\left|\int_{I_{2k}} h - \int_{I_{2k+1}} h\right| \leq \frac{1}{2^n}(2\epsilon) = \frac{\epsilon}{2^{n-1}}. \tag{3.28}$$

Hence,

$$\left|\int_E h \cdot \left(w_1^n - \frac{1}{2}\right)\right| \leq \frac{1}{2} \sum_{k=0}^{2^{n-1}-1} \frac{\epsilon}{2^{n-1}} < \epsilon. \tag{3.29}$$

This shows that w_1^n converges weakly to $\frac{1}{2}$.

Since $w_2^n = 1 - w_1^n$, we have that w_2^n converges weakly to $\frac{1}{2}$, as well. □

Since $\lambda^n(t) = w_1^n(t)\lambda_1(t) + w_2^n(t)\lambda_2(t)$, by Theorem 2.31, we have that K_t is generated by λ^n. This proves that K_t is generated by a rapidly oscillating function.

3.2.3 Rapid, Random Oscillation

Now that we have shown that a rapidly oscillating function satisfies part of the conjecture in [19], we turn to proving that we do not have to control the oscillation as we did before.

In the random case, we begin construction of the sequence of driving functions by defining weight functions. Let $w_1 \in (0,1)$ and $w_2 = 1 - w_1$ be constants. For each $k \in \mathbb{N}$, let X_k be a random variable such that $P(X_k = 1) = w_1$ and $P(X_k = 0) = w_2$ (i.e. X_k is a Bernoulli random variable). For each $n \in \mathbb{N}$ and $k \in \{1, ..., n\}$, define

$$I_k^n = \left[\frac{k-1}{n}, \frac{k}{n}\right). \tag{3.30}$$

For each $n \in \mathbb{N}$, define

$$w_1^n = \sum_{k=1}^{n} X_k \chi_{I_k^n}(t) \quad \text{and} \quad w_2^n = \sum_{k=1}^{n} (1 - X_k)\chi_{I_k^n}(t). \tag{3.31}$$

Then for every $t \in [0,1]$ and $n \in \mathbb{N}$, $w_1^n(t) + w_2^n(t) = 1$ a.s. Further, $w_1^n(t) = 1$ only when $w_2^n(t) = 0$ and vice versa. Let

$$\lambda^n(t) = w_1^n(t)\lambda_1(t) + w_2^n(t)\lambda_2(t). \tag{3.32}$$

For any $n \in \mathbb{N}$, λ^n rapidly (for large n) and randomly oscillates between the values of λ_1 and λ_2. The idea here is that w_j^n turns off and on λ_j. So, essentially we are using the single Loewner equation to approximate the multiple Loewner equation and the weights control which function is turned on or picked in the intervals I_k^n. We will first show that w_j^n converges weakly to w_j for $j = 1, 2$. Then using Theorems 2.31 and 3.2, we will obtain the desired result.

Lemma 3.10. As $n \to \infty$, almost surely w_j^n as in (3.31) converges weakly to w_j for $j = 1, 2$.

We will prove this for $j = 1$ using a standard approach by proving that convergence holds on intervals, for step functions, for non-negative functions, and for L^∞ functions. Then the result will also hold for $j = 2$ as $w_2^n = 1 - w_1^n$.

Claim 3.11. Let $J \subseteq [0,1]$ be an interval. Then almost surely $\int_J w_1^n \to \int_J w_1 = w_1 m(J)$

Proof. Let $\epsilon > 0$ and $J \subseteq [0,1]$ be an interval. Then there exists $N_1 \in \mathbb{N}$ such that for all $n \geq N_1$ there exists $a_n \in \{1, ..., n\}$ and $m_n \in \{0, ..., n - a_n\}$ such that $\bigcup_{k=a_n}^{a_n+m_n} I_k^n \subseteq J$. Then there exists a natural number $N_2 \geq N_1$ such that for all $n \geq N_2$

$$I_n = \bigcup_{k=a_n}^{a_n+m_n} I_k^n \subseteq J \quad \text{and} \quad m(J \setminus I_n) < \frac{\epsilon}{2}. \tag{3.33}$$

So,

$$\left| \int_{J \setminus I_n} w_1^n - w_1 \right| \leq \left| \int_{J \setminus I_n} dt \right| = m(J \setminus I_n) < \frac{\epsilon}{2} \tag{3.34}$$

As $n \to \infty$, $m_n \to \infty$. By the Strong Law of Large Numbers, we have

$$\sum_{k=a_n}^{a_n+m_n} \frac{X_k}{m_n} \to w_1 \text{ a.s.} \tag{3.35}$$

So, there exists $N \geq N_2$ such that for all $n \geq N$

$$\left| \sum_{k=a_n}^{a_n+m_n} \frac{X_k}{m_n} - w_1 \right| < \frac{\epsilon}{2} \text{ a.s.} \tag{3.36}$$

Fix $n \geq N$. Then with probability 1, since $m(I_n) = \frac{1}{n}$,

$$\left| \int_{I_n} w_1^n - w_1 \right| = \left| \frac{m_n}{n} \sum_{k=a_n}^{a_n+m_n} \frac{X_k - w_1}{m_n} \right| = m(I_n) \left| \sum_{k=a_n}^{a_n+m_n} \frac{X_k}{m_n} - w_1 \right| \leq \frac{\epsilon}{2} \tag{3.37}$$

Therefore, as $n \to \infty$, almost surely

$$\int_J w_1^n \to w_1 m(J). \tag{3.38}$$

□

Claim 3.12. Let $h \in L^\infty[0,1]$ be a step function. Then almost surely

$$\int_{[0,1]} h w_1^n \to w_1 \int_{[0,1]} h. \tag{3.39}$$

Proof. Since h is a bounded step function, there exist finitely many nonempty intervals $J_1, ..., J_n$ and $\alpha_1, ..., \alpha_n \in \mathbb{R} \setminus \{0\}$ so that $h = \sum_{i=1}^n \alpha_i \chi_{J_i}$. Then, by the previous claim, there exists N such that for all $n \geq N$ almost surely

$$\left| \int_{J_i} w_1^n - w_1 m(J_i) \right| < \frac{\epsilon}{2 \sum_{i=1}^n |\alpha_i|}. \tag{3.40}$$

Then with probability 1,

$$\left| \int_{[0,1]} h(w_1^n - w_1) \right| \leq \sum_{i=1}^n \left| \alpha_i \int_{J_i} (w_1^n - w_1) \right| \leq \sum_{i=1}^n |\alpha_i| \frac{\epsilon}{2 \sum_{i=1}^n |\alpha_i|} < \epsilon \tag{3.41}$$

This proves the claim. □

Claim 3.13. For $h \in L^\infty[0,1]$ with $h \geq 0$, almost surely

$$\int h w_1^n \to w_1 \int h. \tag{3.42}$$

Proof. Let $h \in L^\infty[0,1]$ with $h \geq 0$. Then there exists a step function $f \in L^\infty[0,1]$ such that $||f - h||_2 \leq \frac{\epsilon}{2}$, where $\| \cdot \|_k$ denotes the $L^k[0,1]$ norm. Then there exists $N \in \mathbb{N}$ such that for all $n \geq N$, almost surely $| \int (w_1^n - w_1)| < \frac{\epsilon}{2(\|f\|_\infty \vee 1)}$. Also, since $0 \leq w_1^n(t) \leq 1$ a.s., $|w_1^n - w_1| \leq 1$ a.s. for all $t \in [0,1]$. So,

$$\left| \int h(w_1^n - w_1) \right| \leq \left| \int f(w_1^n - w_1) \right| + \left| \int (h - f)(w_1^n - w_1) \right| \leq \frac{\epsilon}{2} + ||h - f||_2 < \epsilon \tag{3.43}$$

This proves the claim. □

Claim 3.14. For $h \in L^\infty[0,1]$, almost surely

$$\int h w_1^n \to w_1 \int h. \tag{3.44}$$

Proof. Let $h \in L^\infty[0,1]$. Then $h^+, h^- \in L^\infty[0,1]$ (where $h^+, h^- \geq 0$ and $h = h^+ - h^-$). Then there exists $N \in \mathbb{N}$ such that for all $n \geq N$, almost surely

$$\left| \int_{[0,1]} h^+ (w_1^n - w_1) \right| < \frac{\epsilon}{2} \text{ and } \left| \int_{[0,1]} h^- (w_1^n - w_1) \right| < \frac{\epsilon}{2}. \tag{3.45}$$

Then with probability 1,

$$\left|\int h\left(w_1^n - w_1\right)\right| \le \left|\int h^+\left(w_1^n - w_1\right)\right| + \left|\int h^-\left(w_1^n - w_1\right)\right| < \epsilon. \tag{3.46}$$

$\square$

Proof of Lemma 3.10. By Claim 3.14, we have that w_1^n converges weakly to w_1. Then as $w_2^n = 1 - w_1^n$, we have w_2^n converges weakly to $1 - w_1 = w_2$. So we have the result. $\square$

Proof of Proposition 3.1. Apply Theorem 3.2 to get $\lambda_1, ..., \lambda_n$ continuous functions and constant weights $w_1, ..., w_n \in (0, 1)$. Applying Lemma 3.10 to w_j^n from (3.31), we have that w_j^n converges weakly to w_j in $L^1[0, 1]$ for $j = 1, 2$. Now, using Theorem 2.31, we have that we get the convergence we desire. $\square$

3.3 Simulating the Multiple Loewner Equation

For the multiple Loewner equation, we want to use the same idea as above but our driving function (randomly) oscillates between the driving functions. This is in effect what the proof in Section 3.2.3 does to generate the hulls. Let $\lambda_1, \lambda_2 : [0, T] \to \mathbb{R}$ be driving functions and $w_1, w_2 \in [0, 1]$ be constant weights. For $k \in \{0, ..., N\}$:

1. (Randomly) assign j_k to be either 1 or 2 so that $P(j_k = 1) = w_1$ and $P(j_k = 2) = w_2$
2. Define $\lambda(T \cdot \frac{k}{n}) = \lambda_{j_k}(T \cdot \frac{k}{n})$
3. Repeat steps in previous algorithm

We will investigate this algorithm by revisiting the example done in [19] and mentioned here in Section 3.2.1 that motivates all of our results. Let $\lambda_1 = -1$, $\lambda_2 = 1$, and $w_1 = \frac{1}{2} = w_2$. Recall the hull is given by

$$K_t = \left\{ \sqrt{\frac{2\theta_t}{\sin(2\theta_t)}} (\pm \cos \theta_t + i \sin \theta_t) \right\}. \tag{3.47}$$

First, we will control the oscillation by assigning j_k to be 1 when k is odd and 2 when k is even. The simulations for 1,000 and 10,000 oscillations are given in Figures 3.1 and 3.2. For 1,000 oscillations, the simulated data points are extremely close to the curve. There is a larger spread in the points near the real line since the growth of f_t^c is faster there. For 10,000 oscillations, the simulated data is almost indistinguishable from the curve.

The errors (that is, the maximum distance the data is from the hull) for 1000, 500, 400, 300, 200, 100, 90, 80, 70, 60, 50, 40, 30, 20, 10 controlled oscillations are shown in Figure 3.3, where the blue points correspond to points on the left side (i.e. associated with λ_1) and the red points correspond to points on the right side (i.e. associated with λ_2). Since the last map used in each controlled simulation is f_t^1, all of the right sided points are shifted up from their previous positions. This causes more error for these points. On the other hand, the map shifts the left sided points towards the right and reduces the error for these points. One amazing note is that even for 10 oscillations (11 data points), the error is small enough that simulated points are closer to their respective side than the opposite side (that is, their real parts are on the same side of 0 as their corresponding driving function). Further, for any number of oscillations (≥ 10), we could thicken each side of the hull by the error and they would not intersect (up to $T = 10$).

Second, we switch to randomly oscillating the driving function. We randomly assign j_k to be 1 or 2 by flipping a fair, virtual coin. In each of Figures 3.5 and 3.6 are 10 simulated hulls (non-black curves) with 1,000 and 10,000 oscillations (respectively) and the hull (black curves). For 1,000 oscillations, the simulated hulls have the same overall shape (e.g. they approach each other as their imaginary parts increase), but there is significant variation between the curves. For 10,000 oscillations, the simulated hulls are significantly closer to the hull, but there is still variation between the curves. The upshot is that the random hulls are visually a good replacement for the actual hull. Figure 3.4 gives a histogram of 100 simulations of 1,000 random oscillations where left and right sides correspond to the colors blue and red as before.

It appears that the controlled oscillation (i.e. forcing a switch between driving functions) always outperforms the random oscillation. This intuitively makes sense. Say we grow the -1 hull first using f_t^{-1}. If we use f_t^1 next, the hull corresponding to -1 will be shifted to the

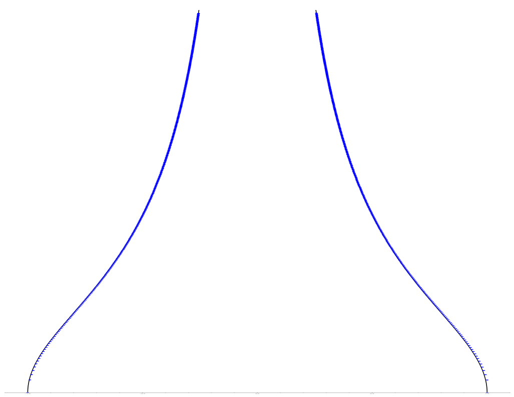

Figure 3.1: 1000 Controlled Oscillations

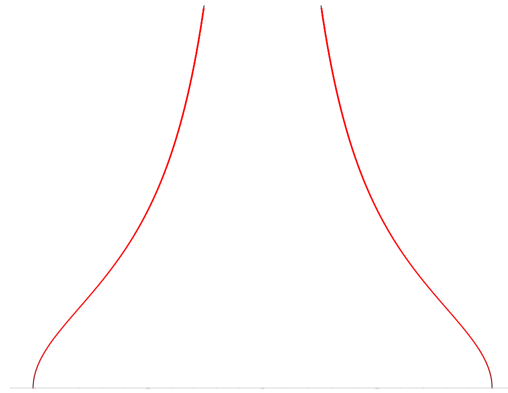

Figure 3.2: 10000 Controlled Oscillations

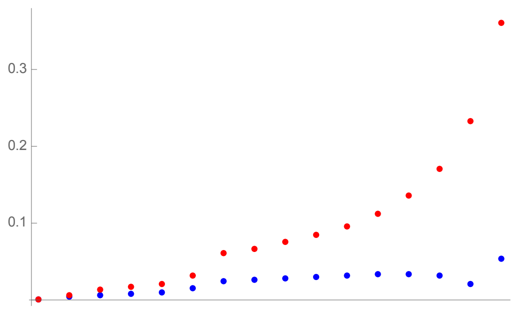

Figure 3.3: Moving from left to right are the plots for the errors of 10000, 1000, 500, 400, 300, 200, 100, 90, 80, 70, 60, 50, 40, 30, 20, 10 Controlled Oscillations

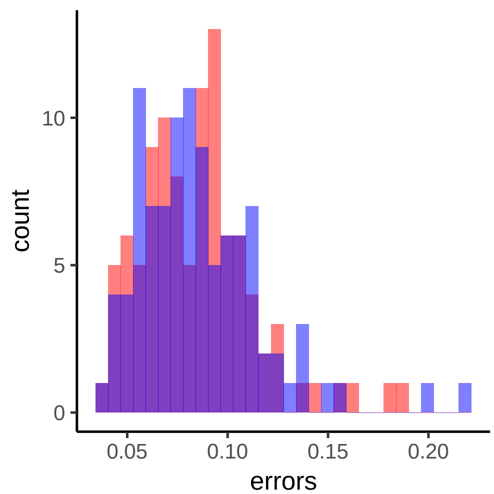

Figure 3.4: Histogram of 100 Errors for 1000 Random Oscillations

right. Instead, if we use f_t^{-1} next, the hull corresponding to -1 will be higher. In the random oscillation case, either of these maps could be used over and over before switching. This would cause the hulls to be higher or more to the left or right than the actual hull. The forced oscillation appears to not allow either side of the hull to get too far away from the actual hull.

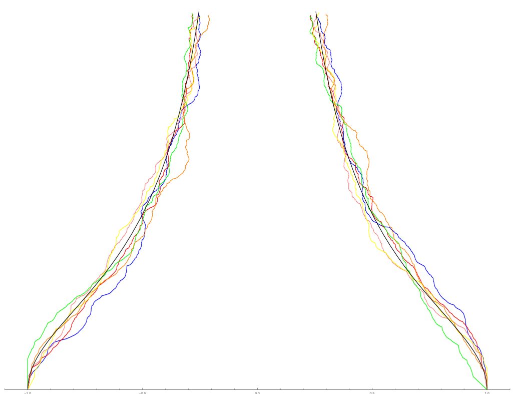

Figure 3.5: 1000 Random Oscillations

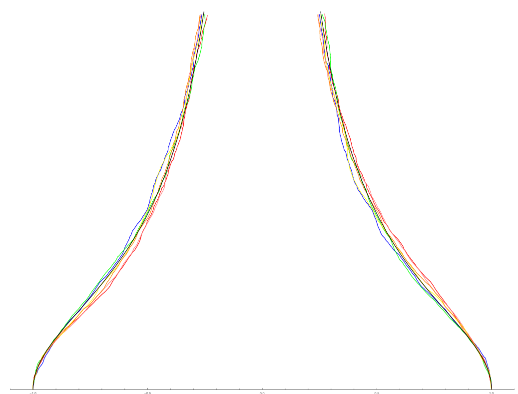

Figure 3.6: 10000 Random Oscillations

Chapter 4

Effect of Random Time Changes on Loewner Hulls

Schramm–Loewner Evolution, denoted SLE_κ, is a family of random curves in the upper halfplane $\mathbb{H}$ that is generated by the random function $\lambda(t) = \sqrt{\kappa}B_t$, where $\kappa \geq 0$ and $(B_t)_{t\geq 0}$ is a one-dimensional standard Brownian motion. Based on κ, SLE_κ exhibits phase transitions. Namely, for $0 \leq \kappa \leq 4$ the curves are simple, for $4 < \kappa < 8$ the curves are not simple, and for $8 \leq \kappa$ the curves are spacefilling; where all of these hold almost surely [42]. In the deterministic setting, it is also known that if we let $\lambda(t)$ be a Hölder-$\frac{1}{2}$ continuous function with norm $\|\lambda\|_{1/2}$, then there are similar phase transitions: for $0 \leq \|\lambda\|_{1/2} < 4$ the curves generated are simple [28], and for $\|\lambda\|_{1/2} < 4.0001$ the curves generated are not spacefilling [27]. It is our goal to analyze what happens to the curves when some of these functions are composed with a continuous, non-decreasing stochastic process $(E_t)_{t\geq 0}$, called a random time change.

Among the simplest yet most important random time changes is the so-called inverse α-stable subordinator, where $\alpha \in (0,1)$ is a parameter. With this specific time change (E_t) assumed independent of (B_t), the time-changed Brownian motion $B \circ E = (B_{E_t})_{t\geq 0}$ has been widely used to model subdiffusions, where particles spread at a slower rate than the usual Brownian particles. Indeed, the variance $\mathbb{E}[(B_{E_t})^2]$ takes the form $c_\alpha t^\alpha$, which grows more slowly for large t than the variance of the Brownian motion. More detailed backgrounds and relevant references about SLE_κ and random time changes are provided in Section 2.

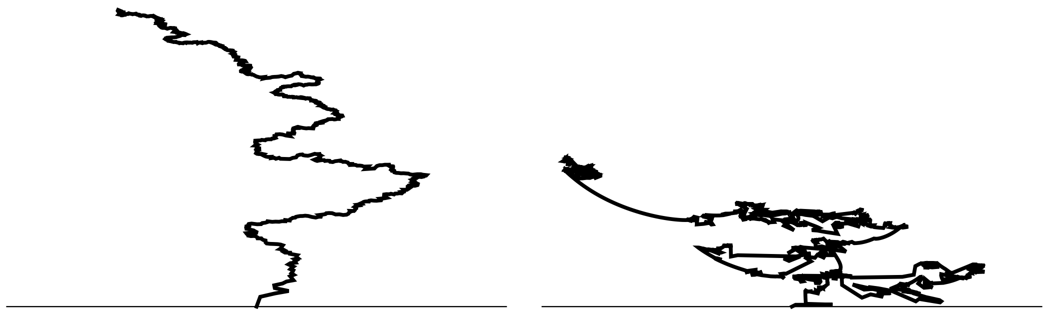

Figure 4.1: Sample SLE_1 curve (left) and sample curve generated by a time-changed Brownian motion (right).

Our main result reveals the fact that the time change extremely modifies the original curves, and phase transitions do not occur. See Figure 4.1 which compares a sample curve in this particular case with a sample curve in the untime-changed setting.

Theorem 4.1. For any $\kappa > 0$, almost surely the time-changed Brownian motion process $(\kappa B_{E_t})_{t\geq 0}$ does not generate a simple curve.

To prove this, we use a result in [26] to first derive general criteria (Theorem 4.9) for verifying whether the curves generated by time-changed functions are simple or non-simple. The proof of Theorem 4.1 also relies on a deep relationship between Brownian motion and a 3-dimensional Bessel process given in [50] and local behaviors of Bessel processes studied in [49].

We also investigate the scaling limits of random curves generated by time-changed self-similar processes. In particular, Corollary 4.7 shows that rescaling the curves generated by $\lambda(t) = \kappa B_{E_t}$ leads to deterministic sets, as observed in [8] for curves generated by a symmetric stable process (without a time change).

To further understand the effect of the random time change, we explore some examples of curves generated by time-changed deterministic functions, including a time-changed Weierstrass function. To aid our analysis of the deterministic examples, we also derive a condition on $\lambda(t)$ that guarantees that the generated curves leave the real line tangentially:

Proposition 4.2. Suppose that $\lambda(0) = 0$ and $\lambda(t) \geq at^r$ where $a > 0$ and $r \in (0, 1/2]$. Then for t small enough, the hull K_t driven by λ is contained in the region $\{x + iy : 0 \leq x, 0 < y < \frac{26}{a} x^{2-2r}\}$.

This proposition may be of independent interest, as it provides a converse of sorts to recent work by Lau and Wu [23]. In particular, Lau and Wu show that if the curve leaves the real line tangentially by lying in the domain $\{x + iy : 0 < x, ax^r < y < bx^r\}$ for $r > 1$, then we have some control on the associated driving function, namely $\limsup_{t\to 0} t^{-1/(r+1)}|\lambda(t)| < \infty$. They also analyze a particular family of tangential curves, which generalizes a result of Prokhorov and Vasil'ev [40].

Generalizations of SLE_κ to the case of the time-changed Brownian motion are considered and numerically analyzed in [38, 9]. However, as far as we know, our investigation in this chapter provides the first theoretical account of geometric properties of random curves associated with a large class of time-changed functions.

Time change is not the only adaptation of SLE that has been considered. Another example of an SLE variant is found in [45] and [14], where an α-stable Lévy process is added to the Brownian motion, which adds jumps to the driving function. It was shown that the phases of the hulls were unchanged by this addition, but the spread of the hull along the real line changes based on α due to the jumps.

We end this section with comments on the organization of the chapter. In Section 2, we discuss the Loewner equation and random time changes. Section 4.2 contains results on rescaled hulls and the proof of Proposition 4.2. In the last section, we state and prove the criteria (Theorem 4.9) for verifying whether the curves generated by time-changed functions are simple or non-simple, we prove Theorem 4.1, and we discuss examples of time-changed deterministic driving fucntions.

4.1 Lévy Processes and Random Time Changes

One of our goals is to consider a Brownian motion that has been time-changed by the inverse of a stable subordinator. We will use the inverse in order for our time change to be continuous. However, knowing how the subordinator behaves will help us see how its inverse behaves. In this subsection, we will set up the necessary definitions and develop some intuition about these processes. The discussion begins with the definition of Lévy processes as they include Brownian motion and stable subordinators as special cases. Throughout this chapter, given stochastic processes are assumed to be defined on a probability space $(\Omega, \mathscr{F}, \mathbb{P})$, take values in $\mathbb{R}$, start at 0, and have right-continuous sample paths with left limits.

A stochastic process $X = (X_t)_{t\geq 0}$ is called a *Lévy process* if it is stochastically continuous (i.e. for $\epsilon > 0$ and $t \geq 0$, $\lim_{s\to t} \mathbb{P}(|X_s - X_t| > \epsilon) = 0$) and has stationary and independent increments. If X is a Lévy process, then for each $t > 0$, the random variable X_t is infinitely divisible and its distribution is characterized by the triplet (b, σ^2, ν) appearing in the so-called Lévy-Khintchine formula

$$\mathbb{E}[e^{iuX_t}] = e^{t\eta(u)} \quad \text{with} \quad \eta(u) = ibu - \frac{1}{2}\sigma^2 u^2 + \int_{\mathbb{R}\setminus\{0\}} (e^{iuy} - 1 - iuy\mathbf{1}_{|y|<1})\nu(\mathrm{d}y),$$

where $\mathbb{E}$ denotes the expectation under $\mathbb{P}$. Here, $b \in \mathbb{R}$, $\sigma^2 \geq 0$, and ν is a Borel measure on $\mathbb{R} \setminus \{0\}$ with $\int_{\mathbb{R}\setminus\{0\}} (|y|^2 \wedge 1)\nu(\mathrm{d}y) < \infty$, called the *Lévy measure* of X. Since sample paths of a Lévy process are assumed to be right-continuous with left limits, they have at most countably many jumps, but for each $\epsilon > 0$, they have only finitely many jumps of size ϵ or larger. The Lévy measure ν controls the jumps of the Lévy process. In particular, Brownian motion is a Lévy process with triplet $(b, \sigma^2, \nu) = (0, 1, 0)$ so that $\mathbb{E}[e^{iuX_t}] = e^{-\frac{1}{2}u^2 t}$.

A Lévy process with non-decreasing sample paths is called a *subordinator.* The distribution of a subordinator $D = (D_t)_{t\geq 0}$ is characterized by its Laplace transform

$$\mathbb{E}[e^{uD_t}] = e^{-t\psi(u)} \quad \text{with} \quad \psi(u) = bu + \int_0^\infty (1 - e^{-uy})\nu(\mathrm{d}y),$$

where the Lévy measure ν satisfies $\nu(-\infty, 0) = 0$ and $\int_0^\infty (y \wedge 1)\nu(\mathrm{d}y) < \infty$. The function $\psi(u)$ is called the *Laplace exponent* of D. In this paper, we only consider a subordinator D with $b = 0$ and $\nu(0, \infty) = \infty$, which implies that D has strictly increasing sample paths with $\lim_{t\to\infty} D_t = \infty$ and the jump times of D are dense in $(0, \infty)$ (see [46]). Examples of theoretically and practically important subordinators include:

- a *stable subordinator* of index $\alpha \in (0, 1)$ (or an α-stable subordinator for short), where $\nu(\mathrm{d}x) = \frac{\alpha}{\Gamma(1-\alpha)} x^{-\alpha-1}\mathbf{1}_{x>0}\,\mathrm{d}x$ and $\psi(u) = u^\alpha$, and
- a *tempered stable subordinator* of index $\alpha \in (0, 1)$ and tempering factor $\theta > 0$, where $\nu(\mathrm{d}x) = \frac{\alpha}{\Gamma(1-\alpha)} e^{-\theta x} x^{-\alpha-1}\mathbf{1}_{x>0}\,\mathrm{d}x$ and $\psi(u) = (u + \theta)^\alpha - \theta^\alpha$.

Tempered stable subordinators may be regarded as a one-parameter extension of stable subordinators via θ. However, they possess very different properties. Indeed, while a stable subordinator has infinite first moment, a tempered stable subordinator has finite moments of all orders due to the factor $e^{-\theta x}$ which diminishes (or "tempers") large jumps of the stable subordinator of the same index (see [43] for a detailed account of more general tempered stable Lévy processes). On the other hand, an α-stable subordinator is the only subordinator which is self-similar with index $1/\alpha$; i.e. $(D_{ct}) \stackrel{\mathrm{d}}{=} (c^{1/\alpha} D_t)$ for all $c > 0$ (see [10]).

The Lévy–Itô decomposition allows us to develop some intuition about the jumps of subordinators, which will in turn help us view their inverses. Given a Lévy process X, for each Borel set A of $\mathbb{R} \setminus \{0\}$ and $t \geq 0$, define

$$N(t, A)(\omega) = \#\{0 \leq s \leq t : \Delta X_s(\omega) \in A\}, \tag{4.1}$$

where ΔX_s is the size of the jump at s. For fixed $t > 0$ and $\omega \in \Omega$, $N(t, \cdot)(\omega)$ is a counting measure on the collection of Borel sets of $\mathbb{R} \setminus \{0\}$. For A bounded below, $(N(t, A))_{t \geq 0}$ is a Poisson process with intensity $\mu(A) = \mathbb{E}(N(1, A))$. $N(t, A)$ is called the Poisson random measure associated with X. For A bounded below, $t > 0$ and $\omega \in \Omega$, define the Poisson integral of x with respect to the random measure as the random finite sum

$$\int_A x N(t, \mathrm{d}x)(\omega) = \sum_{x \in A} x N(t, \{x\})(\omega) = \sum_{0 \leq s \leq t} \Delta X_s(\omega) \mathbf{1}_A(\Delta X_s(\omega)). \tag{4.2}$$

Define $\widetilde{N}$, the compensated Poisson random measure of X, by $\widetilde{N}(t, A) = N(t, A) - \mathbb{E}(N(t, A)) = N(t, A) - t\mu(A)$. The Lévy–Itô decomposition states that any Lévy process X can be expressed as

$$X_t = b_1 t + \sigma B_t + \int_{|x|<1} x \widetilde{N}(t, \mathrm{d}x) + \int_{|x|\geq 1} x N(t, \mathrm{d}x), \tag{4.3}$$

where $b_1 \in \mathbb{R}$ and σB_t is a scaled Brownian motion independent of the Poisson random measure N. Note that the terms $\int_{|x|<1} x \widetilde{N}(t, \mathrm{d}x)$ and $\int_{|x|\geq 1} x N(t, \mathrm{d}x)$ represent small jumps and large jumps of X, respectively. It also follows that X has finite variation if and only if

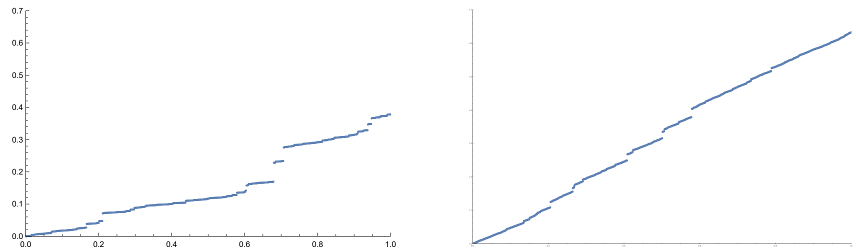

Figure 4.2: Sample paths of a stable subordinator with $\alpha = 0.7$ (left) and $\alpha = 0.9$ (right).

its Lévy–Itô decomposition can be rewritten as

$$X_t = \left(b_1 - \int_{|x|<1} x\nu(\mathrm{d}x)\right) t + \int_{\mathbb{R}\setminus\{0\}} xN(t, \mathrm{d}x). \tag{4.4}$$

An α-stable subordinator D, which is strictly increasing (and hence of finite variation), can be expressed as

$$D_t = \lim_{n\to\infty} \left(c_n t + \int_{x\geq\epsilon_n} xN(t, \mathrm{d}x)\right) = \int_{x>0} xN(t, \mathrm{d}x), \tag{4.5}$$

where $\epsilon_n \downarrow 0$ and $c_n = \mathbb{E}[\int_{0<|x|<\epsilon_n} xN(1, \mathrm{d}x)]$. Hence, we can think of the sample paths of D as approximated by a process that has finitely many jumps, where the jump sizes are bounded below, and between jumps it is linear, see Figure 4.2. On the other hand, the sample paths of D itself can increase only by jumps. This approximation argument comes from the idea of "interlacing," the details of which appear in [1] section 2.6.2.

Define the *inverse* (or the *first hitting time process*) $E = (E_t)_{t\geq 0}$ of a subordinator D by

$$E_t = \inf\{s > 0 : D_s > t\}. \tag{4.6}$$

We refer to E as an *inverse subordinator* for short. With the assumption that $b = 0$ and $\nu(0, \infty) = \infty$, D has strictly increasing paths starting at 0, and hence, its inverse E has continuous, non-decreasing paths starting at 0 which are not constant in a neighborhood of $t = 0$. Indeed, we can think of E as having random long flat periods (corresponding to the large jumps of D) and in between these, E is increasing very quickly (since D has infinitely many small jumps). Note that E is not a Lévy process since it no longer has independent or

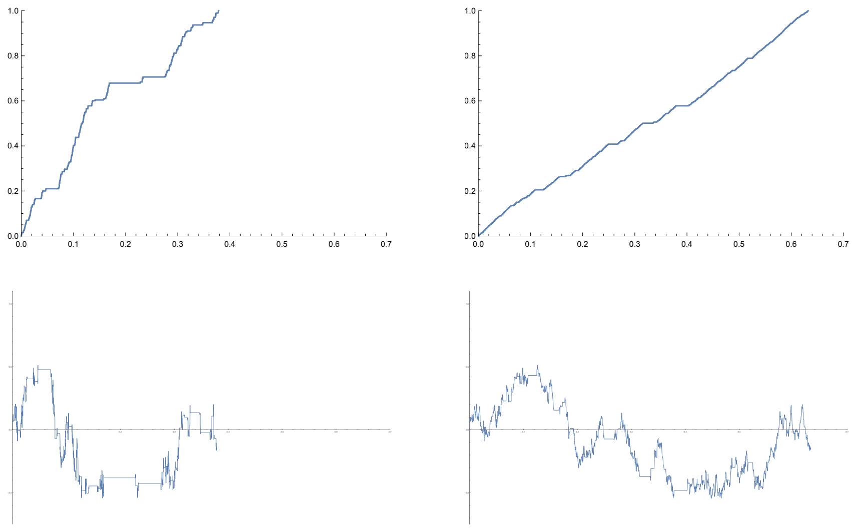

Figure 4.3: Sample paths of an inverse stable subordinator E_t with $\alpha = 0.7$ (top left) and $\alpha = 0.9$ (top right), and the corresponding sample paths of the time-changed Brownian motion B_{E_t} with $\alpha = 0.7$ (bottom left) and $\alpha = 0.9$ (bottom right).

stationary increments (see [32]). On the other hand, E has finite exponential moment; i.e. $\mathbb{E}[e^{cE_t}] < \infty$ for all t (see e.g. [18]).

Now, suppose D is an α-stable subordinator independent of Brownian motion B. Then the self-similarity of D with index $1/\alpha$ implies self-similarity of E with index α (See [32]). Figure 4.3 presents sample paths of the time change E and the corresponding *time-changed Brownian motion* $B \circ E = (B_{E_t})_{t \geq 0}$. The time-changed Brownian motion is non-Markovian and non-Gaussian ([32, 34]). Moreover, the densities $p(t, x)$ of B_{E_t} satisfy the time-fractional order heat equation

$$\frac{\partial^\alpha p(t, x)}{\partial t^\alpha} = \frac{1}{2} \frac{\partial^2 p(t, x)}{\partial x^2},$$

where $\partial^\alpha / \partial t^\alpha$ is the Caputo fractional derivative of order α (see e.g. [13]). The time-changed Brownian motion and stochastic differential equations it drives have been used to model subdiffusions, where particles spread at a slower rate than the usual Brownian particles (see e.g. [35, 33, 30, 15, 22] and references therein). For simulations of inverse subordinators and their associated time-changed processes, see the algorithms presented and discussed in e.g. [12, 18].

4.2 Limiting Hull Behavior

4.2.1 Rescaled Hulls

This section develops results about rescaled hulls for time-changed processes of the form $X \circ E = (X_{E_t})_{t\geq 0}$, where $X = (X_t)_{t\geq 0}$ and $E = (E_t)_{t\geq 0}$ are independent self-similar processes with continuous paths. Note that E is not necessarily non-decreasing and may be allowed to take negative values if the process (X_t) is defined for $t \in \mathbb{R}$; for simplicity of discussion, however, we assume that E is nonnegative. Important examples of the "outer process" X include fractional Brownian motion B^H of Hurst index $H \in (0,1)$, which coincides with Brownian motion when $H = 1/2$. When $H \neq 1/2$, B^H is non-Markovian and its increments are positively correlated if $H > 1/2$ and negatively correlated if $H < 1/2$. On the other hand, an inverse α-stable subordinator can serve as the "inner process" E with self-similarity index $\alpha \in (0,1)$. Since we are allowed to take E to be the identity map, the results presented in this section cover the cases of (untime-changed) self-similar processes as well.

Recall that a process (X_t) is said to be self-similar with index $H > 0$ if $(X_{ct}) \overset{\mathrm{d}}{=} (c^H X_t)$ for all $c > 0$. Note that the self-similarity implies that $X_0 = 0$ a.s. We begin with a simple lemma.

Lemma 4.3. Let K_t be the hull driven by $\lambda(t) = X_{E_t}$, where X is a continuous, self-similar process of index $H > 0$ and E is a nonnegative, continuous, self-similar process of index $\alpha > 0$, independent of X. Then for any $r > 0$, the scaled hulls $(\frac{1}{r}K_{r^2 t})_{t\geq 0}$ and the hulls driven by $(r^{2H\alpha-1}X_{E_t})_{t\geq 0}$ have the same distribution.

Proof. For any fixed $r > 0$, due to the scaling of the Loewner equation, the hulls $\frac{1}{r}K_{r^2 t}$ are driven by $\frac{1}{r}X_{E_{r^2 t}}$. On the other hand, the self-similarities of X and E together with independence imply that (X_{E_t}) is self-similar with index $H\alpha$, so

$$\left(\frac{1}{r}X_{E_{r^2 t}}\right)_{t\geq 0} \overset{\mathrm{d}}{=} \left(\frac{1}{r}(r^2)^{H\alpha}X_{E_t}\right)_{t\geq 0} = (r^{2H\alpha-1}X_{E_t})_{t\geq 0}.$$

Therefore, the hulls generated by $(r^{2H\alpha-1}X_{E_t})_{t\geq 0}$ must have the same distribution as the scaled hulls $(\frac{1}{r}K_{r^2 t})_{t\geq 0}$. $\square$

In [8], Chen and Rohde consider geometric properties of the Loewner hulls that are generated by a symmetric stable process. One of their results (Proposition 3.2 in that paper) shows that rescaling the hulls leads to deterministic sets (and fairly uninteresting sets – either a vertical line segment or the empty set). This is expected because the driving process does not satisfy Brownian scaling, which implies that the Loewner hulls will not satisfy scale-invariance.

The following result, which is analogous to Proposition 3.2 in [8], holds for our time-changed process (X_{E_t}).

Proposition 4.4. Let K_t be the hull driven by X_{E_t}, where X is a continuous, self-similar process of index $H > 0$ and E is a nonnegative, continuous, self-similar process of index $\alpha > 0$, independent of X.

(a) If $2H\alpha < 1$, then as $r \to \infty$, the rescaled hulls $\frac{1}{r}K_{r^2}$ converge to the vertical line segment $[0, 2i]$ (in the Hausdorff metric) in probability. If $2H\alpha > 1$, then the same conclusion holds as $r \to 0$.

(b) Suppose $\mathbb{P}(X_1 = 0) = 0$. If $2H\alpha < 1$, for all $\epsilon > 0$,

$$\lim_{r\to 0} \mathbb{P}\left(\frac{1}{r}K_{r^2} \cap \{y > \epsilon \text{ and } |x| < 1/\epsilon\} \neq \emptyset\right) = 0.$$

If $2H\alpha > 1$, then the same conclusion holds with the limit as $r \to \infty$.

Remark 4.5. *In part (b), we need the constraint $|x| < 1/\epsilon$ on the real part, which can be interpreted as follows. If $2H\alpha < 1$ and r is very small, then $r^{2H\alpha-1}\lambda(t)$ has a very large scaling factor. Near zero, we would not expect to see much hull growth, but far away from zero, we will see the taller parts of the hull that are grown when the driving function is constant.*

The proof utilizes the next lemma, which is entirely deterministic:

Lemma 4.6 ([8] Lemma 3.3)**.** (a) If $\lambda(t) \in [a, b]$ for all $t \in [0, T]$, then $K_T \subset [a, b] \times \mathbb{R}$.

(b) Let $0 < \epsilon < 1$. If $I \subset \mathbb{R}$ is an interval of length $\sqrt{T}$ and $10I$ the concentric interval of size $10\sqrt{T}$, and if

$$\int_0^T \mathbf{1}_{\{\lambda(t)\in 10I\}} \mathrm{d}t \leq \epsilon T, \tag{4.7}$$

then

$$K_T \cap I \times [4\sqrt{\epsilon T}, \infty) = \emptyset. \tag{4.8}$$

Proof of Proposition 4.4. To prove (a), note that by Lemma 4.3, the scaled hull $\frac{1}{r}K_{r^2}$ is equal in distribution to the time $t = 1$ hull generated by $\lambda_r(t) = r^{2H\alpha-1}\lambda(t)$, where $\lambda(t) = X_{E_t}$. Since (X_{E_t}) has continuous paths, $\sup_{0\le t\le 1}|\lambda(t)| < \infty$ a.s. Therefore, if $2H\alpha < 1$, for any $\epsilon > 0$,

$$\lim_{r\to\infty} \mathbb{P}\left(\exists\, t \in [0,1] \text{ such that } |\lambda_r(t)| > \epsilon\right) = \lim_{r\to\infty} \mathbb{P}\left(\sup_{0\le t\le 1} |\lambda(t)| > r^{1-2H\alpha}\epsilon\right) = 0.$$

Hence

$$\lim_{r\to\infty} \mathbb{P}\left(\lambda_r[0,1] \subset [-\epsilon, \epsilon]\right) = 1.$$

By part (a) of Lemma 4.6, this implies that the width of the time 1 hull of $\lambda_r(t)$ is going to 0 in probability, so the same is true for $\frac{1}{r}K_{r^2}$. Since the halfplane capacity of $\frac{1}{r}K_{r^2}$ is 1, we know that it must be converging to the interval $[0, 2i]$ with respect to Hausdorff distance (see the example with $\lambda(t) \equiv c$ in Section 2). The case when $2H\alpha > 1$ is proved in an analogous manner.

To prove (b), let $\epsilon \in (0, 2)$. Once again, by Lemma 4.3, the scaled hull $\frac{1}{r}K_{r^2}$ is equal in distribution to the time $t = 1$ hull generated by $r^{2H\alpha-1}\lambda(t)$ (call this hull $\widetilde{K}_1$). So

$$\mathbb{P}\left(\frac{1}{r}K_{r^2} \cap \{y > \epsilon \text{ and } |x| < 1/\epsilon\} \neq \emptyset\right) = \mathbb{P}\left(\widetilde{K}_1 \cap \{y > \epsilon \text{ and } |x| < 1/\epsilon\} \neq \emptyset\right).$$

Now, if $\widetilde{K}_1 \cap \{y > \epsilon \text{ and } |x| < 1/\epsilon\} \neq \emptyset$, then there exists a (random) interval I of length 1 (not necessarily centered at 0) such that $I \subset (-1/\epsilon, 1/\epsilon)$ and $\widetilde{K}_1 \cap I \times (\epsilon, \infty) \neq \emptyset$. By Lemma 4.6(b) with $T = 1$ and ϵ replaced by $4\sqrt{\epsilon}$, this implies $\int_0^1 \mathbf{1}_{\{r^{2H\alpha-1}\lambda(t)\in 10I\}} \mathrm{d}t > \epsilon^2/16$. Since $\{r^{2H\alpha-1}\lambda(t) \in 10I\} \subset \{|\lambda(t)| \le \delta/\epsilon\}$ with $\delta = 10r^{1-2H\alpha}$, it follows that

$$\mathbb{P}\left(\frac{1}{r}K_{r^2} \cap \{y > \epsilon \text{ and } |x| < 1/\epsilon\} \neq \emptyset\right) \le \mathbb{P}\left(\int_0^1 \mathbf{1}_{\{|\lambda(t)|\le\delta/\epsilon\}}\mathrm{d}t > \frac{\epsilon^2}{16}\right) \tag{4.9}$$

$$\le \frac{16}{\epsilon^2}\int_0^1 \mathbb{P}\left(|\lambda(t)| \le \frac{\delta}{\epsilon}\right) \mathrm{d}t, \tag{4.10}$$

using Markov's inequality. Since $\mathbb{P}(X_1 = 0) = 0$ and the process X is self-similar by assumption, $\mathbb{P}(X_t = 0) = 0$ for each $t > 0$. Moreover, since X and E are independent, $\mathbb{P}(|\lambda(t)| = 0) = \mathbb{P}(X_{E_t} = 0) = \mathbb{E}[\mathbb{P}(X_{E_t} = 0|E_t)] = 0$ for each $t > 0$. Therefore, the above bound tends to 0 upon taking the limit as $\delta \to 0$ (so as $r \to 0$ if $2H\alpha < 1$ or as $r \to \infty$ if $2H\alpha > 1$), which completes the proof. $\square$

Proposition 4.4 immediately yields the following corollary:

Corollary 4.7. Let B be a Brownian motion independent of an inverse α-stable subordinator E. Let K_t be the hull driven by the time-changed Brownian motion B_{E_t}.

(a) As $r \to \infty$, the rescaled hulls $\frac{1}{r}K_{r^2}$ converge to the vertical line segment $[0, 2i]$ (in the Hausdorff metric) in probability.

(b) For all $\epsilon > 0$,

$$\lim_{r\to 0} \mathbb{P}\left(\frac{1}{r}K_{r^2} \cap \{y > \epsilon \text{ and } |x| < 1/\epsilon\} \neq \emptyset\right) = 0.$$

4.2.2 Tangential Hulls

Proposition 4.4(b), in the case that $2H\alpha < 1$, tells us that the initial hull growth stays close to the real line. In some cases, we can describe tangential hull behavior more concretely. In particular, the following deterministic result tells us that if the driving function is moving faster than a square root function at $t = 0$, then the Loewner hull leaves the real line tangentially. The result will be used in Section 4.3.2.

Proposition 4.2. Suppose that $\lambda(0) = 0$ and $\lambda(t) \geq at^r$ where $a > 0$ and $r \in (0, 1/2]$. Then for t small enough, the hull K_t driven by λ is contained in the region $\{x + iy : 0 \leq x, 0 < y < \frac{26}{a}x^{2-2r}\}$.

The proof of this proposition will follow from scaling and the next lemma.

Lemma 4.8. Let $k \geq 26$. Suppose λ is defined on $[0, T]$ for $T \geq 1$ and satisfies that $\lambda(0) = 0$, $\lambda(t) \geq k\sqrt{t}$ for $t \in [0, 1]$, and $\lambda(t) > 3.5$ for $t > 1$. Let K_t be driven by λ. Then $K_t \cap ([1, 2] \times [26/k, \infty)) = \emptyset$ for all t.

Proof. For $t \in [0,1]$, the amount of time that λ spends in $[-3.5, 6.5]$ is at most $(6.5/k)^2$. Therefore, applying Lemma 4.6(b) with $\epsilon = (6.5/k)^2$, we conclude that K_1 does not intersect $[1,2] \times [26/k, \infty)$. Let $z \in [1,2] \times [26/k, \infty)$. The proof of Lemma 4.6(b) further gives that $\mathrm{Re}(g_1(z)) \leq 3.5$. Note that for $t \geq 1$, $\lambda(t) > 3.5$. Thus applying Lemma 4.6(a) to λ on $[1, \infty)$, we see that $g_1(z)$ cannot be part of the hull $g_1(K_t \setminus K_1)$. Thus z is not in the hull K_t for any t. □

Proof of Proposition 4.2. Let $\lambda_n(t) := 2^n \lambda(2^{-2n} t)$ generate the hull K_t^n, and note that $\lambda_n(t) \geq a 2^{n(1-2r)} t^r$. Choose N so that $a 2^{N(1-2r)} \geq 26$ and λ_N is defined on $[0,1]$. For $n \geq N$, Lemma 4.8 applied to $\lambda_n(t)$ implies K_t^n does not intersect $[1,2] \times [(26/a) \cdot 2^{-n(1-2r)}, \infty)$. Thus by scaling, K_t does not intersect $[2^{-n}, 2^{-n+1}] \times [(26/a) \cdot 2^{-n(2-2r)}, \infty)$ for $n \geq N$. Therefore for small t, the hull lies below the curve $y = (26/a)\, x^{2-2r}$. □

4.3 Hulls Generated with Time Change

In this section, we take a look at the geometric behavior of a hull that has been generated by a time-changed driving function, where the random time change is given by an inverse subordinator. In particular, we will consider two cases for the driving function, a time-changed deterministic function and a time-changed Brownian motion; and we ask whether or not the generated hulls are simple curves. Theorem 4.9 gives conditions for determining simpleness or non-simpleness. This result is applied to the time-changed Brownian case to show that the generated hulls are almost surely non-simple curves. We end by discussing some examples of time-changed deterministic functions.

4.3.1 Criteria for Simple and Non-simple Hulls

The results to be presented in this section are applicable to a large class of random time changes, including the inverses of stable and tempered stable subordinators. To discuss them, we first introduce the notion of regular variation. A function $\ell : (0,\infty) \to (0,\infty)$ is said to be *slowly varying at* ∞ if for any $c > 0$,

$$\lim_{u\to\infty} \frac{\ell(cu)}{\ell(u)} = 1.$$

Examples of slowly varying functions include $\ell(u) = (\log u)^\eta$ for any $\eta \in \mathbb{R}$. A function $f : (0,\infty) \to (0,\infty)$ is said to be *regularly varying at* ∞ *with index* $\alpha > 0$ if for any $c > 0$,

$$\lim_{u\to\infty} \frac{f(cu)}{f(u)} = c^\alpha.$$

Every regularly varying function f with index $\alpha > 0$ is represented as $f(u) = u^\alpha \ell(u)$ with ℓ being a slowly varying function. For a general account of this topic, consult [7].

Recall that the Laplace transform of a subordinator $D = (D_t)_{t\geq 0}$ with Lévy measure ν and zero drift is given by

$$\mathbb{E}[e^{-uD_t}] = e^{-t\psi(u)}, \quad \text{where} \quad \psi(u) = \int_0^\infty (1 - e^{-ux})\nu(\mathrm{d}x).$$

As usual, we assume that sample paths of D_t start at 0 and are right-continuous with left limits and that $\nu(0,\infty) = \infty$ (so that the inverse E_t is continuous). In this section, we further assume that the Laplace exponent ψ is regularly varying at ∞ with index $\alpha \in (0,1)$. This includes the two important examples of a subordinator:

- a stable subordinator with index $\alpha \in (0,1)$, where $\psi(u) = u^\alpha$, and
- a tempered stable subordinator with index $\alpha \in (0,1)$ and tempering factor $\theta > 0$, where $\psi(u) = (u+\theta)^\alpha - \theta^\alpha$.

We now state the main theorem of this section. Note that the process X in this theorem can be deterministic.

Theorem 4.9. Let E be the inverse of a subordinator D whose Lévy measure is infinite and Laplace exponent ψ is regularly varying at ∞ with index $\alpha \in (0,1)$. Let X be a stochastic process with continuous paths.

(a) If X is a.s. locally β-Hölder with $\beta > \frac{1}{2\alpha}$, then a.s. $\lambda(t) = X_{E_t}$ generates a simple curve.

(b) If there exist random variables $\tau, \epsilon, c > 0$ and $0 < \beta < \frac{1}{2\alpha}$ so that τ is independent of the subordinator D and a.s. $|X_\tau - X_t| \geq c(\tau - t)^\beta$ for all $t \in (\tau - \epsilon, \tau)$, then a.s. $\lambda(t) = X_{E_t}$ does not generate a simple curve.

The proof relies on previously known deterministic results (Theorems 2.2 and 2.4) and the following two lemmas which give control on the local behavior of the time change. The main idea for proving the second statement is to compare λ with an appropriate square root function that is known to generate a non-simple curve. This is illustrated in Figure 4.4 in the case when X_t is the deterministic function $\sqrt{1-t}$.

Lemma 4.10. Let D be a subordinator whose Lévy measure is infinite and Laplace exponent ψ is regularly varying at ∞ with index $\alpha \in (0,1)$. Then for any $\gamma \in [1, 1/\alpha)$, $\lim_{t\downarrow 0} D_t/t^\gamma = 0$ almost surely.

Proof. Fix $\gamma \in [1, 1/\alpha)$ and note that the function $h(t)/t$, where $h(t) = 2t^\gamma$, is positive, continuous, and non-decreasing on $(0,\infty)$. By Proposition 47.17 of [46] (originally by Fristedt [11]), the desired result follows once we establish $\int_0 \nu[h(t),\infty)\,\mathrm{d}t < \infty$. However, due to the relation (see the discussion following Chapter III, Proposition 1 in [6])

$$\psi(1/x) \sim \Gamma(1-\alpha)\nu(x,\infty) \quad \text{as } x \downarrow 0,$$

it suffices to prove that $\int_0 \psi(1/t^\gamma)\mathrm{d}t < \infty$. Upon writing $\psi(u)$ as $\psi(u) = u^\alpha \ell(u)$ using a slowly varying function ℓ, we obtain

$$\int_0 \psi\Big(\frac{1}{t^\gamma}\Big)\,\mathrm{d}t = \frac{1}{\gamma}\int^\infty x^{\alpha-1-1/\gamma}\ell(x)\,\mathrm{d}x.$$

Since $\alpha - 1 - 1/\gamma < -1$, the latter integral converges due to Proposition 1.5.10 of [7]. $\square$

Lemma 4.11. Let D be a subordinator whose Lévy measure is infinite and Laplace exponent ψ is regularly varying at ∞ with index $\alpha \in (0,1)$. Then the inverse E of D is a.s. locally weak α-Hölder.

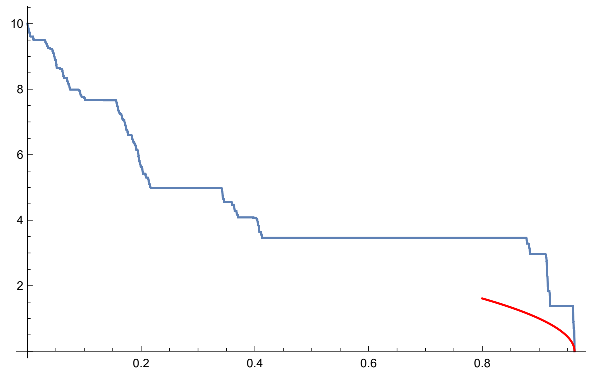

Figure 4.4: The driving function $\sqrt{1-E_t}$ (blue) is decreasing faster than $4\sqrt{T-t}$ (red) near T.

Proof. By Chapter III, Lemma 17 in [6], an inverse subordinator E_t is a.s. locally Hölder with any exponent $\rho \in (0, \underline{\mathrm{ind}}(\psi))$, where $\underline{\mathrm{ind}}(\psi)$ is the *lower index* of ψ defined as

$$\underline{\mathrm{ind}}(\psi) = \sup\left\{\rho > 0 : \lim_{u\to\infty} \frac{\psi(u)}{u^\rho} = \infty\right\}.$$

Writing $\psi(u)$ as $\psi(u) = u^\alpha \ell(u)$ and applying Proposition 1.3.6(v) of [7] yields

$$\lim_{u\to\infty} \frac{\psi(u)}{u^\rho} = \lim_{u\to\infty} u^{\alpha-\rho}\ell(u) = \begin{cases} 0 & \text{if } \rho > \alpha, \\ \infty & \text{if } 0 < \rho < \alpha, \end{cases}$$

which implies $\underline{\mathrm{ind}}(\psi) = \alpha$, thereby completing the proof. □

Proof of Theorem 4.9. To prove (a), assume that X is a.s. locally β-Hölder with $\beta > \frac{1}{2\alpha}$. Since E_t is a.s. locally weak α-Hölder due to Lemma 4.11, it follows that $\lambda(t) = X_{E_t}$ is a.s. locally weak $\alpha\beta$-Hölder, where $\alpha\beta > 1/2$. Thus, for almost every $\omega \in \Omega$, we can partition the time interval $[0, T]$ into a finite number of intervals $J_i := [t_{i-1}, t_i]$, for $i = 1, 2, \cdots, n$, so that on J_i, λ is Lip(1/2) with $||\lambda||_{1/2} < 4$. Therefore the hull $\hat{K}_i$ generated by λ restricted to J_i is a simple curve by Theorem 2.2. The concatenation property allows us to put these pieces together to conclude that

$$K_T = \hat{K}_1 \cup g_{t_1}^{-1}(\hat{K}_2) \cup \cdots \cup g_{t_{n-1}}^{-1}(\hat{K}_n)$$

is a simple curve. Since this holds for almost every $\omega \in \Omega$, the desired result follows.

To prove (b), assume $\tau, \epsilon, c > 0$ and $0 < \beta < \frac{1}{2\alpha}$ so that a.s. $|X_\tau - X_t| \geq c(\tau - t)^\beta$ for all $t \in (\tau - \epsilon, \tau)$. Set $T = D_{\tau-}$, where D_{t-} denotes the left limit of the path at $t > 0$ and $D_{0-} := D_0 = 0$. In other words, the random time T is the first time that $E_t = \tau$. Note that given τ, $(D_{t-})_{t\in[0,\tau]}$ is a subordinator having the same distribution as $(D_t)_{t\in[0,\tau]}$, and therefore, so is the time-reversed process $(D_{\tau-} - D_{(\tau-t)-})_{t\in[0,\tau]}$. Since D and τ are assumed independent, by Lemma 4.10, for any fixed $\gamma \in [1, 1/\alpha)$,

$$\mathbb{P}\left(\lim_{t\downarrow 0} \frac{D_{\tau-} - D_{(\tau-t)-}}{t^\gamma} = 0\right) = \mathbb{E}\left[\mathbb{P}\left(\lim_{t\downarrow 0} \frac{D_{\tau-} - D_{(\tau-t)-}}{t^\gamma} = 0 \;\middle|\; \tau\right)\right] \tag{4.11}$$

$$= \mathbb{E}\left[\mathbb{P}\left(\lim_{t\downarrow 0} \frac{D_t}{t^\gamma} = 0 \;\middle|\; \tau\right)\right] = 1. \tag{4.12}$$

Hence, for any $m > 0$, almost surely, there exists $\delta \in (0, \epsilon)$ such that

$$D_{\tau-} - D_{(\tau-t)-} \leq m t^\gamma \quad \text{for all} \quad t \in [0, \delta].$$

For this particular path, fix $t \in [D_{\tau-\delta}, T)$ and set $r = E_t$, which satisfies $r \in [\tau - \delta, \tau]$ and $t \in [D_{r-}, D_r)$. Then the above condition yields

$$T - t \leq D_{\tau-} - D_{r-} \leq m(\tau - r)^\gamma = m(E_T - E_t)^\gamma.$$

Therefore,

$$|\lambda(T) - \lambda(t)| \geq c(E_T - E_t)^\beta \geq \frac{c}{m^{\beta/\gamma}}(T - t)^{\beta/\gamma} \quad \text{for all} \quad t \in [D_{\tau-\delta}, T).$$

Now, since $\gamma \in [1, 1/\alpha)$ and $m > 0$ are arbitrary, we choose γ so that $\beta/\gamma = 1/2$, and we choose m satisfying $c/\sqrt{m} \geq 4$. An application of Theorem 2.4 implies that almost surely $\lambda(t)$ does not generate a simple curve. $\square$

We now turn to the Brownian case:

Theorem 4.1. Let E be the inverse of a subordinator D whose Lévy measure is infinite and Laplace exponent ψ is regularly varying at ∞ with index $\alpha \in (0, 1)$. Let B be a Brownian

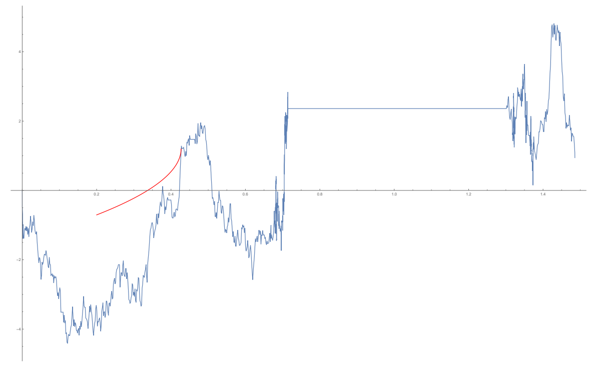

Figure 4.5: Time-changed Brownian motion sample path (blue) moving faster than $4\sqrt{T-t}+B_{E_T}$ (red) near T.

motion independent of D. Then almost surely, the time-changed Brownian motion process $\lambda(t) = B_{E_t}$ does not generate a simple curve.

In order to apply Theorem 4.9, we wish to control the growth of the time-changed Brownian motion with an appropriate square root function, as illustrated in Figure 4.5. We obtain this control through the relationship between Brownian motion and 3-dimensional Bessel processes, as given in the following two results. Recall that we say Y is a d-dimensional Bessel process if it satisfies $\mathrm{d}Y_t = \frac{a}{Y_t}\mathrm{d}t + \mathrm{d}B_t$ for $a = \frac{d-1}{2}$. For more details about Bessel processes, see [24] section 1.10. For a continuous real-valued process X and $0 < c < \infty$, define

$$\tau_c^X = \inf\{t > 0 : X_t = c\} \text{ and } \sigma_c^X = \sup\{t > 0 : X_t = c\}. \tag{4.13}$$

Proposition 4.12 ([50])**.** Let B be a Brownian motion starting at 0, Y a 3-dimensional Bessel process starting at 0, and let $0 < c < \infty$. Let $\tau_c = \tau_c^B$. Then the two processes

$$\{c - B_{\tau_c - t} : 0 \le t \le \tau_c\} \text{ and } \{Y_t : 0 \le t \le \sigma_c^Y\} \tag{4.14}$$

are identical in distribution.

Theorem 4.13 ([49])**.** Let $\varphi(t) \downarrow 0$ when $t \downarrow 0$ and let Y be a d-dimensional Bessel process. Then for $d \ge 2$,

$$\mathbb{P}(Y_t < \varphi(t)\sqrt{t} \text{ i.o. } t \downarrow 0) = 1 \text{ or } 0 \tag{4.15}$$

according as

$$\int_0^\infty \varphi(t)^{d-2}\frac{\mathrm{d}t}{t} = \infty \text{ or } < \infty \quad (d > 2); \tag{4.16}$$

$$\int_0^\infty \frac{1}{|\log \varphi(t)|}\frac{\mathrm{d}t}{t} = \infty \text{ or } < \infty \quad (d = 2). \tag{4.17}$$

In our proof of Theorem 4.1, we will use $\varphi(t) = (\log \frac{1}{t})^{-\eta}$ for $\eta > 0$ and $d = 3$. Then $\varphi(t) \downarrow 0$ when $t \downarrow 0$. Also, $\int_0^\infty \varphi(t)\frac{\mathrm{d}t}{t} = \infty$ for $\eta \leq 1$ and $\int_0^\infty \varphi(t)\frac{\mathrm{d}t}{t} < \infty$ for $\eta > 1$.

Proof of Theorem 4.1. Let $0 < c < \infty$ and $\tau_c = \tau_c^B$. By Proposition 4.12, $(c - B_{\tau_c - t})_{0 \leq t \leq \tau_c}$ has the same distribution as $(Y_t)_{0 \leq t \leq \sigma_c}$ for a 3-dimensional Bessel process Y where $\sigma_c = \sigma_c^Y$. By Theorem 4.13 and the discussion before this theorem, if $\eta > 1$

$$\mathbb{P}\left(Y_t < \frac{\sqrt{t}}{(\log \frac{1}{t})^\eta} \text{ i.o. } t \downarrow 0\right) = 0. \tag{4.18}$$

As such, for $a \in (\frac{1}{2}, \frac{1}{2\alpha})$ and some $k > 0$, almost surely there exists $\epsilon > 0$ so that $Y_t \geq kt^a$ for $t \in [0, \epsilon]$. Therefore, almost surely there exists $\epsilon > 0$ with $B_{\tau_c} - B_t \geq k(\tau_c - t)^a$ for $t \in [\tau_c - \epsilon, \tau_c]$. Since B_t is assumed independent of D_t, the random time $\tau_c = \tau_c^B$ is also independent of D_t. An application of Theorem 4.9(b) completes the proof. □

4.3.2 Examples of Time-Changed Deterministic Functions

In this section we consider two deterministic functions ϕ whose Loewner hulls have previously been analyzed. To highlight the effect of the time change on driving functions, we look at the behavior of the hulls driven by $\lambda(t) = \phi(E_t)$, where E is an inverse α-stable subordinator.

Example 4.14. The Loewner hulls driven by $\phi(t) = c\sqrt{t}$ are line-segments starting from 0, with an angle determined by the constant c. See [19]. In particular, the hulls are always simple curves. With the driving function $\lambda(t) = c\sqrt{E_t}$, we see different hull behavior in two regimes, when $\alpha > 1/2$ and when $\alpha < 1/2$. See Figure 4.6.

Suppose first that $\alpha > 1/2$. Let K_t be the hull generated by λ, let $\epsilon > 0$, and let τ_ϵ be the first time that $E_t = \epsilon$. We first consider λ restricted to the interval $[\tau_\epsilon, \infty)$ which generates the hull $g_{\tau_\epsilon}(K_t \setminus K_{\tau_\epsilon})$. Since ϕ is C^1 on $[\epsilon, \infty)$, Theorem 4.9(a) implies that $g_{\tau_\epsilon}(K_t \setminus K_{\tau_\epsilon})$ is a simple curve. Thus $K_t \setminus K_{\tau_\epsilon}$ must be a simple curve for $t > \tau_\epsilon$, and so we can define $\gamma(t)$,

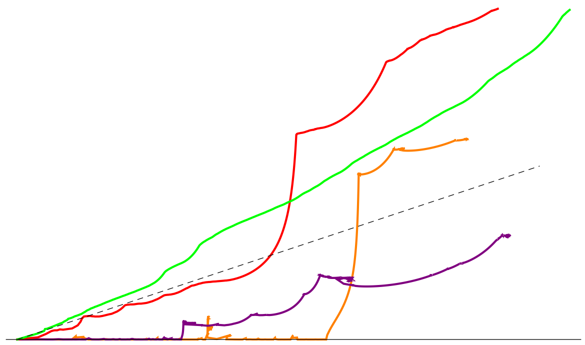

Figure 4.6: Sample hulls generated by $\sqrt{E_t}$, where E_t is an inverse α-stable subordinator ($\alpha = 0.9$ in green, $\alpha = 0.7$ in red, $\alpha = 0.4$ in purple and $\alpha = 0.3$ in orange). The black dashed line represents a hull generated by $\sqrt{t}$ (without a time change).

for $t \in (0, \infty)$, so that $K_b \setminus K_a = \gamma[a, b]$. Further, using the continuity of λ we can argue that $\gamma(t) \to 0$ as $t \to 0^+$. Thus almost surely γ is a simple curve defined on $[0, \infty)$, and $K_t = \gamma[0, t]$. Proposition 4.2 and Lemma 4.10 show that γ leaves the real line tangentially.

Suppose next that $\alpha < 1/2$. Arguing as above shows that the hull must still leave the real line tangentially. However the hull is no longer a simple curve. In particular, we can apply Theorem 4.9(b) with $\beta = 1$ for any fixed time $\tau > 0$. This shows that the hulls generated by λ are far from being simple curves, as they are non-simple at the first time that E_t reaches height τ. Since this is true for all $\tau > 0$ and since E_t is almost surely not constant in a neighborhood of 0 (otherwise D_0 would be positive, which contradicts the assumption $D_0 = 0$), we find that almost surely K_t is non-simple for all $t > 0$.

Example 4.15. For our last example, we consider the case when $\lambda(t) = c\,W(E_t)$, where $W(t) = \sum_{n=0}^{\infty} 2^{-n/2} \cos(2^n t)$ is the Weierstrass function. Since this function is continuous but nowhere differentiable, it serves as a deterministic analogue of Brownian motion. Similar to SLE, the Loewner hulls driven by $c\,W$, studied in [26], have a phase transition. In particular for c small enough $c\,W$ generates simple curves, but for c large enough the hulls are not simple. In [26], it is also shown that near a local maximum W_t grows faster than an appropriately scaled square root curve. Therefore, Theorem 4.9(b) implies that $c\,W(E_t)$ does not generate a simple curve. Since these local maximums are dense, we can further conclude that almost surely the Loewner hull K_t is non-simple for all $t > 0$. See Figure 4.7.

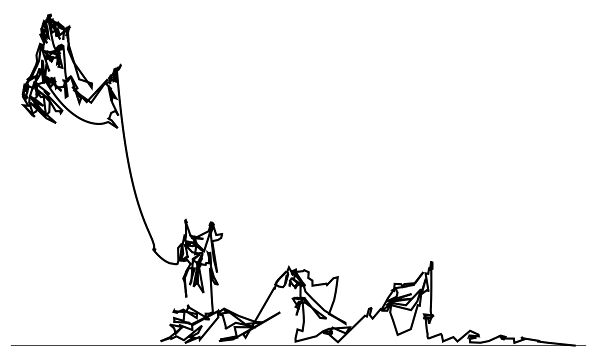

Figure 4.7: Sample hull generated by $W(E_t)$ where E_t is an inverse 0.7-stable subordinator.

Chapter 5

Constructing Spacefilling Loewner Curves

Let $\mathscr{S}$ denote the set of Lipschitz-1/2 functions that generate spacefilling curves. The purpose of this section is to discuss our work towards finding the constant κ so that if $\lambda \in \mathscr{S}$, then the Lipschitz-1/2 norm of λ is at least κ. Our idea for constructing a spacefilling curve is motivated by the Peano spacefilling curve construction. We want to build a family of Lipschitz-1/2 driving functions, with norm controllable by a parameter c, that generate spacefilling curves (for large enough c).

We begin this chapter by discussing the construction of a Peano spacefilling curve. This is followed by the creation of our candidate spacefilling curves and simulations of the candidate hulls. Next we show some general results about Lipschitz-1/2 functions. This is followed by the construction of our candidate driving function and some of its properties. After this we build two other families of driving functions that we will use to numerically investigate the behavior of the candidate hulls. This chapter concludes with the numerical data.

This entire project is built on work that Bridget Jones did during her time as an undergraduate at the University of Tennessee. In particular, Bridget proved Corollary 5.6, which is the entire motivation for Proposition 5.5. She also studied the Lipschitz-1/2 norm of our driving function family numerically.

Note 5.1. For this chapter if $\varphi : [0, T] \to \mathbb{R}$, then $\|\varphi\|$ denotes its Lipschitz-1/2 norm.

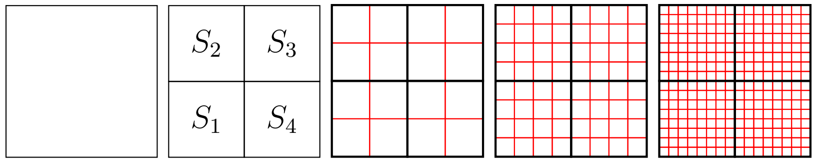

Figure 5.1: Division of the unit square

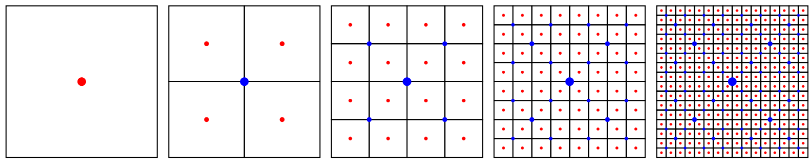

Figure 5.2: Centers of new iteration squares (red) and all prior centers (blue)

5.1 Peano Spacefilling Curve Construction

Peano [39] crafted the first known example of a spacefilling curve and the famous Hilbert curve [16] was created the next year. Here, we will construct a Peano curve which is a map $f : [0,1] \to [0,1] \times [0,1]$ with $f([0,1]) = [0,1] \times [0,1]$. The map f will be a limit of functions f_n which we explicitly construct. We will go through its construction to motivate our construction of the candidate spacefilling curves generated from the Loewner equation.

We begin by breaking up the unit square into smaller squares as shown in Figure 5.1. Starting with the unit square, we divide it up into four equal disjoint squares. Denote these squares starting at 0 and moving clockwise as S_1, S_2, S_3, and S_4. Next we shrink this division of the unit square by 2 and place it in each S_i, which divides the unit square into 16 squares. We then repeat this processes so that the nth iteration divides the unit square into 4^n squares. Note that the set of centers at any iteration is rotation invariant.

With the processes of subdividing the unit square in hand, we turn to the construction of the curve itself. We want to create a sequence of functions so that the nth function in the sequence travels through the centers of each of the 4^n subsquares (e.g. f_0 will travel through

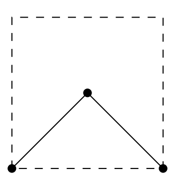

Figure 5.3: Graph of f_0

center of unit square, f_1 will travel through the center of unit square and the four squares in the first subdivision, etc.) which are shown in Figure 5.2. We will start with f_0, which we want to start at 0, hit the center of the square $(\frac{1}{2}+\frac{i}{2})$ at time $\frac{1}{2}$, and end at 1. We will do this by fixing $f_0(0) = 0$, $f_0(\frac{1}{2}) = \frac{1}{2}+\frac{i}{2}$, and $f_0(1) = 1$ and then fitting a line between these points. The graph of f_0 is shown in Figure 5.3 Now, the construction of f_1 from f_0 will satisfy the following:

- $f_1(t) \in S_i$ for $t \in [\frac{i-1}{4}, \frac{i}{4}]$
- $f_1(\frac{2i-1}{8})$ is at the center of S_i
- $f_1|_{[\frac{i-1}{4},\frac{i}{4}]}$ is a scaled, shifted, and rotated version of $f_0(4t-i)$

We want this construction to be recursive, so we will construct f_{n+1} from f_n for $n \in \mathbb{N}$. For $n \in \mathbb{N}$, we shrink f_n by 2 and construct f_{n+1} with the following four steps:

1. In S_1, rotate $\frac{1}{2}f_n(4t)$ by 90°, then flip it across the x-axis and rotate it 180°.
2. In S_2, shift $\frac{1}{2}f_n(4t-1)$ up by $\frac{1}{2}$.
3. In S_3, shift $\frac{1}{2}f_n(4t-2)$ up and to the right by $\frac{1}{2}$.
4. In S_4, rotate $\frac{1}{2}f_n(4t-3)$ by 90°, then flip it across the x-axis and shift it up by $\frac{1}{2}$ and to the right by 1.

The construction of f_1 from $\frac{1}{2}f_0$ is shown in Figure 5.4 and a few iterations of the sequence are shown in Figure 5.5. We now have our sequence (f_n).

We now outline why f is spacefilling; for details see [16] or [37] (specifically pages 272-274). For $t \in [0,1]$, define $f(t)$ as the limit of $(f_n(t))_n$. Since the domain of f is compact, we have that f_n converges to f uniformly. Further since f_n is continuous, so is f. Since f_n travels through the center of each square of the 4^n squares (and so does any subsequent f_m), f travels through the center of each of the squares of every iteration. Let C be the set of centers of the squares of every iteration, which means $\overline{C} = [0,1]\times[0,1]$. Since $[0,1]$ is compact and f is continuous,

$$\overline{C} = [0,1]\times[0,1] \subseteq f([0,1]) \subseteq [0,1]\times[0,1]. \tag{5.1}$$

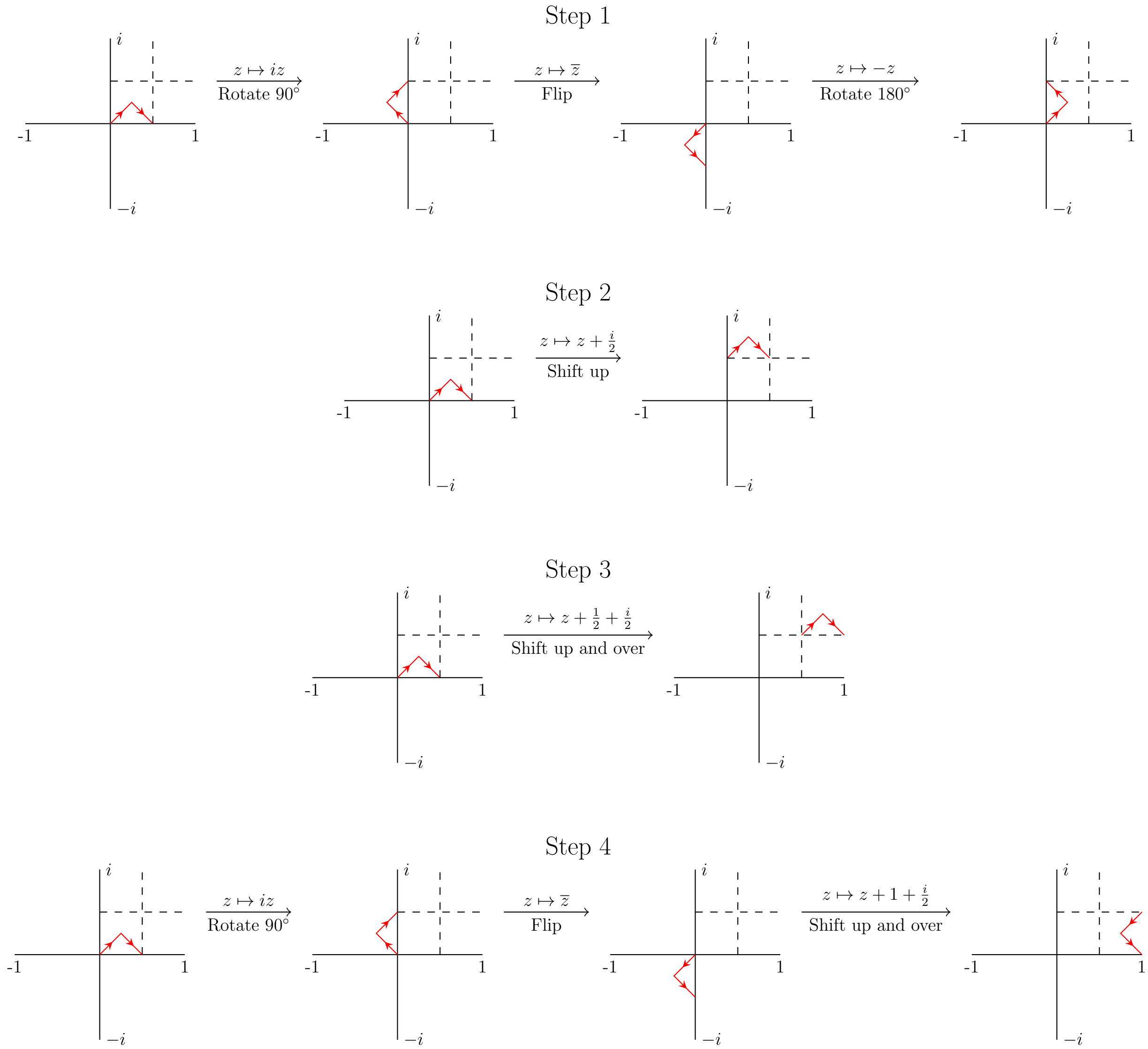

Figure 5.4: Steps for Constructing Iterations of Peano Spacefilling Curve

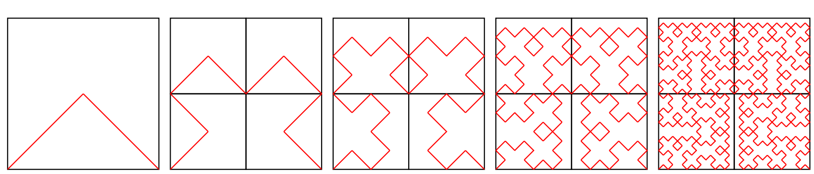

Figure 5.5: First five functions in Peano curve limit

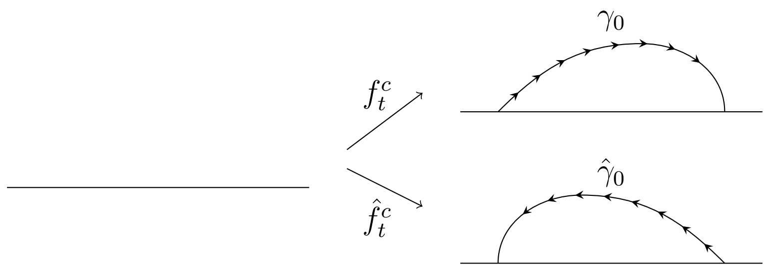

Figure 5.6: Graphs of γ_0 and $\hat{\gamma}_0$

This shows that f is spacefilling.

We now summarize this construction process:

- Start with a region and a continuous curve in that region
- Subdivide the region
- Modify the curve so that it intersects each subdivision and is continuous
- Repeat this recursively

The limit curve will be continuous and travel through these ever shrinking subdivisions, which means it will fill the area. We will attempt to do the same thing, but we will add an extra layer of conformal behavior governed by the Loewner equation.

5.2 Simulation of Candidate Hulls

For $c \geq 4$, $c\sqrt{1-t}$ generates a curve at time 1 that intersects the real line in two places. We want to take this curve and divide it up (as in the typical construction of spacefilling curves), but we want our next curve to be generated by a driving function that is similar to our original one. Similar in this case will mean that our new driving function will be scaled and shifted concatenations of our original driving function. Let f_t^c be the solution to the upward Loewner equation driven by $c\sqrt{t}$ with trace γ_0. Define $\hat{f}_t^c$ to be the solution upward Loewner equation driven by $c - c\sqrt{t}$ with trace $\hat{\gamma}_0$. The two traces are reflections of each other (see Figure 5.6). An example of this type of the construction is as follows (see Figure 5.7 for visualization of this process):

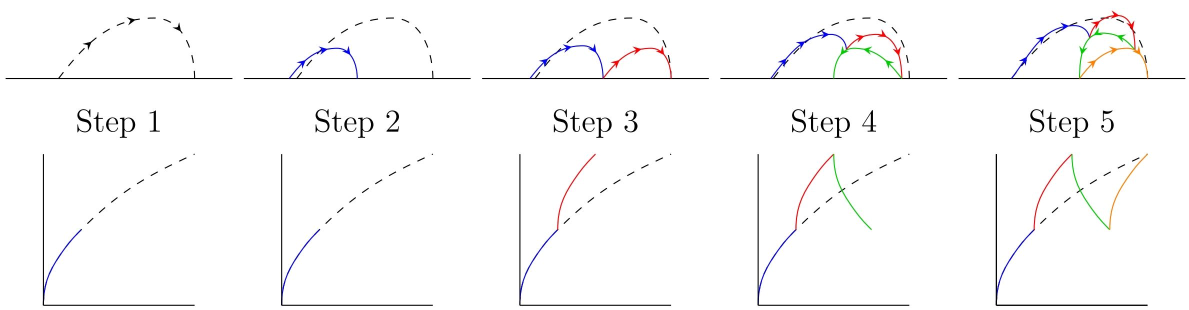

Figure 5.7: Spacefilling construction (top row) and corresponding driving function (bottom row)

1. Let γ_0 be the trace generated by f_t^c.

2. Let $\gamma_1 = \frac{1}{2}\gamma_0$.

3. Apply $\frac{1}{2}f_t^c + \frac{c}{2}$ to γ_1 then add $\frac{1}{2}\gamma_0 + \frac{c}{2}$ to γ_1.

4. Apply $\frac{1}{2}\hat{f}_t^c + \frac{c}{2}$ to γ_1 then add $\frac{1}{2}\hat{\gamma}_0 + \frac{c}{2}$ to γ_1.

5. Apply $\frac{1}{2}f_t^c + \frac{c}{2}$ to γ_1 then add $\frac{1}{2}\gamma_0 + \frac{c}{2}$ to γ_1.

We will repeat this in order to get each iteration after this. The shifting in the construction is so that one curve ends where the next begins. A key observation of this construction is that the half-plane capacity of the hull in step 5 has half-plane capacity 1 and the half-plane capacity of the hull in step 2 (when scaled appropriately) is 1 divided by the square of the scale. In this particular construction, we scale the hull in step 1 by $\frac{1}{2}$, which means the half-plane capacity of the hull in step 2 is $\frac{1}{4}$. We can do this for any $c \geq 4$, so this construction gives us a family of curves parameterized by c.

The curve in step 5 is four conformal copies of the curve in step 1. The hull in step 5 is also not too different than the hull in step 1. One major difference between this curve and the Hilbert spacefilling curve is that we did not force our curves to travel through particular points in the step 1 hull. Our curve still divides the hull into different pieces like the Hilbert spacefilling curve. This gives us hope that recursively repeating this process will limit into a spacefilling curve.

We now examine simulations of these curves for particular c values. A word of warning: these simulations are not exactly what the hulls look like, they are just approximations. For

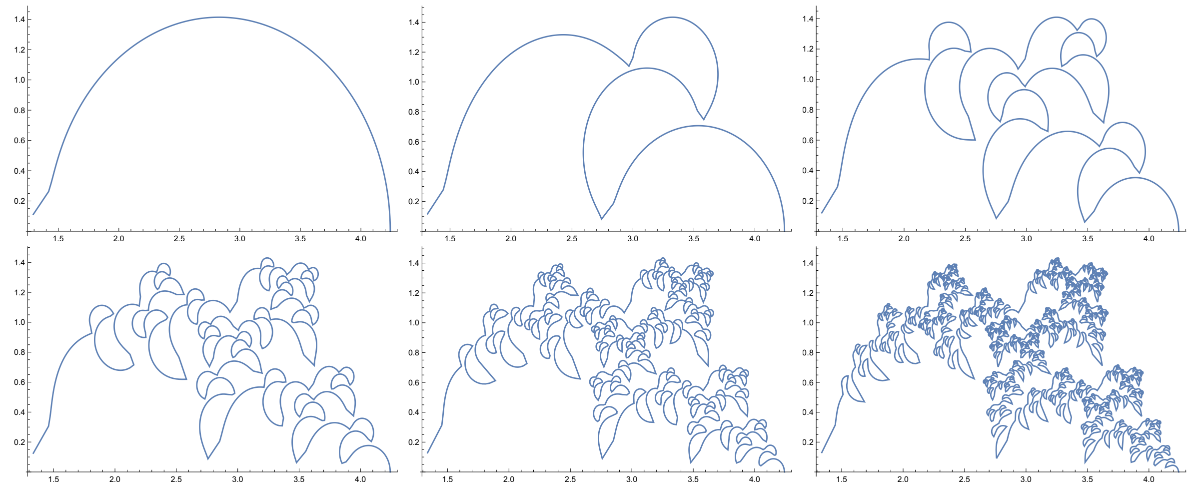

Figure 5.8: Graphs of Hulls for $c = 3\sqrt{2}$

instance, when the curve travels under itself, the simulations clearly show a gap between the steps 2 and 3 curves and the step 4 curve. However, by construction these curves do intersect, since the curves from steps 2 and 3 touch the real line which is moved up to make the curve in step 4. Another instance of the simulations not accurately conveying reality is the behavior of the hull along the real line. The entire hull is moving up in the simulations, but in reality the hull stays on the real line. Furthermore, the more times we iterate this, the more sample points we need in order for our simulations to appear accurate. For example, if 100 sample points make the original curve appear accurate, then at least 400 sample points would be needed to make the first iteration appear accurate. This makes good simulations expensive.

For $c = 3\sqrt{2}$, the first six iterations are in Figure 5.8. Upon initial inspection, it appears that with each iteration the curve roughly divides up the previous iteration of the curve. For example, moving from the iteration with four parts to the iteration with sixteen parts, each old piece has four new pieces inside of it. This seems to indicate that this sequence of curves obeys the general idea of constructing spacefilling curves. When further inspected, it appears that there is a large empty space forming in the bottom left. This might not seem like a problem at first because the rest of the curve appears to divide up any other empty space. However, if this empty space is in one part of the hull, it must appear in every part of the hull because of the recursive nature of this construction. We formally state this result

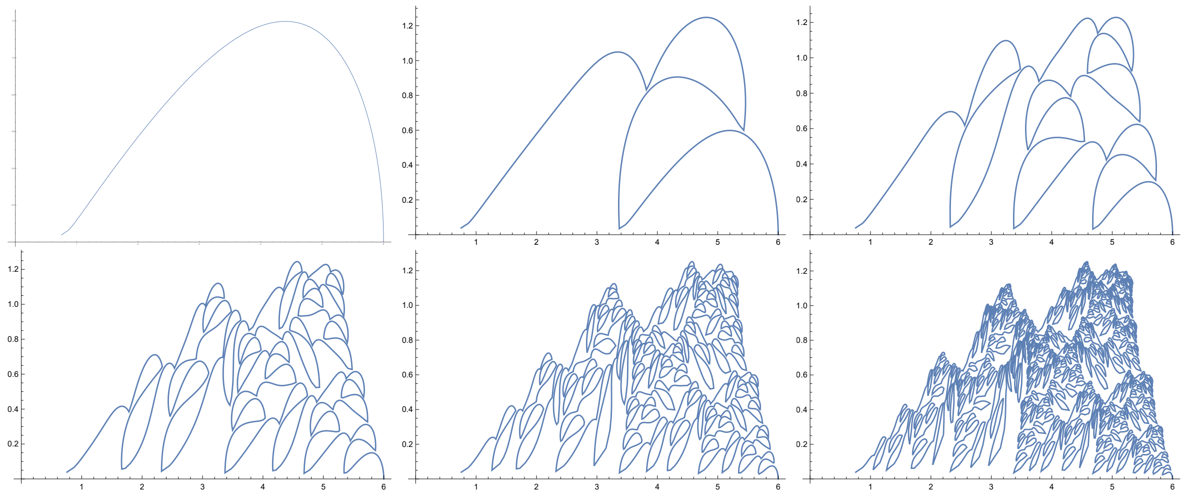

Figure 5.9: Graphs of Hulls for $c = 6$

in Proposition 5.2. This indicates that the limit curve for $c = 3\sqrt{2}$ is not spacefilling. All hope is not yet lost for our construction though.

For $c = 6$, the first six iterations are in Figure 5.9. Just as in the $c = 3\sqrt{2}$ case, any iteration of the curve appears to appropriately divide the previous iteration. Also, the large empty space that appeared in $c = 3\sqrt{2}$ does not seem to appear in this case. However, there does appear to be significant stretching of the curve above $x = 3$. There might also be a long (but thin) bubble of empty space forming in this case as well. The stretching poses a potential problem because it might prevent the limiting hull from being a continuous curve. Since there is significant change in behavior from $3\sqrt{2}$ to 6, it is still posiible that we will generate a spacefilling curve for large enough values of c.

Our last simulated hull is when $c = 16$. As in the previous cases, each iteration appropriately divides the iteration before. Moreover, the division seems to be somewhat uniform. On the other hand, there is significant stretching above $x = 8$ (i.e. at $x = \frac{c}{2}$, which is the same location as in the $c = 6$ case). This stretching is due to the fact that there are three pieces mapping up starting around $x = 8$. Since the first piece ends at $x = 8$, the curve gets pulled up and stretched there since there is not much movement before $x = 8$. The upshot is that all of the potential problems seem to be getting better as c increases.

In conclusion, from these three simulations the limit curves appear to either not be spacefilling (due to empty space) or the limit curves are not continuous (due to stretching).

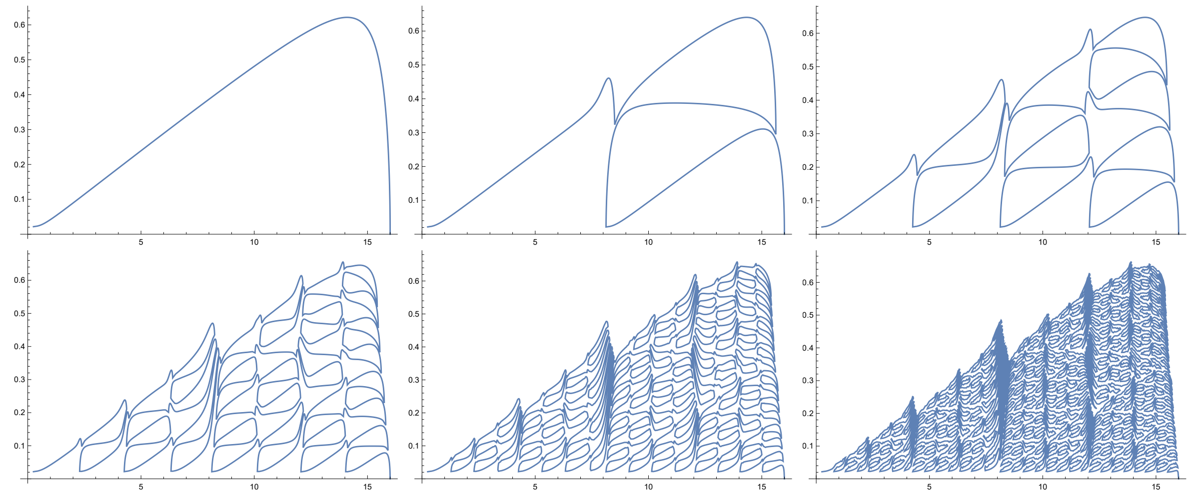

Figure 5.10: Graphs of Hulls for $c = 16$

Since these are just simulations, it is possible that the stretching we see is misleading and will not cause discontinuity of our limit curve. Even if it does, it is worth investigating with more rigor rather than relying entirely on simulations. Additionally, as c increases, the base of the hull increases and the height of the hull decreases. So, for large enough c values, the continuity might not be a problem.

Conjecture 5.2. Let γ_n be as in the construction and K^n be the corresponding hull. Suppose $\gamma(t) = \lim_{n\to\infty} \gamma_n(t)$ exists and is continuous. Suppose there exists $z_0 \in \mathbb{C}$, $r > 0$, and $N \in \mathbb{N}$ so that for all $n \geq N$ $\mathrm{B}(z_0, r) \subseteq K^n$ and $\gamma_n[0,1] \cap \overline{B(z_0, r)} = \emptyset$. Then the area of $\gamma[0,1]$ is 0.

5.3 Properties of Lipschitz-1/2 Functions

Definition 5.3. Let $\varphi : [0, T] \to \mathbb{R}$. Define

$$\mathrm{Lip}_\varphi(s, t) = \frac{|\varphi(s) - \varphi(t)|}{\sqrt{|s-t|}}. \tag{5.2}$$

Lemma 5.4. Let $\varphi : [0, T] \to \mathbb{R}$. Then

(a) $\|\varphi\| = \frac{1}{2}\|\varphi(4t)\|$,

(b) $\|\varphi\| = \|\varphi(T - t)\|$,

(c) $\|c\varphi\| = |c| \cdot \|\varphi\|$ for $c \in \mathbb{R}$.

Proposition 5.5. Let $\alpha : [0, T] \to \mathbb{R}$ be a Lipschitz-1/2 function. Let $\epsilon > 0$ and define $\varphi : [0, T + \epsilon] \to \mathbb{R}$ by

$$\varphi(t) = \begin{cases} \alpha(t) & t \in [0, T] \\ \sqrt{t - T} + \alpha(T) & t \in [T, T + \epsilon] \end{cases} \tag{5.3}$$

Then $\|\varphi\| \le \sqrt{1 + \|\alpha\|^2}$. Furthermore, if $\epsilon^2 \le \sup\{\frac{T-s}{\alpha(T)-\alpha(s)} : s \in [0, T)\}$ and $\|\varphi\| > \|\alpha\| \vee 1$, then

$$\|\varphi\| = \sup_{s \in [0,T)} \mathrm{Lip}_\varphi(s, T + \epsilon). \tag{5.4}$$

Proof. Let $s, t \in [0, T + \epsilon]$ with $s \neq t$. If $s, t \in [0, T]$ or $s, t \in [T, T + \epsilon]$, then $\mathrm{Lip}_\varphi(s, t)$ is bounded by $\|\alpha\|$ or 1, respectively. Without loss of generality, suppose $0 \le s < T < t \le T + \epsilon$. Then

$$\mathrm{Lip}_\varphi(s, t) = \frac{|\sqrt{t - T} + \alpha(T) - \alpha(s)|}{\sqrt{t - s}}. \tag{5.5}$$

We now consider three different cases and think of s as fixed and t as varying (i.e. $\mathrm{Lip}_\varphi(s, t)$ is a function of t).

Case 1: If $\alpha(T) \ge \alpha(s)$, then for $T < t \le T + \epsilon$

$$\mathrm{Lip}_\varphi(s, t) = \frac{\sqrt{t - T} + \alpha(T) - \alpha(s)}{\sqrt{t - s}}. \tag{5.6}$$

So,

$$\frac{\partial}{\partial t}\mathrm{Lip}_\varphi(s, t) = \frac{T - s + (\alpha(s) - \alpha(T))\sqrt{t - T}}{2\sqrt{t - T}(t - s)^{3/2}}, \tag{5.7}$$

which means that the extrema of $\mathrm{Lip}_\varphi(s, t)$ occur at $T, T + \epsilon$, or $T + \left(\frac{T-s}{\alpha(T)-\alpha(s)}\right)^2$. Since $\alpha(T) \ge \alpha(s)$,

$$\frac{\partial}{\partial t}\mathrm{Lip}_\varphi(s, t) > 0 \text{ for } t < T + \epsilon \wedge \left[T + \left(\frac{T - s}{\alpha(T) - \alpha(s)}\right)^2\right]. \tag{5.8}$$

If $\epsilon \geq \left(\frac{T-s}{\alpha(T)-\alpha(s)}\right)^2$, then

$$\frac{\partial}{\partial t}\mathrm{Lip}_\varphi(s,t) < 0 \text{ for } T + \left(\frac{T-s}{\alpha(T)-\alpha(s)}\right)^2 < t \leq T+\epsilon. \tag{5.9}$$

So, the maximum occurs at $T + \left(\frac{T-s}{\alpha(T)-\alpha(s)}\right)^2$ if this is less than $T+\epsilon$, otherwise the maximum occurs at $T+\epsilon$. Observe that

$$\mathrm{Lip}_\varphi\left(s, T + \left(\frac{T-s}{\alpha(T)-\alpha(s)}\right)^2\right) = \frac{\frac{T-s}{\alpha(T)-\alpha(s)} + \alpha(T)-\alpha(s)}{\sqrt{T-s+\left(\frac{T-s}{\alpha(T)-\alpha(s)}\right)^2}} \tag{5.10}$$

$$= \frac{T-s+(\alpha(T)-\alpha(s))^2}{\sqrt{T-s}\sqrt{T-s+(\alpha(T)-\alpha(s))^2}} \tag{5.11}$$

$$= \sqrt{\frac{T-s+(\alpha(T)-\alpha(s))^2}{T-s}} \tag{5.12}$$

$$= \sqrt{1+\left(\frac{\alpha(T)-\alpha(s)}{\sqrt{T-s}}\right)^2} \leq \sqrt{1+\|\alpha\|^2}. \tag{5.13}$$

Case 2: If $\sqrt{\epsilon}+\alpha(T) \leq \alpha(s)$, then for $T < t \leq T+\epsilon$

$$\mathrm{Lip}_\varphi(s,t) = -\frac{\sqrt{t-T}+\alpha(T)-\alpha(s)}{\sqrt{t-s}}. \tag{5.14}$$

So,

$$\frac{\partial}{\partial t}\mathrm{Lip}_\varphi(s,t) = -\frac{T-s+(\alpha(s)-\alpha(T))\sqrt{t-T}}{2\sqrt{t-T}(t-s)^{3/2}}. \tag{5.15}$$

Since $\alpha(s) > \alpha(T)$, we have that

$$T-s+(\alpha(s)-\alpha(T))\sqrt{t-T} > 0 \tag{5.16}$$

for $t \in (T, T+\epsilon]$. So, $\frac{\partial}{\partial t}\mathrm{Lip}_\varphi(s,t) < 0$ for $t \in (T, T+\epsilon]$.Thus the maximum occurs at T.

Case 3: If there is $t_0 \in (T, T+\epsilon)$ so that

$$\sqrt{t_0 - T} + \alpha(T) = \alpha(s). \tag{5.17}$$

Note that $\mathrm{Lip}_\varphi(s, t_0) = 0$. If $T < t < \frac{s+t_0}{2}$, there exists $s_0 \in (s, T)$ so that $\alpha(s_0) = \varphi(t)$. So,

$$\begin{aligned}
\mathrm{Lip}_\varphi(s,t) &= \frac{\alpha(s) - \varphi(t)}{\sqrt{t-s}} && (5.18)\\
&= \frac{\alpha(s) - \alpha(s_0)}{\sqrt{t-s}} && (5.19)\\
&< \frac{\alpha(s) - \alpha(s_0)}{\sqrt{s_0-s}} && (5.20)\\
&\leq \|\alpha\|. && (5.21)
\end{aligned}$$

If $\frac{s+t_0}{2} \leq t \leq T+\epsilon$ and $t \neq t_0$, then $|s-t| \geq |t_0 - t|$. So,

$$\begin{aligned}
\mathrm{Lip}_\varphi(s,t) &= \frac{|\alpha(s) - \sqrt{t-T} - \alpha(T)|}{\sqrt{t-s}} && (5.22)\\
&= \frac{|\sqrt{t_0-T} + \alpha(T) - \sqrt{t-T} - \alpha(T)|}{\sqrt{t-s}} && (5.23)\\
&= \frac{|\sqrt{t_0-T} - \sqrt{t-T}|}{\sqrt{t-s}} && (5.24)\\
&\leq \frac{|\sqrt{t_0-T} - \sqrt{t-T}|}{\sqrt{|t-t_0|}} && (5.25)\\
&\leq 1 && (5.26)
\end{aligned}$$

The above cases show that $\|\varphi\| \leq \sqrt{1 + \|\alpha\|^2}$.

If $\epsilon \leq \left(\frac{T-s}{\alpha(T)-\alpha(s)}\right)^2$ for all $s \in [0,T)$, then $\left(\frac{T-s}{\alpha(T)-\alpha(s)}\right)^2 \notin (T, T+\epsilon]$ for any $s \in [0,T)$. Since this is the only critical point in the previous cases, we have that the maximum must occur at an endpoint (i.e. T or $T+\epsilon$) for any fixed $s \in [0,T)$. If we assume that $\|\varphi\| > \|\alpha\| \vee 1$, then the maximum cannot occur at T. So,

$$\|\varphi\| = \sup_{s \in [0,T)} \mathrm{Lip}_\varphi(s, T+\epsilon). \tag{5.27}$$

$\square$

Corollary 5.6. Let $m > 0$ and $0 < T_1 < T_2$. Define $\varphi : [0, T_2] \to \mathbb{R}$ by

$$\varphi(t) = \begin{cases} -\sqrt{T_1 - t} & t \in [0, T_1) \\ m\sqrt{t - T_1} & t \in [T_1, T_2] \end{cases} \tag{5.28}$$

Then $\|\varphi\| \leq \sqrt{1 + m^2}$.

Proof. Let $\phi(t) = \frac{1}{m}\varphi(t)$. Since $\| - \frac{1}{m}\sqrt{T_1 - t}\| = \frac{1}{m}$, Corollary 5.6 gives us that $\|\phi\| \leq \sqrt{1 + \left(\frac{1}{m}\right)^2}$. So,

$$\|\varphi\| = \|m\phi\| \leq m\sqrt{1 + \left(\frac{1}{m}\right)^2} = \sqrt{1 + m^2}. \tag{5.29}$$

$\square$

5.4 Candidate Family of Driving Functions

We now define our driving function that will be scaled to create the driving function family that are candidates for generating spacefilling curves. Note that ξ_n and ξ will be the driving functions for the upward Loewner equation and λ_n and λ will be the driving functions for the downward Loewner equation.

Definition 5.7. Define $\xi_0 : [0, 1] \to [0, 1]$ by $\xi_0(t) = \sqrt{t}$. For $n \in \mathbb{N}$, define $\xi_n : [0, 1] \to [0, 1]$ recursively by

$$\xi_n(t) = \begin{cases} \frac{1}{2}\xi_{n-1}(4t) & t \in [0, \frac{1}{4}] \\ \frac{1}{2}\xi_{n-1}(4t - 1) + \frac{1}{2} & t \in [\frac{1}{4}, \frac{1}{2}] \\ -\frac{1}{2}\xi_{n-1}(4t - 2) + 1 & t \in [\frac{1}{2}, \frac{3}{4}] \\ \frac{1}{2}\xi_{n-1}(4t - 3) + \frac{1}{2} & t \in [\frac{3}{4}, 1] \end{cases} \tag{5.30}$$

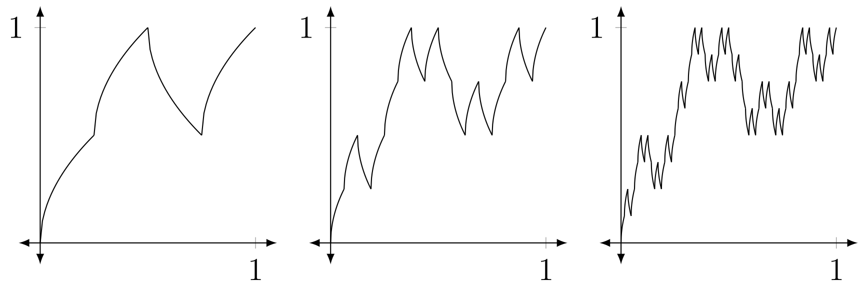

Figure 5.11: Graphs of ξ_1, ξ_2, and ξ_3

Alternatively, we could define

$$\tau(l) = \begin{cases} 1 & l = 0, 1, 3 \\ -1 & l = 2 \end{cases} \quad \text{and } \sigma(l) = \begin{cases} \frac{1}{2} & l = 1, 3 \\ 1 & l = 2 \\ 0 & l = 0 \end{cases} \tag{5.31}$$

Then $\xi_n(t) = \frac{\tau(l)}{2}\xi_{n-1}(4t - l) + \sigma(l)$ for $t \in [\frac{l}{4}, \frac{l+1}{4}]$. The plots of ξ_1, ξ_2, and ξ_3 are shown in Figure 5.11

Definition 5.8. For each $n \in \mathbb{N}$, let $\lambda_n(t) = \xi_n(1 - t)$.

Remark 5.9. This means that λ_n can be expressed recursively as follows:

$$\lambda_n(t) = \begin{cases} \frac{1}{2}\lambda_{n-1}(4t) + \frac{1}{2} & t \in [0, \frac{1}{4}] \\ -\frac{1}{2}\lambda_{n-1}(4t - 1) + 1 & t \in [\frac{1}{4}, \frac{1}{2}] \\ \frac{1}{2}\lambda_{n-1}(4t - 2) + \frac{1}{2} & t \in [\frac{1}{2}, \frac{3}{4}] \\ \frac{1}{2}\lambda_{n-1}(4t - 3) & t \in [\frac{3}{4}, 1] \end{cases} \tag{5.32}$$

Remark 5.10. By Lemma 5.4, for all $n \in \mathbb{N}$, $||\lambda_n|| = ||\xi_n||$.

We now prove a few useful results about ξ_n, which we will use later to give uniform convergence of the sequence.

Lemma 5.11. For $n \in \mathbb{N}$ and $k \in \{0, 1, ..., 4^n - 1\}$,

$$\left|\xi_n\left(\frac{k}{4^n}\right) - \xi_n\left(\frac{k+1}{4^n}\right)\right| = \frac{1}{2^n}. \tag{5.33}$$

Proof. We proceed by induction on n. For $n = 0$, $\xi_0(0) = 0$ and $\xi_0(1) = 1$, so the result holds. Fix $n \in \mathbb{N}$. Suppose the result holds for $n - 1$. Let $k \in \{0, 1, ..., 4^n - 1\}$. Then for some $l \in \{0, 1, 2, 3\}$, $\frac{k}{4^n}, \frac{k+1}{4^n} \in [\frac{l}{4}, \frac{l+1}{4}]$. So,

$$\left|\xi_n\left(\frac{k}{4^n}\right) - \xi_n\left(\frac{k+1}{4^n}\right)\right| = \frac{1}{2}\left|\xi_{n-1}\left(\frac{k}{4^{n-1}} - l\right) - \xi_{n-1}\left(\frac{k+1}{4^{n-1}} - l\right)\right| = \frac{1}{2}\frac{1}{2^{n-1}} = \frac{1}{2^n} \tag{5.34}$$

as $k - 4^{n-1}l \in \{0, 1, ..., 4^{n-1} - 1\}$. □

Lemma 5.12. Let $n \in \mathbb{N}$.

(a) $\xi_n(0) = 0$ and $\xi_n(1) = 1$

(b) For $m \geq n$ and $x \in \{0, \frac{1}{4^n}, \frac{2}{4^n}, ..., 1\}$, $\xi_n(x) = \xi_m(x)$.

Proof of (a). We will induct on n. For $n = 0$, $\xi_0(0) = 0$ and $\xi_0(1) = 1$. Fix $n \in \mathbb{N}$. Suppose this holds for $n - 1$. Then

$$\xi_n(0) = \frac{1}{2}\xi_{n-1}(4 \cdot 0) = 0 \tag{5.35}$$

and

$$\xi_n(1) = \frac{1}{2}\xi_{n-1}(4 \cdot 1 - 3) + \frac{1}{2} = \frac{1}{2} + \frac{1}{2} = 1. \tag{5.36}$$

□

Proof of (b). We will again induct on n. Part (a) gives the base case when $n = 0$. Suppose the result holds for $n - 1$ - that is, for all $m \geq n - 1$ and $x \in \{0, \frac{1}{4^{n-1}}, ..., 1\}$, $\xi_m(x) = \xi_{n-1}(x)$. Let $x \in \{0, \frac{1}{4^n}, \frac{2}{4^n}, ..., 1\}$. Then for some $l \in \{0, 1, 2, 3\}$, $x \in [\frac{l}{4}, \frac{l+1}{4}]$. So,

$$\xi_n(x) = \frac{\tau(l)}{2}\xi_{n-1}(4x - l) + \sigma(l). \tag{5.37}$$

By the induction hypothesis for $m > n - 1$,

$$\xi_n(x) = \frac{\tau(l)}{2}\xi_{n-1}(4x - l) + \sigma(l) = \frac{\tau(l)}{2}\xi_{m-1}(4x - l) + \sigma(l) = \xi_m(x). \tag{5.38}$$

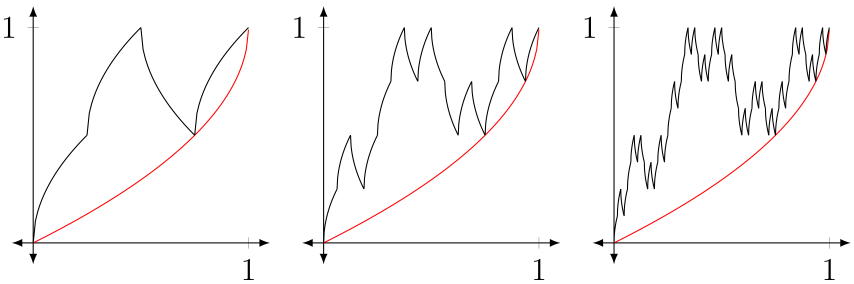

Figure 5.12: Graph of u in red along with ξ_1 (left), ξ_2 (middle), and ξ_3 (right)

□

Our goal is to prove that $\xi : [0,1] \to \mathbb{R}$ defined as the pointwise limit of $\xi_n(t)$ is a Lipschitz-1/2 function and $\|\xi\| \leq 2$. Our approach will be to prove $\|\xi_n\|$ is bounded by a sequence that converges to 2 as $n \to \infty$ and leverage this to show the same for $\|\xi\|$. In order to prove this, we will strategically bound ξ_n above and below by functions with computable Lipschitz-1/2 norm that will bound $\|\xi_n\|$. Essentially, what we will do is this:

- Show that for some $a \in (0,1)$ there exist u and β_n so that $u(t) \leq \xi_n(t)$ for $0 \leq t \leq a$ and $\beta_n(t) \geq \xi_n(t)$ for $a \leq t \leq 1$. (Lemmas 5.13, 5.15, 5.16, 5.18)
- Show $\|\xi_n\| > \|\beta_n\| \vee \|u\|$. (Lemma 5.17)
- This gives (Lemma 5.17)

$$\|\xi_n\| = \sup\left\{\frac{\beta_n(t) - u(s)}{\sqrt{t-s}} : 0 \leq s < a < t \leq 1\right\}. \tag{5.39}$$

- Show that $\|u\chi_{[0,a]} + \beta_n\chi_{(a,1]}\| \leq 2$. (Lemma 5.20)
- This gives $\|\xi_n\| \leq 2$. (Lemma 5.22)
- Finally, we will use all of the above to show that $\|\xi\| \leq 2$ also. (Proposition 5.23)

We begin by defining the function that bounds ξ_n below. We will denote this function by u since it will be *under* ξ_n. The graph of u on ξ_1, ξ_2, and ξ_3 is shown in Figure 5.12.

Lemma 5.13. Define $u : [0,1] \to [0,1]$ by $u(t) = 1 - \sqrt{1-t}$. Then for all $n \in \mathbb{N}$, $u(t) \leq \xi_n(t)$ for all $t \in [0,1]$ with equality only when $t \in \{1, 1 - \frac{1}{4^k} : k \in \{0,1,...,n\}\}$.

Proof. We will use induction on n.

For $n = 0$, $\xi_n(t) = \sqrt{t}$. The only solutions to $\sqrt{t} = 1 - \sqrt{1-t}$ are $t = 0, 1$, which means $\xi_0(t) = u(t)$ only when $t = 0, 1$. Between 0 and 1, since $\xi_0(\frac{1}{2}) = \frac{1}{\sqrt{2}} > \frac{\sqrt{2}-1}{\sqrt{2}} = u(\frac{1}{2})$, we have that $u(t) < \xi_n(t)$. Thus, $u(t) \leq \xi_n(t)$ on $[0, 1]$.

Suppose this holds for $n - 1$. We now show the result for $\xi_n(t)$ by considering cases on t.

Case 1: Suppose $t = 0$. Then $u(t) = 0 = \xi_n(t)$.

Case 2: Suppose $t \in (0, \frac{1}{4}]$. Then $\xi_n(t) = \frac{1}{2}\xi_{n-1}(4t) \geq \frac{1}{2}u(4t)$ by the induction hypothesis on ξ_{n-1} as $4t \in [0, 1]$. So,

$$\xi_n(t) \geq \frac{1}{2}u(4t) = -\frac{1}{2}\sqrt{1-4t} + \frac{1}{2} = -\sqrt{\frac{1}{4} - t} + \frac{1}{2} \tag{5.40}$$

Since $1 - \frac{1}{4^k} \notin (0, \frac{1}{4}]$ for any k, we want $\xi_n(t) > u(t)$. It suffices to check that

$$\frac{1}{2} - \sqrt{\frac{1}{4} - t} > 1 - \sqrt{1-t} \tag{5.41}$$

for $t \in (0, \frac{1}{4}]$.

Case 3: Suppose $t \in (\frac{1}{4}, \frac{3}{4})$. $\xi_n(t) \geq \frac{1}{2} > u(t)$ as u is strictly increasing and

$$u\left(\frac{3}{4}\right) = -\sqrt{1 - \frac{3}{4}} + 1 = \frac{1}{2}. \tag{5.42}$$

Case 4: Suppose $t \in [\frac{3}{4}, 1]$. Then $\xi_n(t) = \frac{1}{2}\xi_{n-1}(4t-3) + \frac{1}{2}$. By the induction hypothesis, we have that $\xi_{n-1}(4t-3) \geq u(4t-3)$ with equality only for $4t - 3 \in \{1, 1 - \frac{1}{4^k} : k \in \{0, ..., n-1\}\}$. This means that $\xi_{n-1}(4t-3) = u(4t-3)$ only when

$t \in \{1, 1 - \frac{1}{4^k} : k \in \{1, ..., n\}\}$. Using this we have the following:

$$\begin{aligned}
\xi_n(t) &= \tfrac{1}{2}\xi_{n-1}(4t-3) + \tfrac{1}{2} \\
&\geq \tfrac{1}{2}u(4t-3) + \tfrac{1}{2} \\
&= \tfrac{1}{2}(-\sqrt{1-(4t-3)} + 1) + \tfrac{1}{2} \\
&= -\sqrt{1-t} + 1 \\
&= u(t)
\end{aligned} \tag{5.43}$$

with equality only when $t \in \{1, 1 - \frac{1}{4^k} : k \in \{1, ..., n\}\}$.

□

The previous lemma shows that u lies under ξ_n for all n. Contrary to this, the function that bounds ξ_n above will depend on n. We begin the process of constructing this function by first investigating a sequence that relates to ξ_n which will be used to define the upper bound function.

Definition 5.14. For $n \in \mathbb{N}$, let

$$a_n = \frac{2^n\sqrt{3}}{\sqrt{2+4^n}}. \tag{5.44}$$

Lemma 5.15. For $n \in \mathbb{N}$ we have the following:

(a) $a_n > a_{n-1}$

(b) $\frac{1}{4} \leq \frac{1}{a_n^2} \leq \frac{1}{2}$

(c) $\frac{1}{a_n^2} = \frac{1}{2}(1 - \sum_{m=1}^{n-1} \frac{1}{4^m})$

(d) $\frac{1}{4}\left(\frac{1}{a_{n-1}^2} + 1\right) = \frac{1}{a_n^2}$

Proof of (a). For $n \in \mathbb{N}$,

$$\sqrt{2+4^n} = 2\sqrt{\frac{1}{2} + 4^{n-1}} < 2\sqrt{2+4^{n-1}}. \tag{5.45}$$

So,

$$2^{n-1}\sqrt{3}\sqrt{2+4^n} < 2^n\sqrt{3}\sqrt{2+4^{n-1}}. \tag{5.46}$$

Thus,

$$a_{n-1} = \frac{2^{n-1}\sqrt{3}}{\sqrt{2+4^{n-1}}} < \frac{2^n\sqrt{3}}{\sqrt{2+4^n}} = a_n. \tag{5.47}$$

$\square$

Proof of (b). By part (a), $a_n \geq a_1 = \sqrt{2}$ for all $n \in \mathbb{N}$. Also

$$a_n^2 = \frac{3\cdot 4^n}{2+4^n} < \frac{3\cdot 4^n}{4^n} = 3. \tag{5.48}$$

These two facts mean $\frac{1}{4} < \frac{1}{3} < \frac{1}{a_n^2} \leq \frac{1}{2}$. $\square$

Proof of (c). Since $\frac{2+4^n}{3\cdot 4^n} = \frac{1}{a_n^2}$, it suffices to show

$$2+4^n = \frac{3\cdot 4^n}{2}\left(1 - \sum_{m=1}^{n-1}\frac{1}{4^m}\right). \tag{5.49}$$

We have the following:

$$\begin{aligned}
\tfrac{3\cdot 4^n}{2}\left(1-\textstyle\sum_{m=1}^{n-1}\tfrac{1}{4^m}\right) &= 6\left(4^{n-1}-\textstyle\sum_{m=1}^{n-1}4^{n-1-m}\right)\\
&= 6\left(4^{n-1}-\textstyle\sum_{m=0}^{n-2}4^m\right)\\
&= 6\left(4^{n-1}-\tfrac{1}{3}(4^{n-1}-1)\right)\\
&= 6\left(\tfrac{1}{3}(3\cdot 4^{n-1}-4^{n-1}+1)\right)\\
&= 2(2\cdot 4^{n-1}+1)\\
&= 4^n+2
\end{aligned} \tag{5.50}$$

$\square$

Proof of (d). Observe the following:

$$
\begin{aligned}
\tfrac{1}{4}\left(\tfrac{1}{a_{n-1}^2}+1\right) &= \tfrac{1}{4}(\tfrac{1}{2}(1-\textstyle\sum_{m=1}^{n-2}\tfrac{1}{4^m})+1) \\
&= \tfrac{1}{4}(\tfrac{1}{2}(4-\textstyle\sum_{m=0}^{n-2}\tfrac{1}{4^m})) \\
&= \tfrac{1}{2}(1-\textstyle\sum_{m=0}^{n-2}\tfrac{1}{4^{m+1}}) \\
&= \tfrac{1}{2}(1-\textstyle\sum_{m=1}^{n-1}\tfrac{1}{4^m}) \\
&= \tfrac{1}{a_n^2}
\end{aligned}
\tag{5.51}
$$

□

Lemma 5.16. For $n \in \mathbb{N}$, $\xi_n\left(\frac{1}{a_n^2}\right) = 1$.

Proof. We will proceed by induction on n.

For $n = 1$, $\frac{1}{a_1^2} = \frac{1}{\sqrt{2}^2} = \frac{1}{2}$ and

$$\xi_1\left(\frac{1}{2}\right) = \frac{1}{2}\xi_0\left(4\left(\frac{1}{2}\right)-1\right)+\frac{1}{2} = \frac{1}{2}\sqrt{1}+\frac{1}{2} = 1. \tag{5.52}$$

Let $n \in \mathbb{N}$ and suppose $\xi_k(\frac{1}{a_k^2}) = 1$ for $k \leq n-1$. By Lemma 5.15, we have that $\frac{1}{a_{n-1}^2} = \frac{4}{a_n^2} - 1$. Since $\frac{1}{4} < \frac{1}{a_n^2} < \frac{1}{2}$, we have

$$\xi_n\left(\frac{1}{a_n^2}\right) = \frac{1}{2}\xi_{n-1}\left(\frac{4}{a_n^2}-1\right)+\frac{1}{2} = \frac{1}{2}\xi_{n-1}\left(\frac{1}{a_{n-1}^2}\right)+\frac{1}{2} = \frac{1}{2}+\frac{1}{2} = 1. \tag{5.53}$$

□

Lemma 5.17. For $n \in \mathbb{N}$, we have the following:

(a) $\|\xi_n\| \geq \|\xi_{n-1}\|$

(b) $\|\xi_n\| = \|\xi_n|_{[0,\frac{1}{a_n^2}]}\|$

(c) If $\|\xi_n\| > \|\xi_{n-1}\|$, then

$$\|\xi_n\| = \sup\left\{\mathrm{Lip}_{\xi_n}(s,t) : s \in \left[0,\frac{1}{4}\right), t \in \left(\frac{1}{4},\frac{1}{a_n^2}\right]\right\} \tag{5.54}$$

Proof of (a). Since $\xi_n|_{[0,\frac{1}{4}]}(t) = \frac{1}{2}\xi_{n-1}(4t)$, by Lemma 5.4,

$$\|\xi_n\| \geq \|\xi_n|_{[0,\frac{1}{4}]}\| = \|\xi_{n-1}\|. \tag{5.55}$$

□

Proof of (b). Let $s, t \in [0,1]$ with $s \neq t$. We will show that $\mathrm{Lip}_{\xi_n}(s,t) \leq \|\xi_n|_{[0,\frac{1}{a_n^2}]}\|$. If $\xi_n(s) = \xi_n(t)$, then $\mathrm{Lip}_{\xi_n}(s,t) = 0 \leq \|\xi_n|_{[0,\frac{1}{a_n^2}]}\|$. Let $s \in \left[\frac{l_s}{4}, \frac{l_s+1}{4}\right]$ and $t \in \left[\frac{l_t}{4}, \frac{l_t+1}{4}\right]$ for the smallest $l_s, l_t \in \{0,1,2,3\}$.

Case 1: Suppose $l_s = l_t := l$. Then as $\xi_n|_{[\frac{l}{4},\frac{l+1}{4}]}(x) = \frac{\tau(l)}{2}\xi_{n-1}(4x-l) + \sigma(l)$, by Lemma 5.4,

$$\mathrm{Lip}_{\xi_n}(s,t) \leq \|\xi_n|_{[\frac{l}{4},\frac{l+1}{4}]}\| = \|\xi_{n-1}\| = \|\xi_n|_{[0,\frac{1}{4}]}\| \leq \|\xi_n|_{[0,\frac{1}{a_n^2}]}\|. \tag{5.56}$$

Case 2: Suppose $l_s \neq l_t$ and $l_s, l_t \in \{1,2,3\}$. Note that

$$\xi_n\left(\left[\frac{l_s}{4}, \frac{l_s+1}{4}\right]\right) = \left[\frac{1}{2}, 1\right] = \xi_n\left(\left[\frac{l_t}{4}, \frac{l_t+1}{4}\right]\right). \tag{5.57}$$

Since ξ_n is continuous and $\xi_n(s) \neq \xi_n(t)$, there exists $s_0 \in [\frac{l_t}{4}, \frac{l_t+1}{4}]$ so that $\xi_n(s_0) = \xi_n(s)$ or $t_0 \in [\frac{l_s}{4}, \frac{l_s+1}{4}]$ so that $\xi_n(t_0) = \xi_n(t)$. Without loss of generality, we will assume that there exists $s_0 \in [\frac{l_t}{4}, \frac{l_t+1}{4}]$ so that $\xi_n(s_0) = \xi_n(s)$. Then as $|s-t| \geq |s_0 - t|$,

$$\mathrm{Lip}_{\xi_n}(s,t) \leq \mathrm{Lip}_{\xi_n}(s_0,t) \leq \|\xi_n|_{[\frac{l_t}{4},\frac{l_t+1}{4}]}\| \leq \|\xi_n|_{[0,\frac{1}{a_n^2}]}\|. \tag{5.58}$$

Case 3: Either $l_s = 0$ or $l_t = 0$. Without loss of generality, we will assume $l_s = 0$. So, $s \in [0, \frac{1}{4})$ and $t \in (\frac{1}{4}, 1]$. If $\xi_n(t) = \frac{1}{2} = \xi_n(\frac{1}{4})$, then

$$\mathrm{Lip}_{\xi_n}(s,t) = \frac{|\xi_n(\frac{1}{4}) - \xi_n(s)|}{\sqrt{|t-s|}} < \frac{|\xi_n(\frac{1}{4}) - \xi_n(s)|}{\sqrt{|\frac{1}{4} - s|}} \leq ||\xi_{n-1}|| \tag{5.59}$$

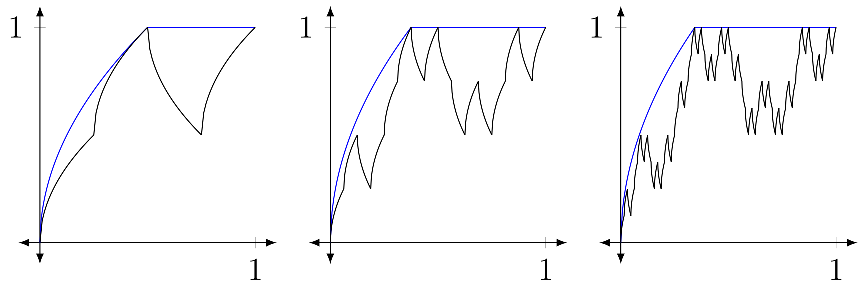

Figure 5.13: Graph of β_1, β_2, and β_3 in blue along with ξ_1, ξ_2, and ξ_3

If $\xi_n(t) \neq \frac{1}{2}$, then $\xi_n(t) \in (\frac{1}{2}, 1]$. Since $\xi_n((\frac{1}{4}, \frac{1}{a_n^2}]) \supseteq (\frac{1}{2}, 1]$, there exists $t_0 \in (\frac{1}{4}, \frac{1}{a_n^2}]$ so that $\xi_n(t) = \xi_n(t_0)$. Hence

$$\mathrm{Lip}_{\xi_n}(s,t) = \frac{|\xi_n(t_0) - \xi_n(s)|}{\sqrt{|t-s|}} \leq \frac{|\xi_n(t_0) - \xi_n(s)|}{\sqrt{|t_0-s|}} \leq ||\xi_n|_{[0,\frac{1}{a_n^2}]}|| \tag{5.60}$$

□

Proof of (c). From the proof of part (b), unless $s \in [0, \frac{1}{4})$ and $t \in (\frac{1}{4}, \frac{1}{a_n^2}]$, we have that $\mathrm{Lip}_{\xi_n}(s,t) \leq \|\xi_{n-1}\|$. Since $\|\xi_{n-1}\| < \|\xi_n\|$, we have the result. □

We now have enough information to define the family of functions that will *bound* ξ_n above, denoted β_n. The graphs of β_1, β_2, and β_3 are shown in Figure 5.13.

Lemma 5.18. For $n \in \mathbb{N}$, define $\beta_n : [0,1] \to \mathbb{R}$ by

$$\beta_n(t) = \begin{cases} a_n\sqrt{t} & t \in [0, \frac{1}{a_n^2}] \\ 1 & t \in [\frac{1}{a_n^2}, 1] \end{cases} \tag{5.61}$$

Then $\beta_n(t) \geq \xi_n(t)$ for all $t \in [0,1]$ with equality only for $t = 0, \frac{1}{a_n^2}$ or $t > \frac{1}{a_n^2}$ with $\xi_n(t) = 1$.

Proof. We once again we use induction on n. For $n = 1$, $a_1 = \sqrt{2}$ and $\beta_1(t) = \sqrt{2t}$. First note that $\xi_1(0) = 0 = \beta_1(0)$ and $\xi_1(\frac{1}{2}) = 1 = \beta_1(\frac{1}{2})$.

Case 1: Suppose $t \in (0, \frac{1}{4}]$. Then $\xi_1(t) = \sqrt{t} < \sqrt{2t} = \beta_1(t)$.

Case 2: Suppose $t \in (\frac{1}{4}, \frac{1}{2})$. Then

$$\xi_1(t) = \frac{1}{2}\xi_0(4t-1) + \frac{1}{2} = \sqrt{t - \frac{1}{4}} + \frac{1}{2}. \tag{5.62}$$

Now, if $\xi_1(t) = \beta_1(t)$, then $\sqrt{t - \frac{1}{4}} + \frac{1}{2} = \sqrt{2t}$, which only holds when $t = \frac{1}{2}$. Since $\xi_1(\frac{1}{4}) > \beta_1(\frac{1}{4})$, we have that $\xi_1(t) > \beta_1(t)$ for $t \in (\frac{1}{4}, \frac{1}{2})$.

Case 3: Suppose $t \in (\frac{1}{2}, 1]$. Then $\xi_1(t) \leq 1 < \beta_1(t)$.

This proves $\xi_1(t) \leq \beta_1(t)$ with equality only for $t = 0, \frac{1}{2} = \frac{1}{a_1^2}$.

Suppose this holds for $n-1$. We will once again consider cases on t. Note that $\xi_n(0) = 0 = \beta_n(0)$ and $\xi_n(\frac{1}{a_n^2}) = 1 = a_n\sqrt{\frac{1}{a_n^2}} = \beta_n(\frac{1}{a_n^2})$.

Case 1: Suppose $t \in (0, \frac{1}{4}]$, then

$$\xi_n(t) = \frac{1}{2}\xi_{n-1}(4t) \leq \frac{1}{2}\beta_{n-1}(4t) = \frac{a_{n-1}}{2}\sqrt{4t} = a_{n-1}\sqrt{t} = \beta_{n-1}(t) < \beta_n(t) \tag{5.63}$$

as $a_n > a_{n-1}$.

Case 2: Suppose $t \in (\frac{1}{4}, \frac{1}{a_n^2})$, then

$$\xi_n(t) = \frac{1}{2}\xi_{n-1}(4t-1) + \frac{1}{2} \leq \frac{1}{2}\beta_{n-1}(4t-1) + \frac{1}{2} = a_{n-1}\sqrt{t - \frac{1}{4}} + \frac{1}{2} = \beta_{n-1}\left(t - \frac{1}{4}\right) + \frac{1}{2} \tag{5.64}$$

Now,

$$\beta_n(t) = \beta_{n-1}\left(t - \frac{1}{4}\right) + \frac{1}{2} \text{ only when } t = \frac{1}{a_n^2}, \frac{1}{4^{n+1}}\left(\frac{2+4^n}{3}\right)^3. \tag{5.65}$$

Also, $\frac{1}{a_n^2} < \frac{1}{4^{n+1}}(\frac{2+4^n}{3})^3$, which shows

$$\xi_n(t) \leq \beta_{n-1}\left(t - \frac{1}{4}\right) + \frac{1}{2} < \beta_n(t). \tag{5.66}$$

Case 3: Suppose $t \in (\frac{1}{a_n^2}, 1]$. Then $\xi_n(t) \leq 1 = \beta_n(t)$.

Therefore, $\beta_n(t) \geq \xi_n(t)$ for all $t \in [0, 1]$ with equality only when $t = 0, \frac{1}{a_n^2}$ or $t > \frac{1}{a_n^2}$ with $\xi_n(t) = 1$. $\square$

Now that we have that ξ_n is bounded by Lip($\frac{1}{2}$) functions above and below, we will use the recursion of ξ_n to create a function ϕ_n with the property that $||\phi_n|| \geq ||\xi_n||$.

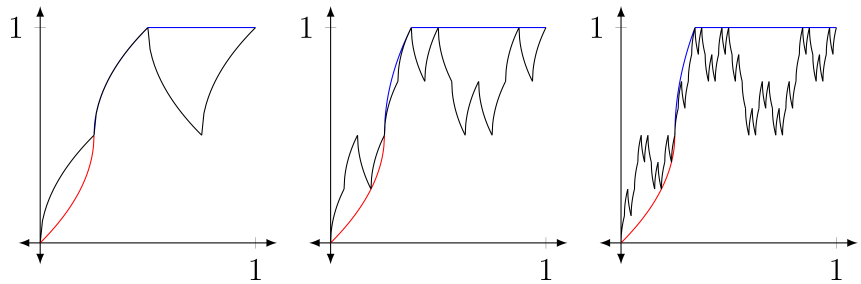

Figure 5.14: Graph of ϕ_1, ϕ_2, and ϕ_3 in red and blue along with ξ_1, ξ_2, and ξ_3

Definition 5.19. For $n \in \mathbb{N}$, define $\phi_n : [0,1] \to \mathbb{R}$ by

$$\phi_n(t) = \begin{cases} \frac{1}{2}u(4t) & [0, \frac{1}{4}] \\ \\ \frac{1}{2}\beta_{n-1}(4t-1) + \frac{1}{2} & [\frac{1}{4}, \frac{1}{a_n^2}] \\ \\ 1 & [\frac{1}{a_n^2}, 1] \end{cases} \tag{5.67}$$

The graphs of ϕ_1 and ϕ_2 are shown in Figure 5.14. Also in Figure 5.14 are the graphs of $\frac{1}{2}u(4t)$ (red) and $\frac{1}{2}\beta_{n-1}(4t-1) + \frac{1}{2}$ (blue).

Lemma 5.20. For $n \in \mathbb{N}$, $||\phi_n|| \leq \sqrt{1 + a_{n-1}^2}$.

Proof. We will prove $||\phi_n|| = ||\phi_n|_{[0, \frac{1}{a_n^2}]}||$. Once we have this, by the Proposition 5.6

$$||\phi_n|| = ||\phi_n|_{[0, \frac{1}{a_n^2}]}|| \leq \sqrt{1 + a_{n-1}^2}. \tag{5.68}$$

Case 1: Suppose $s, t \in \left[\frac{1}{a_n^2}, 1\right]$. Then $\phi_n(s) = \phi_n(t) = 1$. So,

$$\mathrm{Lip}_{\phi_n}(s,t) = 0 < ||\phi_n|_{[0, \frac{1}{a_n^2}]}||. \tag{5.69}$$

Case 2: Suppose $s \in [0, \frac{1}{a_n^2})$, $t \in (\frac{1}{a_n^2}, 1]$. Then $\phi_n(t) = 1$ and

$$\mathrm{Lip}_{\phi_n}(s,t) = \frac{|1 - \phi_n(s)|}{\sqrt{t-s}} < \frac{|\phi_n(\frac{1}{a_n^2}) - \phi_n(s)|}{\sqrt{\frac{1}{a_n^2} - s}} \leq ||\phi_n|_{[0, \frac{1}{a_n^2}]}||. \tag{5.70}$$

This shows $||\phi_n|| = ||\phi_n|_{[0,\frac{1}{a_n^2}]}||$, which completes the proof. $\square$

Lemma 5.21. For $n \in \mathbb{N}$, we have the following:

(a) for $t \in [0, \frac{1}{4}]$, $\phi_n(t) \leq \xi_n(t)$

(b) for $t \in [\frac{1}{4}, 1]$, $\phi_n(t) \geq \xi_n(t)$

Proof. Let $t \in [0, 1]$.

Case 1: Suppose $t \in \left[0, \frac{1}{4}\right]$. By Lemma 5.13, $\frac{1}{2}\xi_{n-1}(4t) \geq \frac{1}{2}\alpha(4t)$. So,

$$\phi_n(t) = \frac{1}{2}\alpha(4t) \leq \frac{1}{2}\xi_{n-1}(4t) = \xi_n(t). \tag{5.71}$$

Case 2: Suppose $t \in \left[\frac{1}{4}, \frac{1}{a_n^2}\right]$. By Lemma 5.18,

$$\frac{1}{2}\beta_{n-1}(4t-1) + \frac{1}{2} \geq \frac{1}{2}\xi_{n-1}(4t-1) + \frac{1}{2}. \tag{5.72}$$

So,

$$\phi_n(t) = \frac{1}{2}\beta_{n-1}(4t-1) + \frac{1}{2} \geq \frac{1}{2}\xi_{n-1}(4t-1) + \frac{1}{2} = \xi_n(t). \tag{5.73}$$

Case 3: Suppose $t \in \left[\frac{1}{a_n^2}, 1\right]$. Then $\phi_n(t) = 1 \geq \xi_n(t)$.

$\square$

We now have the results we need to bound $\|\xi_n\|$.

Lemma 5.22. For $n \in \mathbb{N}$, $||\xi_n|| \leq \sqrt{1 + a_{n-1}^2}$.

Proof. Let $n \in \mathbb{N}$. If $||\xi_n|| > ||\xi_{n-1}||$, then by Lemma 5.17,

$$\|\xi_n\| = \sup\left\{\mathrm{Lip}_{\xi_n}(s,t) : 0 \leq s < \frac{1}{4} < t \leq \frac{1}{a_n^2}\right\}. \tag{5.74}$$

If $s \in [0, \frac{1}{4})$ and $t \in (\frac{1}{4}, \frac{1}{a_n^2}]$ by Lemma 5.21 we have that

$$\phi_n(s) \leq \xi_n(s) \leq \xi_n(t) \leq \phi_n(t), \tag{5.75}$$

since the contruction of ξ_n guarantees $\xi_n(s) \leq \xi_n(t)$. So,

$$\mathrm{Lip}_{\xi_n}(s,t) = \frac{\xi_n(t) - \xi_n(s)}{\sqrt{|t-s|}} \leq \frac{\phi_n(t) - \phi_n(s)}{\sqrt{|t-s|}} \leq ||\phi_n|| \leq \sqrt{1 + a_{n-1}^2}, \tag{5.76}$$

which means $\|\xi_n\| \leq \sqrt{1 + a_{n-1}^2}$.

On the other hand, if $||\xi_n|| = ||\xi_{n-1}||$, then there exists a minimal $N \in \mathbb{N}$ so that $||\xi_k|| = ||\xi_N||$ for $k \in \{N, ..., n\}$. If $N = 0$, then $||\xi_n|| = 1 \leq ||\phi_n||$. If $N > 0$, then $||\xi_{N-1}|| < ||\xi_N||$ and so

$$||\xi_n|| = ||\xi_N|| \leq ||\phi_N|| \leq \sqrt{1 + a_{N-1}^2} < \sqrt{1 + a_{n-1}^2}. \tag{5.77}$$

Therefore, $||\xi_n|| \leq \sqrt{1 + a_{n-1}^2}$. □

The previous lemma shows that $\|\xi_n\| \leq 2$ for all n. This means that the sequence is equicontinuous: let $\epsilon > 0$ and define $\delta = \frac{\epsilon^2}{4}$. Then for $s, t \in [0,1]$ with $|s - t| < \delta$, we have

$$|\xi_n(t) - \xi_n(s)| \leq 2\sqrt{|t-s|} < 2\sqrt{\frac{\epsilon^2}{4}} = \epsilon. \tag{5.78}$$

Since $|\xi_n(t)| \leq 1$ for $t \in [0,1]$, we could use Arzela-Ascoli to obtain a convergent subsequence. However, we want to show that the *entire* sequence converges and the Lipschitz-1/2 norm of the limit is at most 2 as well. This leads us to the following proposition:

Proposition 5.23. Let $\xi : [0,1] \to \mathbb{R}$ be defined by $\xi(t) = \lim_{n\to\infty} \xi_n(t)$. Then ξ is continuous, $\xi \in \mathrm{Lip}(\frac{1}{2})$, and $\|\xi\| \leq 2$.

Proof. We first prove that $\lim_{n\to\infty} \xi_n(t)$ exists for each $t \in [0,1]$. Let $\epsilon > 0$. We can find $N \in \mathbb{N}$ so that $\frac{1}{2^{N-1}} < \epsilon$. Then there exists $k \in \{0, 1, ..., 4^N\}$ so that $\frac{k}{4^N} \leq t \leq \frac{k+1}{4^N}$. For $n \geq n$, by Lemma 5.11

$$\left| \xi_n\left(\frac{k}{4^N}\right) - \xi_n\left(\frac{k+1}{4^N}\right) \right| = \frac{1}{2^N}. \tag{5.79}$$

By construction and Lemma 5.12 for $x \in [\frac{k}{4^N}, \frac{k+1}{4^N}]$,

$$\xi_n(x) \in \left[\xi_N\left(\frac{k}{4^N}\right) \wedge \xi_N\left(\frac{k+1}{4^N}\right), \xi_N\left(\frac{k}{4^N}\right) \vee \xi_N\left(\frac{k+1}{4^N}\right) \right]. \tag{5.80}$$

Thus, for $n, m \geq N$ as $\xi_n(\frac{k}{4^N}) = \xi_m(\frac{k}{4^N})$, we have

$$|\xi_n(t) - \xi_m(t)| \leq \left|\xi_n(t) - \xi_n\left(\frac{k}{4^N}\right)\right| + \left|\xi_m\left(\frac{k}{4^N}\right) - \xi_m(t)\right| \leq 2\left|\xi_n\left(\frac{k+1}{4^N}\right) - \xi_n\left(\frac{k}{4^N}\right)\right| < \epsilon. \tag{5.81}$$

This shows that for each $t \in [0, 1]$, $(\xi_n(t))_{n\in\mathbb{N}}$ is a Cauchy sequence and so it converges.

Since ξ_n converges to ξ pointwise on a compact set, we have uniform convergence. As ξ_n is continuous for each $n \in \mathbb{N}$, ξ is continuous too.

Define $\phi : [0, 1] \to \mathbb{R}$ by

$$\phi(t) = \begin{cases} \frac{1}{2}u(4t) & [0, \frac{1}{4}] \\ \sqrt{3t} & [\frac{1}{4}, \frac{1}{3}] \\ 1 & [\frac{1}{3}, 1] \end{cases} \tag{5.82}$$

Since $\beta_n(t) \to \sqrt{3t}$ for $t \in [\frac{1}{4}, \frac{1}{3}]$, ϕ_n converges to ϕ uniformly. By Proposition 5.6, $\|\phi\| \leq \sqrt{1 + (\sqrt{3})^2} = 2$. Further, using Lemma 5.21, we have that

- if $t \in [0, \frac{1}{4}]$, $\phi(t) \leq \xi(t)$
- if $t \in [\frac{1}{4}, 1]$, $\phi(t) \geq \xi(t)$

This means that $\|\xi\| \leq \|\phi\| = 2$ (using the same proof as in Lemma 5.22). Therefore, $\|\xi\| \leq 2$ and $\xi \in \text{Lip}(\frac{1}{2})$. □

5.5 Piecewise Constant Bounds for Candidate Driving Functions

In this section, we approximate λ to give bounds on the hull generated by λ. Specifically, we are looking at how the hull intersects the real line. We want to obtain appropriate bounds in order to analyze the hull's behavior to indicate whether the trace (if it exists) is spacefilling or not. We will obtain these bounds by squeezing the driving function between functions whose Loewner chains we can compute (i.e. piecewise constant functions).

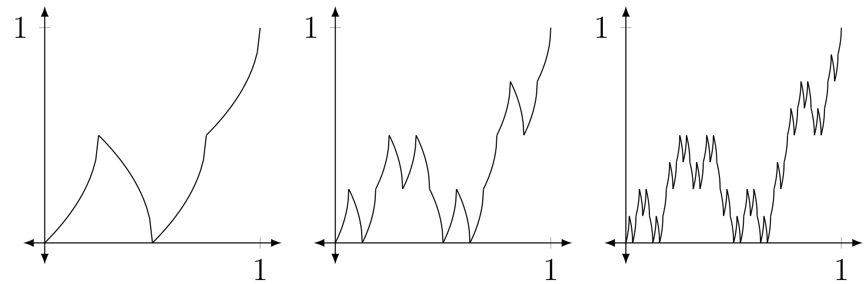

Figure 5.15: Graphs of $\widetilde{\lambda}_1$, $\widetilde{\lambda}_2$, and $\widetilde{\lambda}_3$

The graph of ξ starts at 0 and ends at 1, whereas the graph of λ starts at 1 and ends at 0. It is convenient to look at a slightly different configuration of λ in this section, so that the graph looks more like ξ.

Definition 5.24. For $n \in \mathbb{N}$, let $\widetilde{\lambda}_n(t) = 1 - \lambda_n(t)$. So,

$$\widetilde{\lambda}_n(t) = \begin{cases} \frac{1}{2} - \frac{1}{2}\widetilde{\lambda}_{n-1}(4t) & t \in [0, \frac{1}{4}] \\ \frac{1}{2}\widetilde{\lambda}_{n-1}(4t-1) & t \in [\frac{1}{4}, \frac{1}{2}] \\ \frac{1}{2} - \frac{1}{2}\widetilde{\lambda}_{n-1}(4t-2) & t \in [\frac{1}{2}, \frac{3}{4}] \\ 1 - \frac{1}{2}\widetilde{\lambda}_{n-1}(4t-3) & t \in [\frac{3}{4}, 1] \end{cases} \tag{5.83}$$

Also, $\widetilde{\lambda}(t) = 1 - \lambda(t)$. Alternatively, we could define

$$\tau_0(l) = \begin{cases} 1 & l = 0, 2, 3 \\ -1 & l = 1 \end{cases} \text{ and } \sigma_0(l) = \begin{cases} \frac{1}{2} & l = 0, 2 \\ 1 & l = 1 \\ 0 & l = 3 \end{cases}. \tag{5.84}$$

This would mean that $\widetilde{\lambda}_n(t) = \sigma_0(l) - \frac{\tau_0(l)}{2}\widetilde{\lambda}_{n-1}(4t - l)$. The graphs of $\widetilde{\lambda}_1$, $\widetilde{\lambda}_2$, and $\widetilde{\lambda}_3$ are shown in Figure 5.15.

With this definition, $\widetilde{\lambda}$ and $\widetilde{\lambda}_n$ start at 0 and end at 1. Also, if L_t and K_t are the hulls generated by λ and $\widetilde{\lambda}$, respectively, then $K_t = 1 + \mathscr{R}(L_t)$. (Recall that $\mathscr{R}(A)$ is the reflection of A across the imaginary axis.) This means that whenever we prove something about K_t, we have proven an analogous result for L_t. The next lemma gives us more control over $\widetilde{\lambda}$.

Lemma 5.25. For $k \in \mathbb{N}$, $n \in \{0, 1, ..., k\}$, and $t \in [1 - \frac{1}{4^n}, 1]$, we have

$$\widetilde{\lambda}_k(t) = \frac{1}{2^n}\widetilde{\lambda}_{k-n}(4^n t - (4^n - 1)) + \sum_{i=1}^{n} \frac{1}{2^i}. \tag{5.85}$$

Furthermore,

$$\widetilde{\lambda}(t) = \frac{1}{2^n}\widetilde{\lambda}(4^n t - (4^n - 1)) + \sum_{i=1}^{n} \frac{1}{2^i} \tag{5.86}$$

for $t \in [1 - \frac{1}{4^n}, 1]$.

Proof. The furthermore statement follows by taking the limit as $k \to \infty$. So, we will prove the first result.

Fix $k \in \mathbb{N}$. Let $n = 1$ and $t \in [\frac{3}{4}, 1]$. Then

$$\widetilde{\lambda}_k(t) = \frac{1}{2}\widetilde{\lambda}_{k-1}(4t - 3) + \frac{1}{2}, \tag{5.87}$$

which gives the base case.

Suppose this result holds for $n - 1$. Let $t \in [1 - \frac{1}{4^n}, 1]$. Since $[1 - \frac{1}{4^n}, 1] \subseteq [1 - \frac{1}{4^{n-1}}, 1]$, by the induction hypothesis we have

$$\widetilde{\lambda}_k(t) = \frac{1}{2^{n-1}}\widetilde{\lambda}_{k-(n-1)}(4^{n-1} t - (4^{n-1} - 1)) + \sum_{i=1}^{n-1} \frac{1}{2^i}. \tag{5.88}$$

Since $1 - \frac{1}{4^n} \leq t \leq 1$, we have that $\frac{3}{4} \leq 4t - 3 \leq 1$ and so by construction

$$\begin{aligned}
\widetilde{\lambda}_k(t) &= \frac{1}{2^{n-1}}\widetilde{\lambda}_{k-(n-1)}(4^{n-1} t - (4^{n-1} - 1)) + \sum_{i=1}^{n-1} \frac{1}{2^i} && (5.89)\\
&= \frac{1}{2^{n-1}}\left(\frac{1}{2}\widetilde{\lambda}_{k-(n-1)-1}(4(4^{n-1} t - (4^{n-1} - 1)) - 3) + \frac{1}{2}\right) + \sum_{i=1}^{n-1} \frac{1}{2^i} && (5.90)\\
&= \frac{1}{2^n}\widetilde{\lambda}_{k-n}(4^n t - (4^n - 1)) + \sum_{i=1}^{n} \frac{1}{2^i} && (5.91)\\
& && (5.92)
\end{aligned}$$

□

We know that $\widetilde{\lambda}$ is bounded above by 1 and bounded below by 0. We will use these bounds and the recursion of $\widetilde{\lambda}$ in order to construct a sequence of functions that are piecewise constant. Since we can explicitly compute the Loewner chain corresponding to a constant function, we can explicitly compute the Loewner chain corresponding to a piecewise constant function since it is just a concatenation of constant maps.

Definition 5.26. For $n \in \mathbb{N}$, define $\eta_n, \widetilde{\eta}_n : [0,1] \to \mathbb{R}$ by $\eta_0(t) = 0$, $\widetilde{\eta}_0(t) = 1$,

$$\eta_n(t) = \begin{cases} \frac{1}{2} - \frac{1}{2}\widetilde{\eta}_{n-1}(4t) & t \in [0, \frac{1}{4}] \\ \frac{1}{2}\eta_{n-1}(4t-1) & t \in [\frac{1}{4}, \frac{1}{2}] \\ \frac{1}{2} - \frac{1}{2}\widetilde{\eta}_{n-1}(4t-2) & t \in [\frac{1}{2}, \frac{3}{4}] \\ 1 - \frac{1}{2}\widetilde{\eta}_{n-1}(4t-3) & t \in [\frac{3}{4}, 1] \end{cases} \tag{5.93}$$

and

$$\widetilde{\eta}_n(t) = \begin{cases} \frac{1}{2} - \frac{1}{2}\eta_{n-1}(4t) & t \in [0, \frac{1}{4}] \\ \frac{1}{2}\widetilde{\eta}_{n-1}(4t-1) & t \in [\frac{1}{4}, \frac{1}{2}] \\ \frac{1}{2} - \frac{1}{2}\eta_{n-1}(4t-2) & t \in [\frac{1}{2}, \frac{3}{4}] \\ 1 - \frac{1}{2}\eta_{n-1}(4t-3) & t \in [\frac{3}{4}, 1] \end{cases}. \tag{5.94}$$

Using τ_0 and σ_0, for $t \in [\frac{l}{4}, \frac{l+1}{4}]$ we have

$$\eta_n(t) = \sigma_0(l) - \frac{\tau_0(l)}{2}\widetilde{\eta}_{n-1}(4t-l) \tag{5.95}$$

if $l \neq 1$ and if $l = 1$

$$\eta_n(t) = \sigma_0(l) - \frac{\tau_0(l)}{2}\eta_{n-1}(4t-l). \tag{5.96}$$

We have a similar formulation for $\widetilde{\eta}_n$. The graphs of η_i and $\widetilde{\eta}_i$ are shown in Figure 5.16.

Lemma 5.27. For $n \in \mathbb{N}$, $\eta_n(t) + \frac{1}{2^n} = \widetilde{\eta}_n(t)$.

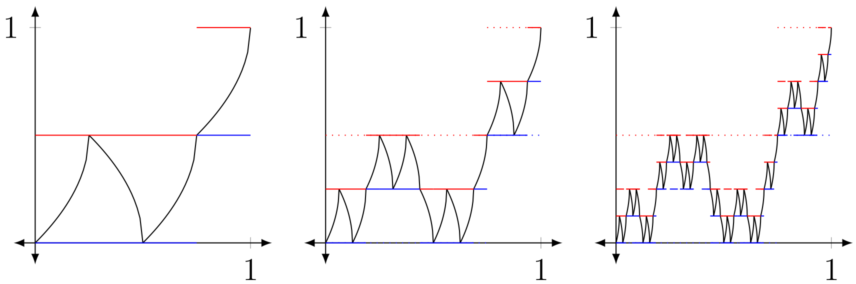

Figure 5.16: Graphs of $\widetilde{\lambda}_i$, η_i, and $\widetilde{\eta}_i$ for $i = 1, 2, 3$

Proof. For $n = 0$, $\eta_0(t) + 1 = 1 = \widetilde{\eta}_n(t)$. Suppose this holds for $n - 1$. Let $t \in [\frac{l}{4}, \frac{l+1}{4}]$. If $l = 0, 2, 3$, then

$$\begin{aligned}
\eta_n(t) &= \sigma_0(l) - \frac{\tau_0(l)}{2}\widetilde{\eta}_{n-1}(4t - l) && (5.97)\\
&= \sigma_0(l) - \frac{1}{2}\widetilde{\eta}_{n-1}(4t - l) && (5.98)\\
&= \sigma_0(l) - \frac{1}{2}\left(\eta_{n-1}(t) + \frac{1}{2^{n-1}}\right) && (5.99)\\
&= \sigma_0(l) - \frac{1}{2}\eta_{n-1}(t) + \frac{1}{2^n} && (5.100)\\
&= \widetilde{\eta}_n(t) - \frac{1}{2^n}. && (5.101)
\end{aligned}$$

If $l = 1$, then

$$\begin{aligned}
\eta_n(t) &= \frac{1}{2}\eta_{n-1}(4t - 1) && (5.102)\\
&= \frac{1}{2}\left(\widetilde{\eta}_{n-1}(4t - 1) - \frac{1}{2^{n-1}}\right) && (5.103)\\
&= \frac{1}{2}\widetilde{\eta}_{n-1}(4t - 1) - \frac{1}{2^n} && (5.104)\\
&= \widetilde{\eta}_n(t) - \frac{1}{2^n}. && (5.105)
\end{aligned}$$

$\square$

The next lemma justifies our use of η and η_n.

Lemma 5.28. For $n \in \mathbb{N}$ and $m \geq n$, $\eta_n(t) \leq \widetilde{\lambda}_m(t) \leq \widetilde{\eta}_n(t)$ for $0 \leq t \leq 1$. Moreover, $\eta_n(t) \leq \widetilde{\lambda}(t) \leq \widetilde{\eta}_n(t)$ for $0 \leq t \leq 1$.

Proof. We will first prove that $\eta_n(t) \leq \widetilde{\lambda}_n(t) \leq \widetilde{\eta}_n(t)$ by induction. For $n = 0$, $\eta_0(t) = 0 \leq \widetilde{\lambda}_0(t) \leq 1 = \widetilde{\eta}_0(t)$ giving us the base case. Suppose this holds for $n-1$. Let $t \in [\frac{l}{4}, \frac{l+1}{4}]$. If $l \neq 1$, then

$$\begin{aligned}
\eta_n(t) &= \sigma_0(l) - \frac{\tau_0(l)}{2}\widetilde{\eta}_{n-1}(4t-l) && (5.106)\\
&= \sigma_0(l) - \frac{1}{2}\widetilde{\eta}_{n-1}(4t-l) && (5.107)\\
&\leq \sigma_0(l) - \frac{1}{2}\widetilde{\lambda}_{n-1}(4t-l) && (5.108)\\
&\leq \sigma_0(l) - \frac{1}{2}\eta_{n-1}(4t-l) && (5.109)\\
&= \sigma_0(l) - \frac{\tau_0(l)}{2}\eta_{n-1}(4t-l) && (5.110)\\
&= \widetilde{\eta}_n(t). && (5.111)
\end{aligned}$$

If $l = 1$, then

$$\eta_n(t) = \frac{1}{2}\eta_{n-1}(4t-1) \leq \frac{1}{2}\widetilde{\lambda}_{n-1}(4t-1) \leq \frac{1}{2}\widetilde{\eta}_{n-1}(4t-1) = \widetilde{\eta}_n(t). \tag{5.112}$$

Since $\widetilde{\lambda}_n(t) = \sigma_0(l) + \frac{\tau_0(l)}{2}\widetilde{\lambda}_{n-1}(4t-l)$, we have the result.

Now, fix $n \in \mathbb{N}$. We will induct on m. The base case of $m = n$ is given above. Suppose the result holds for $m-1$. Then by replacing $\widetilde{\lambda}_{n-1}$ by $\widetilde{\lambda}_m$ in the argument above, we have the result. ∎

The next proposition uses the Loewner chains generated by η_n and $\widetilde{\eta}_n$ in order to gain information about where points move under the Loewner chain generated by $c\widetilde{\lambda}$. The recursion of $\widetilde{\lambda}$ comes in to play significantly here. Since $\widetilde{\lambda}|_{[1-\frac{1}{4^n},1]}$ is just a scaled and shifted version of $\widetilde{\lambda}$, we know that the Loewner chain generated by $c\widetilde{\lambda}$, g_t, obeys the corresponding scaling and shifting. This means that if we watch where a point goes at time $\frac{3}{4}$, then the point's trajectory at any time $1 - \frac{1}{4^n}$ will be the same just scaled and shifted. Figure 5.17 shows possible trajectories of points under g_t. The red line shows that $H_{\frac{3}{4}}(x) > c$, which shows that $g_{\frac{3}{4}}(x)$ is at least c and so the point is not in the hull. The blue line shows that $\widetilde{H}_{\frac{3}{4}}(x)$ stays in the scaled interval, which means that $g_{\frac{3}{4}}(x)$ is bounded by the largest

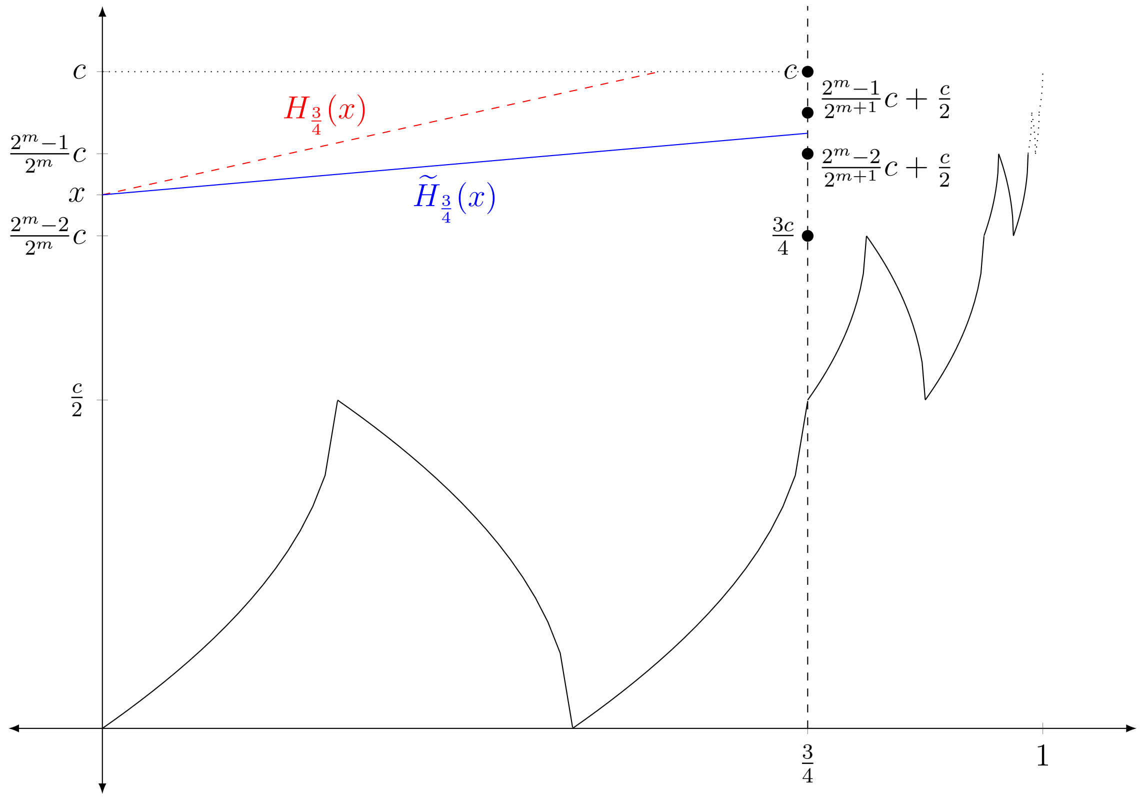

Figure 5.17: Two informative trajectories of a point

endpoint of the interval. By scaling, we know that $g_1(x) \leq c$ and the point is in the hull at least by time 1. Essentially, there are two approximations that give use information:

- if $H_t(x) > c$ for some $t \in [0, 1]$, then $x \notin K_1$
- if $\widetilde{H}_{\frac{3}{4}}(x) \leq \frac{x}{2} + \frac{c}{2}$ for some $t \in [0, 1]$, then $x \in K_1$

The other two approximations (i.e. $H_t(x) \leq c$ and $\widetilde{H}_{\frac{3}{4}}(x) > \frac{x}{2} + \frac{c}{2}$) fail to provide any information about K_1 because the inequalities do not provide bounds on $g_t(x)$ since $H_t(x) \leq g_t(x) \leq \widetilde{H}_t(x)$ for appropriate x-values.

Proposition 5.29. *Let $c > 4$ and K_t be the hull driven by $c\widetilde{\lambda}$ with Loewner chain g_t. Let $k \in \mathbb{N}$. Let H_t and $\widetilde{H}_t$ be the Loewner chains generated by $c\eta_k$ and $c\widetilde{\eta}_k$, respectively.*

(a) *If $x \geq c$, then $x \notin K_1$.*

(b) *If $c \geq 4\sqrt{3}$, then $\frac{c}{2} \in K_1$.*

(c) *If $\frac{2^m-2}{2^m}c \leq x \leq \frac{2^m-1}{2^m}c$ for some $m \geq 2$ and $\widetilde{H}_{\frac{3}{4}}(x) \leq \frac{2^{m+1}-2}{2^{m+1}}c$, then $x \in K_1$.*

(d) *If $H_t(x) > c\widetilde{\lambda}(t)$ for $0 \le t \le 1$, then $x \notin K_1$.*

Proof of (a). Let $x \ge c$. Then as $x > c\widetilde{\lambda}(0)$, $\partial_t g_t(x)|_{t=0} > 0$. So, $g_t(x) > c \ge \widetilde{\lambda}(t)$ for $t \in (0,1]$. This means that $x \notin K_1$. □

Proof of (b). First, note that $\frac{c}{2} \ge c\widetilde{\lambda}(t)$ for $0 \le t \le \frac{3}{4}$. Let $h_t(z)$ be the Loewner chain generated by $\frac{c}{2}$. Since $c\widetilde{\lambda}(t) = 0 < \frac{c}{2} = h_0(\frac{c}{2})$, $\frac{c}{2} < h_t(\frac{c}{2})$ for $t > 0$ (here we are looking at $h_t(\frac{c}{2})$ as the largest prime end of $\frac{c}{2}$ under h_t). Now, by Corollary 2.20, $g_t(\frac{c}{2}) \le h_t(\frac{c}{2})$ for $t \in [0, \frac{3}{4}]$ and $\frac{c}{2} \notin K_{\frac{3}{4}}$. Since h_t is driven by a constant function, we explicitly have

$$h_t(z) = \sqrt{\left(z - \frac{c}{2}\right)^2 + 4t} + \frac{c}{2}. \tag{5.113}$$

Solving $h_{\frac{3}{4}}(\frac{c}{2}) \le \frac{3c}{4}$ for c, we get that $c \ge 4\sqrt{3}$. So, for $c \ge 4\sqrt{3}$

$$g_{\frac{3}{4}}\left(\frac{c}{2}\right) \le h_{\frac{3}{4}}\left(\frac{c}{2}\right) \le \frac{3c}{4}. \tag{5.114}$$

However, by Loewner shifting and scaling, we have that

$$g_{1-\frac{1}{4^n}}\left(\frac{c}{2}\right) \le \sum_{k=1}^{n} \frac{c}{2^n}. \tag{5.115}$$

Taking $n \to \infty$ gives $g_1(\frac{c}{2}) \le c$ and so $\frac{c}{2} \in K_1$. □

Remark 5.30. The previous part of the proposition shows the usefulness of the functions $\widetilde{\eta}_n$ ($\widetilde{\eta}_n(t) = \frac{c}{2}$ for $t \in [0, \frac{3}{4}]$). However, the direct computation used in the previous lemma cannot be used to show that $\frac{c}{2} \notin K_1$ for c less than a particular value. The reason for this is because the Loewner chain generated by $\eta_0(t) \equiv 0$ is $h_t(z) = \sqrt{z^2 + 4t}$ and $c \le h_1(\frac{c}{2})$ only when $c \le \frac{4}{3}$, but we only consider $c > 4$. (This also will not work using $\eta_1(t)$, the second iteration of the lower bound function, either.)

Proof of (c). First, if $k = 1$, $t = 0$, $m = 2$, and $x = \frac{c}{2}$, we have the result from part (b). We will now assume that not all four of these equalities hold at the same time (this is to guarantee $g_t(x) = \frac{c}{2} = c\widetilde{\eta}_k(t)$ cannot happen). By Lemma 5.28, we have that $\widetilde{\eta}_k(t) \ge \widetilde{\lambda}(t)$ for $t \in [0,1]$. Also, $g_t(x) \ge \frac{c}{2} \ge c\widetilde{\eta}_k(t)$ for $t \in [0, \frac{3}{4}]$ (but not all three are equal). So, by

Corollary 2.20, $\widetilde{H}_t(x) \geq g_t(x)$ for $t \in [0, \frac{3}{4}]$ and by assumption

$$\frac{2^{m+1}-2}{2^{m+1}} \geq \widetilde{H}_{\frac{3}{4}}(x) \geq g_{\frac{3}{4}}(x). \tag{5.116}$$

Let $t_n = 1 - \frac{1}{4^n}$. We claim that for each n, $g_{t_n}(x) \leq \frac{2^{m+n}-2}{2^{m+n}}c$, which we will show by induction. The base case ($n = 1$) is given by the previous equation. Suppose for $n-1$ that

$$g_{t_n}(x) \leq \frac{2^{m+n-1}-2}{2^{m+n-1}}c. \tag{5.117}$$

By Lemma 5.25, we have

$$\widetilde{\lambda}(t_n) = \frac{1}{2^{n-1}}\widetilde{\lambda}(4^{n-1}t_n - (4^{n-1}-1)) + \sum_{i=1}^{n-1}\frac{1}{2^i} = \frac{1}{2^{n-1}}\widetilde{\lambda}\left(\frac{3}{4}\right) + \sum_{i=1}^{n-1}\frac{1}{2^i}. \tag{5.118}$$

By Loewner shifting, scaling, and concatenation,

$$\begin{aligned}
g_{t_n}(x) &= g_{t_{n-1},t_n}(g_{t_{n-1}}(x)) && (5.119)\\
&= \frac{1}{2^{n-1}}g_{\frac{3}{4}}\left(2^{n-1}\left(g_{t_{n-1}}(x) - \sum_{i=1}^{n-1}\frac{c}{2^i}\right)\right) + \sum_{i=1}^{n-1}\frac{c}{2^i} && (5.120)\\
&\leq \frac{1}{2^{n-1}}g_{\frac{3}{4}}\left(c2^{n-1}\left(\frac{2^{m+n-1}-2}{2^{m+n-1}} - \frac{2^{n-1}-1}{2^{n-1}}\right)\right) + \sum_{i=1}^{n-1}\frac{c}{2^i} && (5.121)\\
&= \frac{1}{2^{n-1}}g_{\frac{3}{4}}\left(\frac{2^m-2}{2^m}c\right) + \sum_{i=1}^{n-1}\frac{c}{2^i} && (5.122)\\
&\leq \frac{1}{2^{n-1}}g_{\frac{3}{4}}(x) + \sum_{i=1}^{n-1}\frac{c}{2^i} && (5.123)\\
&\leq \frac{1}{2^{n-1}}\left(\frac{2^{m+1}-2}{2^{m+1}}c\right) + \frac{2^{n-1}-1}{2^{n-1}}c && (5.124)\\
&= \frac{2^{m+n}-2}{2^{m+n}}c. && (5.125)
\end{aligned}$$

This proves the claim.

Since

$$\lim_{n\to\infty}\frac{2^{m+n}-2}{2^{m+n}}c = c = c\widetilde{\lambda}(1), \tag{5.126}$$

we have that $g_t(x) = c\widetilde{\lambda}(t)$ for some $t \in (\frac{3}{4}, 1]$, which means $x \in K_1$. $\square$

Proof of (d). This is immediate from Proposition 2.19 since

$$g_t(x) - c\widetilde{\lambda}(t) \geq H_t(x) - c\widetilde{\lambda}(t) > 0. \tag{5.127}$$

$\square$

Proposition 5.31. *For $c \in \mathbb{R}$, let g_t^c be the Loewner chain generated by $c\widetilde{\lambda}$ and K_t^c be its hull. If $4 \leq c_1 < c_2$ and $\frac{1}{2} < x < 1$, then $c_1 x \in K_1^{c_1}$ implies $c_1 x + (c_2 - c_1) \in K_1^{c_2}$. In particular, if $c_1 x \in K_1^{c_1}$, then $c_2 x \in K_1^{c_2}$.*

Proof. Note that $\widetilde{\lambda}(t) \leq 1$ for $t \in [0, 1]$. Since $c_1 < c_2$, $c_2 - c_1 \geq (c_2 - c_1)\widetilde{\lambda}(t)$ which means

$$c_1\widetilde{\lambda}(t) \geq c_2\widetilde{\lambda}(t) - (c_2 - c_1). \tag{5.128}$$

The hull generated by $c_2\widetilde{\lambda}(t) - (c_2 - c_1)$ is $K_t^{c_2} - (c_2 - c_1)$. So, if we show that $c_1 x \in K_t^{c_2} - (c_2 - c_1)$, we will have the desired result that $c_1 x + (c_2 - c_1) \in K_1^{c_2}$. For notational convenience, let $\hat{\lambda} = c_2\widetilde{\lambda}(t) - (c_2 - c_1)$ and $\hat{g}_t(z)$ be its corresponding Loewner chain with hull $\hat{K}_t$.

We now show our main result. We will do this by showing that if $c_1 x \notin \hat{K}_t$ for $t < 1$, then there is a sequence $s_n \uparrow 1$ so that $\hat{g}_{s_n} = c_1\widetilde{\lambda}(s_n)$. By continuity, we will have $c_1 x \in \hat{K}_1$.

If $c_1 x \in K_t^{c_1}$ only for $t = 1$, then by Proposition 2.19, $\hat{g}_t(c_1 x) \leq g_t^{c_1}(c_1 x)$ for $t < 1$. So, taking the limit as t goes to 1 gives that

$$\hat{g}_1(c_1 x) \leq g_1^{c_1}(c_1 x) = c_1\widetilde{\lambda}(1) = \hat{\lambda}(1). \tag{5.129}$$

This shows that $c_1 x \in \hat{K}_1$.

On the other hand, if $c_1 x \in K_t^{c_1}$ for some $t < 1$, then there exists $s_0 \leq t$ so that $\hat{g}_{s_0}(c_1 x) = c_1\widetilde{\lambda}(s_0)$. If $c_1 x \notin \hat{K}_1$, then there exists $s_1 > t$ so that $\hat{g}_{s_1}(c_1 x) = c_1\widetilde{\lambda}(s_1)$. Since $c_1 x > \frac{c_1}{2} \geq c_1\widetilde{\lambda}(t)$ for $t \geq \frac{3}{4}$, $c_1 x \notin K_t^{c_1}$ for $t \geq \frac{3}{4}$. So, there exists $N \in \mathbb{N}$ so that $s_1 < 1 - \frac{1}{4^N}$. If

$$g^{c_1}_{1-\frac{1}{4^N}}(x_0) = \frac{c_1 x}{2^N} + \left(\sum_{k=1}^{N} \frac{c_1}{2}\right), \tag{5.130}$$

then as $c_1 x \in K_{s_1}^{c_1}$, $x_0 > c_1 x$. Then by Proposition 2.19 as $c_1 x \notin \hat{K}_1$,

$$g_{1-\frac{1}{4^N}}^{c_1}(x_0) \geq \hat{g}_{1-\frac{1}{4^N}}(c_1 x). \tag{5.131}$$

Since $c_1 x$ is caught before time 1, by scaling x_0 is also caught before time 1. This means that there exists $s_1 < s_2 < 1$ so that $\hat{g}_{s_2}(c_1 x) = c_1 \widetilde{\lambda}(s_2)$. This in turn means that either $c_1 x \in \hat{K}_t$ for some $t < 1$ or there exists a sequence $s_n \uparrow 1$ so that $\hat{g}_{s_n}(c_1 x) = c_1 \widetilde{\lambda}(s_n)$ for all n which gives that $\hat{g}_1(c_1 x) = c_1 \widetilde{\lambda}(1) = \hat{\lambda}(1)$. Therefore, $c_1 x \in \hat{K}_1$.

In particular, since $x < 1$, $(c_2 - c_1)x < c_2 - c_1$ and $0 < c_2 x < c_1 x + (c_2 - c_1)$. By above, we have that $c_1 x + (c_2 - c_1) \in K_1^{c_2}$. Since $0 = c_2 \widetilde{\lambda}(0)$, $0 \in K_1^{c_2}$ also. As $K_1^{c_2} \cap \mathbb{R}$ is connected,

$$c_2 x \in [0, c_1 x + (c_2 - c_1)] \subseteq K_1^{c_2}. \tag{5.132}$$

□

5.6 Numerical Approximations of Candidate Hulls

In this section, we present the numerical approximations from our upper and lower bounding driving functions. Our goal is to use the upper bound driving function ($\widetilde{\eta}$) to guarantee that points are not caught and the lower bound function (η) to prove that points must be caught by time 1. Proposition 5.31 shows that if we prove that $0 < x_0$ is in the hull generated by $c_1 \widetilde{\lambda}(t)$ then for $c_1 < c_2$ x_0 is in the hull generated by $c_2 \widetilde{\lambda}(t)$. What this means is if we numerically show that x_0 is not caught by $c_2 \widetilde{\lambda}$ by time 1, then x_0 is not caught by $c_1 \widetilde{\lambda}$ by time 1 for $c_1 < c_2$ either. Similarly, if we numerically show that x_0 is caught by $c_1 \widetilde{\lambda}$ by time 1, the x_0 is also caught by $c_2 \widetilde{\lambda}$ by time 1 for $c_2 > c_1$. An example of this is shown in Figure 5.18.

Overall what we hope to gain from these numerical simulations is details about the hull and when points are caught. For example, if a whole interval of real points is caught at the same time, this indicates that the hull formed a bubble along the real line. Ideally, for a spacefilling curve, each real point should be caught at a distinct time. Another way we can use these simulations is by watching where $\frac{c}{2}$ goes starting at time $\frac{1}{4}$. If we show that

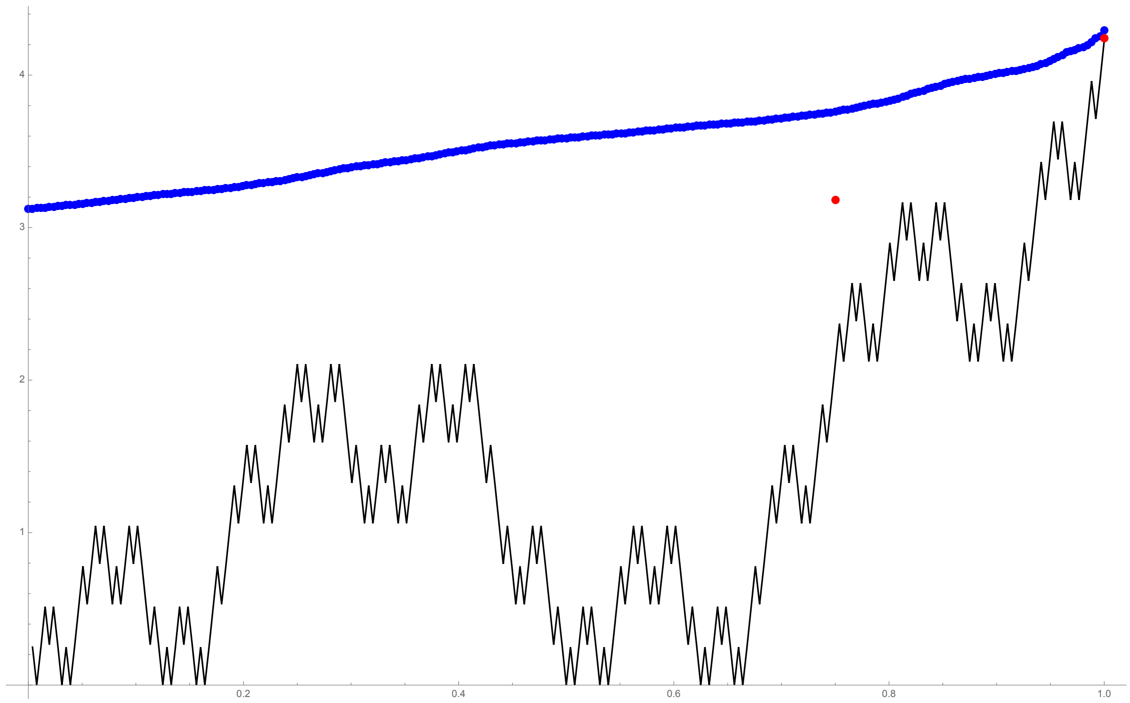

Figure 5.18: Trajectory of $\frac{3c}{4}$ for $c = 3\sqrt{2}$ under H_t for iteration 8 showing $\frac{3c}{4} \notin K_1$

$g_{\frac{1}{4},t}(\frac{c}{2}) > \widetilde{\lambda}(t)$ for $t < t_0$, then no real points are caught in the interval $[\frac{1}{4}, t]$ for $t < t_0$. We already know that $g_{\frac{1}{4},t}(\frac{c}{2}) > \widetilde{\lambda}(t)$ for $t \in (\frac{1}{4}, \frac{3}{4}]$, so these simulations allow use to extend this.

Our simulations were carried out in Mathematica. Table 5.1 gives information about where points move under the Loewner chain corresponding to $\widetilde{\eta}_k$. The first line shows that $\widetilde{H}_{\frac{3}{4}}(\frac{c}{2}) \geq \frac{3c}{4}$ for $c = 4.1$, which means that no information is gained about the behavior of g_t. On the other hand, line 7 shows that $\widetilde{H}_{\frac{3}{4}}(\frac{3c}{4}) < \frac{7c}{8}$ for $c = 4.75$ and $k = 5$. This means that $g_1(\frac{3c}{4}) \leq c$ and $\frac{3c}{4} \in K_1$ for $c \geq 4.75$. Table 5.2 is read similarly. Table 5.3 shows information about what happens under g_t between $\frac{1}{4}$ and $\frac{3}{4}$.

5.7 Future Directions

What we have shown is not the end of this story. There are still questions that we have not answered and options in construction that we have not explored.

First, we know that

$$\lim_{n\to\infty} \eta_n(t) = \lim_{n\to\infty} \widetilde{\eta}_n(t) = \lim_{n\to\infty} \widetilde{\lambda}_n(t) = \widetilde{\lambda}(t). \tag{5.133}$$

Table 5.1: Numerical Simulations for $\widetilde{\eta}_k$

c	z_0	k	$\widetilde{H}_{\frac{3}{4}}(z_0) < \frac{c+z_0}{2}$	$g_1(z_0) < c$	$z_0 \in K_1^c$
4.1	$\frac{c}{2}$	12	no	no	fail
4.1	$\frac{c}{2}$	15	no	no	fail
4.1	$\frac{c}{2} + \frac{c+\sqrt{c^2-16}}{8}$	12	no	no	fail
4.2	$\frac{c}{2}$	8	yes	yes	yes
4.2	$\frac{c}{2} + \frac{c+\sqrt{c^2-16}}{8}$	12	yes	yes	yes
4.5	$\frac{c}{2} + \frac{c+\sqrt{c^2-16}}{8}$	10	yes	yes	yes
4.5	$\frac{3c}{4}$	12	no	no	fail
4.75	$\frac{3c}{4}$	5	yes	yes	yes
6	$\frac{7c}{8}$	12	no	no	fail
6.1	$\frac{7c}{8}$	10	yes	yes	yes
$4\sqrt{3}$	$\frac{c}{2}$	5	yes	yes	yes
8	$\frac{15c}{16}$	12	no	no	fail
9	$\frac{15c}{16}$	10	yes	yes	yes
11	$\frac{31c}{32}$	12	no	no	fail
12	$\frac{31c}{32}$	10	yes	yes	yes
16	$\frac{63c}{64}$	12	no	no	fail
16.5	$\frac{63c}{64}$	10	yes	yes	yes
22	$\frac{127c}{128}$	12	no	no	fail
23	$\frac{127c}{128}$	10	yes	yes	yes
32	$\frac{255c}{256}$	12	no	no	fail
33	$\frac{255c}{256}$	10	yes	yes	yes

Table 5.2: Numerical Simulations for η_k

c	z_0	k	$H_{\frac{3}{4}}(z_0) > \frac{c+z_0}{2}$	$H_1(z_0) > c$	$g_1(z_0) > c$	$z_0 \in K_1$
4.1	$\frac{c}{2}$	12	yes	no	fail	fail
4.1	$\frac{c}{2} + 0.1$	12	yes	no	fail	fail
4.01	$\frac{c}{2}$	12	yes	no	fail	fail
4.001	$\frac{c}{2}$	12	yes	no	fail	fail
4.001	$\frac{c}{2} + 0.1$	14	yes	no	fail	fail
4.25	$\frac{3c}{4}$	12	yes	yes	yes	yes
5.5	$\frac{7c}{8}$	12	yes	yes	yes	yes
7.9	$\frac{15c}{16}$	12	yes	yes	yes	yes
11	$\frac{31c}{32}$	12	yes	yes	yes	yes
15.5	$\frac{63c}{64}$	12	yes	yes	yes	yes
21.5	$\frac{127c}{128}$	12	yes	yes	yes	yes
31	$\frac{255c}{256}$	10	yes	yes	yes	yes
4.001	$\frac{1.1c}{2}$	12	yes	no	fail	fail
4.001	$\frac{1.25c}{2}$	14	yes	no	fail	fail

Table 5.3: Numerical Simulation for $g_{\frac{1}{4},\frac{3}{4}}$

c	z_0	k	$g_{\frac{1}{4},\frac{3}{4}}(z_0)$ Info
4	$\frac{c}{2}$	3	$\leq \frac{3c}{4}$
4.001	$\frac{c}{2}$	5	$> \frac{c}{2} + \frac{1}{8}(c + \sqrt{c^2 - 16})$
4.1	$\frac{c}{2}$	3	$\leq \frac{3c}{4}$
4.2	$\frac{c}{2}$	5	$> \frac{c}{2} + \frac{1}{8}(c + \sqrt{c^2 - 16})$
4.2	$\frac{c}{2}$	3	$\leq \frac{3c}{4}$
$3\sqrt{2}$	$\frac{c}{2}$	5	$> \frac{c}{2} + \frac{1}{8}(c + \sqrt{c^2 - 16})$
$3\sqrt{2}$	$\frac{c}{2}$	5	$\leq \frac{3c}{4}$
$4\sqrt{3}$	$\frac{c}{2}$	3	$\leq \frac{3c}{4}$

This means that the hulls generated by η_n, $\widetilde{\eta}_n$, and $\widetilde{\lambda}_n$ converge to the same limit in the Carathéodory sense. Similarly, we know that if we replace the square roots in $\widetilde{\lambda}_n$ with straight line segments, the limit hull is the same. Do these facts help us leverage insight into the hull?

Second, for any iteration we know that the trace exists, since it is the concatenation of other curves. However, in the limit, we do not have the same justification for proving that the trace exists. This begs us to ask, does the trace even exist? If we could show that the limit of the curves exists, then this limit would indeed be the trace. Unfortunately, we have not shown that the curves we generate converge pointwise. One way to prove that these curves converge would be to show that the curves are equicontinuous, which would mean that the stretching is essentially the same for every curve. Since the height of the hulls decrease as c increases, it might be the case that there is a large enough c so that the stretching does not break continuity. Also, it appears that for large c, that if the limit of the curves exists, then it would be spacefilling. Can we bound the stretching in such a way that we can find large enough c so that the limit curve exists?

Finally, what if we did a different construction altogether? Bridget Jones also investigated constructions that divided the curves generated by $c\sqrt{1-t}$ into nine pieces (this would mean scaling by $\frac{1}{3}$ instead of $\frac{1}{2}$). She aptly names these constructions 9-schemes. The plots of the first iteration of three 9-schemes are shown in Figure 5.19 with corresponding hulls in Figure 5.20. First, does the analysis we did of our driving function carry over to analyzing the driving functions we would build from the 9-schemes? Specifically, can we bound their Lipschitz-1/2 norm similarly? Second, will we see the empty space in the 9-schemes like we did here? Will we see the same stretching? Finally, can we show that the 9-schemes generate a continuous limit curve that is spacefilling?

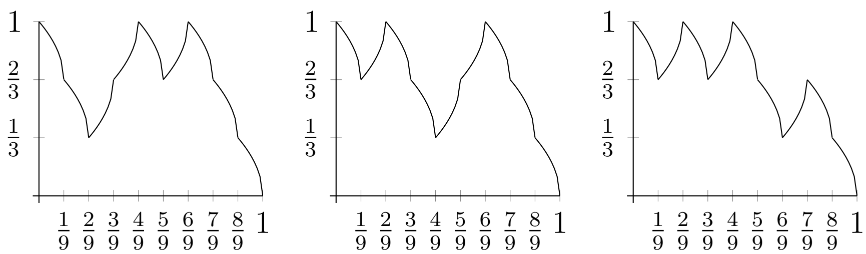

Figure 5.19: Graphs of first iteration of three different 9-schemes

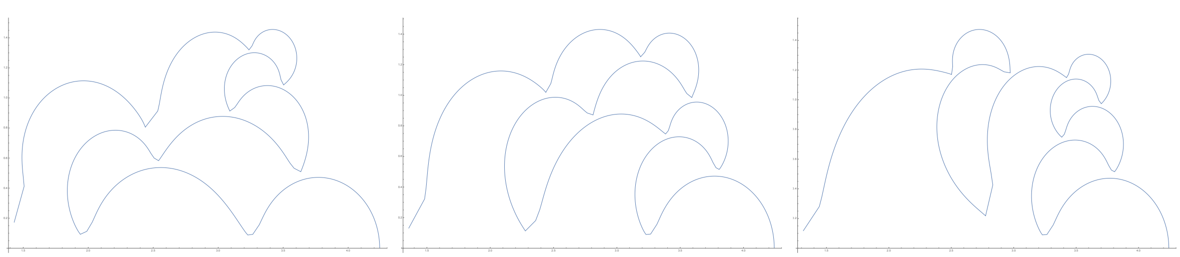

Figure 5.20: Hulls from first iterations of three different 9-schemes

Bibliography

[1] Applebaum, D. (2009). *Lévy Processes and Stochastic Calculus*. Cambridge University Press, New York, second edition. 45

[2] Bauer, M. and Bernard, D. (2006). 2d growth processes: SLE and Loewner chains. *Physics Reports*, 432:115–221. 1

[3] Bauer, M., Bernard, D., and Kytölä, K. (2005). Multiple Schramm–Loewner evolutions and statistical mechanics martingales. *J Stat Phys*, 120(5-6):1125–1163. 1

[4] Bauer, R. (2003). Discrete Loewner evolution. *Ann. Fac. Sci. Toulouse Math.*, 12:433–451. 23

[5] Berestycki, N., Sheffield, S., and Sun, X. (2014). Equivalence of Liouville measure and Gaussian free field. *ArXiv e-prints*. 1

[6] Bertoin, J. (1998). *Lévy processes*. Cambridge University Press. 53, 54

[7] Bingham, N. H., Goldie, C. M., and Teugels, J. L. (1987). *Regular Variation*. Cambridge University Press, New York. 52, 53, 54

[8] Chen, Z.-Q. and Rohde, S. (2009). Schramm–Loewner equations driven by symmetric stable processes. *Communications in Mathematical Physics*, 285:799–824. 2, 13, 41, 48

[9] Credidio, H. F., Moreira, A. A., Herrmann, H. J., and Andrade, J. S. (2016). Stochastic Loewner evolution relates anomalous diffusion and anisotropic percolation. *Phys. Rev. E*, 93:042124. 42

[10] Embrechts, P. and Maejima, M. (2002). *Selfsimilar Processes*. Princeton University Press. 44

[11] Fristedt, B. E. (1967). Sample function behavior of increasing processes with stationary independent increaments. *Pacific Journal of Mathematics*, 21(1):21–33. 53

[12] Gadja, J. and Magdziarz, M. (2010). Fractional Fokker–Planck equation with tempered α-stable waiting times: Langevin picture and computer simulation. *Physical Review E*, 82:011117. 46

[13] Gorenflo, R. and Mainardi, F. (1997). *Fractional Calculus*, pages 223–276. Springer Vienna, Vienna. 46

[14] Guan, Q. and Winkel, M. (2008). SLE and α-SLE driven by Lévy processes. *Ann. Probab*, 36(4):1221–1266. 42

[15] Hahn, M., Kobayashi, K., and Umarov, S. (2012). SDEs driven by a time-changed Lévy process and their associated time-fractional order pseudo-differential equations. *Journal of Theoretical Probability*, 25(1):262–279. 46

[16] Hilbert, D. (1891). Ueber die stetige abbildung einer line auf ein Flächenstück. *D. Math. Ann.*, 38:459–460. 61, 62

[17] Inc, W. R. (2018). Mathematica, Version 11.3. Champaign, IL. 4

[18] Jum, E. and Kobayashi, K. (2016). A strong and weak approximation scheme for stochastic differential equations driven by a time-changed Brownian motion. *Probability and Mathematical Statistics*, 36(2):201–220. 46

[19] Kadanoff, L. P., Kager, W., and Nienhuis, B. (2004). Exact solutions for Loewner evolutions. *Journal of Statistical Physics*, 115(3):805–822. 2, 9, 24, 30, 31, 32, 36, 57

[20] Kennedy, T. (2007). A fast algorithm for simulating the chordal Schramm–Loewner evolution. *Journal of Statistical Physics*, 128(5):1125–1137. 23

[21] Kennedy, T. (2009). Numerical computations for the Schramm-Loewner evolutions. *J. Stat. Phys.*, 137:839–856. 23

[22] Kobayashi, K. (2011). Stochastic calculus for a time-changed semimartingale and the associated stochastic differential equations. *Journal of Theoretical Probability*, 24(3):789–820. 46

[23] Lau, K.-S. and Wu, H.-H. (2016). On tangential slit solution of the Loewner equation. *Ann. Acad. Sci. Fenn.*, 41:681–691. 42

[24] Lawler, G. F. (2005). *Conformally Invariant Processes in the Plane*. American Mathematical Society, Rhode Island. 6, 7, 10, 11, 13, 14, 56

[25] Lawler, G. F., Schramm, O., and Werner, W. (2001). Values of Brownian intersection exponents i: Half-plane exponents. *Acta Math.*, 187(2):237–273. 13, 14

[26] Lind, J. and Robins, J. (2016). Loewner deformations driven by the Weierstrass function. *Involve*, 10(1):151–164. 9, 41, 58

[27] Lind, J. and Rohde, S. (2012). Space-filling curves and phases of the Loewner equation. *Indiana University Mathematics Journal*, 61(6):2231–2249. 3, 9, 40

[28] Lind, J. R. (2005). A sharp condition for the Loewner equation to generate slits. *Annales Academiae Scientiarum Fennicae. Mathematica*, 30(1):143–158. 9, 40

[29] Loewner, K. (1923). Untersuchungen ber schlichte konforme abbildungen des einheitskreises. i. *Mathematische Annalen*, 89(1):103–121. 1

[30] Magdziarz, M. and Schilling, R. L. (2015). Asymptotic properties of brownian motion delayed by inverse subordinators. *Proceedings of the American Mathematical Society*, 143:4485–4501. 46

[31] Marshall, D. E. and Rohde, S. (2005). The Loewner differential equation and slit mappings. *J. Amer. Math. Soc.*, 18:763–778. 23

[32] Meerschaert, M. and Scheffler, H. (2004). Limit theorems for continuous-time random walks with infinite mean waiting times. *Journal of Applied Probability*, 41(3):623–638. 46

[33] Meerschaert, M. M., Nane, E., and Vellaisamy, P. (2009). Fractional cauchy problems on bounded domains. *The Annals of Probability*, 37(3):979–1007. 46

[34] Meerschaert, M. M. and Scheffler, H.-P. (2008). Triangular array limits for continuous time random walks. *Stochastic Processes and their Applications*, 118(9):1606–1633. 46

[35] Meerschaert, M. M. and Sikorskii, A. (2011). *Stochastic Models for Fractional Calculus*. De Gruyter. 46

[36] Miller, J. (2017). Liouville quantum gravity as a metric space and a scaling limit. *ArXiv e-prints*. 1

[37] Munkres, J. (2000). *Topology.* Prentice Hall, 2 edition. 62

[38] Nezhadhaghighi, M. G., Rajabpour, M. A., and Rouhani, S. (2011). First-passage-time processes and subordinated Schramm–Loewner evolution. *Phys. Rev. E*, 84:011134. 42

[39] Peano, G. (1890). Sur une courbe qui remplit toute une aire plane. *G. Math. Ann.*, 36:157–160. 61

[40] Prokhorov, D. and Vasil'ev, A. (2009). Singular and tangent slit solutions to the Loewner equation. *Analysis and Mathematical Physics*, 2009:455–463. 42

[41] Rempe-Gillen, L. (2008). On prime ends and local connectivity. *Bull. Lond. Math. Soc.*, 40:817–826. 16

[42] Rohde, S. and Schramm, O. (2005). Basic properties of SLE. *Annals of Mathematics*, 161(2):883–924. 8, 40

[43] Rosiński, J. (2007). Tempering stable processes. *Stochastic Processes and their Applications*, 117(6):677–707. 44

[44] Roth, O. and Schleissinger, S. (2017). The Schramm-Loewner equation for multiple slits. *J. Anal. Math.*, 131(1):73–99. 2, 11, 16, 20, 22, 24, 25, 26, 27, 28, 30

[45] Rushkin, I., Oikonomou, P., Kadanoff, L. P., and Gruzberg, I. A. (2006). Stochastic Loewner evolution driven by Lévy processes. *J. Stat. Mech. Theory Exp.*, 1(P01001):1–21. 42

[46] Sato, K.-I. (1999). *Lévy Processes and Infinitely Divisible Distributions.* Cambridge University Press, New York. 43, 53

[47] Schleissinger, S. (2014). Embedding problems in Loewner theory. *Ph.D. Thesis, Julius-Maximilians-Universität.* 11

[48] Schramm, O. (2000). Scaling limits of loop-erased random walks and uniform spanning trees. *Isr. J. Math.*, 118(1):221–288. 1

[49] Shiga, T. and Watanabe, S. (1973). Bessel diffusions as a one-parameter family of diffusion processes. *Zeitschrift für Wahrscheinlichkeitstheorie und verwandte Gebiete. (German) [Probability Theory and Related Fields]*, 27(1):37–46. 41, 56

[50] Williams, D. (1974). Path decomposition and continuity of local time for one-dimensional diffusions. *Proceedings of the London Mathematical Society*, 28(3):738–768. 41, 56

Appendix

A Mathematica Code for Simulating Loewner Equation

```
Clear["Global`*"];
T=1; (*Driving function defined on [0,T]*)
n=1000; (*Number of samples*)
c=1;  (*Scaling constant*)
(*Driving function*)
L[t_]:=Sin[10*t];
flip[z_]:=If[Im[z]>=0,z,-z];(*Defines function that makes all imaginary parts
   positive, fixes branch problem*)
f[z0_,z_]:=z0+flip[Sqrt[(z-z0)^2-4*T/n]];(*Conformal map: This is the solution to
    the upward L.E. with constant driving function equal to z0*)

Plot[L[t],{t,0,T}](*Plots driving function from 0 to T*)

dfdata=Table[N[c*L[T*i/n]],{i,0,n,1}];(*Creates table of samples from driving
   functions*)
data=Reverse[dfdata];
zvals={data[[1]]}; (*Base point*)
For[i=1, i<= n, i++,zvals=Prepend[Map[Function[z,f[data[[i]],z]],zvals],data[[i
   +1]]]];(*Runs L.E. on samples*)
If you want to generate watch the hulls grow in the upward LE, comment out
   previous line and run next line
(*For[i=1, i  n,i++,Subscript[q, i]={0}];
For[i=1,  i  n, i++,
Subscript[q, i]=zvals;
zvals=Prepend[Map[Function[z,f[data[[i]],z]],zvals],data[[i+1]]]];*)
ListLinePlot[{Re[#],Im[#]}&/@zvals](*Creates graphs of hull*)

ListPlot[{Re[#],Im[#]}&/@zvals] (*Graphs samples*)
```

```
(*Animate[ListLinePlot[{Re[#],Im[#]}&/@Subscript[q, j],PlotRange
   {{0,5},{0,1.6}}],{j,1,n,1}]*)
```

B Mathematica Code for Simulating Multiple Loewner Equation

```
Clear["Global`*"];
This notebook can simulate hulls from the multiple Loewner equation for constant
   equal weights.
T=10; (*Driving function defined on [0,T]*)
n=1000; (*Number of samples*)
m=2; (*Number of driving functions*)
(*Driving functions: labelled Subscript[L, i][t_] for i=1,...,m*)
Subscript[L, 1][t_]:=-1;
Subscript[L, 2][t_]:=1;
(*Subscript[L, 3][t_]:=Sin[10*t]+2;*)
(*For i=0,...,n, randomly picks driving function for interval [i/n,(i+1)/n]*)
(*For[i=0, in ,i++,Subscript[j, i]=RandomInteger[{1,m}]];*)
(*To run functions in order (as in controlled setting), uncomment the following*)
For[k=1,k<=m,k++,Do[Subscript[j, i]=k,{i,k-1,n,m}]];
flip[z_]:=If[Im[z]>=0,z,-z];(*Defines function that makes all imaginary parts
   positive, fixes branch problem*)
f[z0_,z_]:=z0+flip[Sqrt[(z-z0)^2-4*T/n]];(*"Conformal map"*)
(*Plot[L[t],{t,0,T}];*)(*Plots driving function from 0 to T*)
data=Reverse[Table[N[Subscript[L, Subscript[j, i]][T*i/n]],{i,0,n,1}]];(*Creates
   table of samples from driving functions*)
points=Table[Subscript[j, i],{i,0,n,1}];(*Creates index that indicates what
   driving function each sample was plugged into*)
zvals={Subscript[L, Subscript[j, n]][T]}; (*Base point*)
For[k=1,k<= m+1,k++,Subscript[list, k]={}];(*Creates empty list for points
   plugged into each driving function*)
For[i=1, i<= n, i++, zvals=Prepend[Map[Function[z,f[data[[i]],z]],zvals],data[[i
   +1]]]];(*Runs L.E. on samples*)
(*zvals=Drop[zvals,1];*)
```

```
(*Sorts samples into lists based on which driving function they were plugged into
   *)
For[k=1,k<= m,k++,
For[i=1,i<= n,i++,
If[points[[i]]==k,Subscript[list, k]=Prepend[Subscript[list, k],zvals[[i]]]]]];
For[k=1,k<= m,k++,Subscript[list, k]=Append[Subscript[list, k],Subscript[L, k
   ][0]]];
(*Adds driving function base points to zvals*)
For[k=1,k<=m,k++,zvals=Prepend[zvals,Subscript[L, k][0]]];
For[k=1,k<= m,k++,Subscript[p, k]=ListLinePlot[{Re[#],Im[#]}&/@Subscript[list, k
   ]]] (*Creates graphs based on previous lists*)
Show[Subscript[p, 1],Subscript[p, 2],PlotRange -> {{-2.1,2.1},{0,6}},AxesOrigin->
    {0,0}] (*Graphs hulls, might need to adjust PlotRange*)

ListPlot[{Re[#],Im[#]}&/@zvals] (*Graphs samples*)
```

C Mathematica Code for Simulating Time-Changed Hulls

```
T=1; (*Final Time*)
n=1000; (*Number of Samples*) (*Could possibly add m which gives number of
   samples of subordinator or inverse subordinator*)
alpha=.9;
c=8; (*Scale of driving function*)
Simulating Inverse Subordinator
delta=N[T/n];
subordtime=Table[N[i],{i,0,T,delta}];
Ta={0};
Z={0};
For[j=2,j<= n+1,j++,
V=RandomVariate[UniformDistribution[{-Pi/2,Pi/2}]];
U=RandomVariate[UniformDistribution[]];
W=-Log[U];
S1=Sin[alpha*(V+Pi/2)];
S2=Cos[V-alpha*(V+Pi/2)];
S3=(S2/W)^((1-alpha)/alpha);
S4=(Cos[V])^(1/alpha);
Z=Append[Z,((delta)^(1/alpha))*(S1/S4)*S3];
Ta=Append[Ta,N[Ta[[j-1]]+Z[[j]]]];
];
Tadata=Transpose@{subordtime,Ta};
(*ListPlot[Tadata]*)
time=Table[N[i],{i,0,Max[Ta],Max[Ta]/n}];
S={0};
For[j=2,j<= Length[time],j++,
For[i=1,i<= n,i++,
If[time[[j]]>= Ta[[i]]&&time[[j]]<Ta[[i+1]],S=Append[S,subordtime[[i]]]]]];
```

```
S=Append[S,subordtime[[n+1]]];
Sdata=Transpose@{time,S};
```

Simulating Loewner Equation

```
flip[z_]:=If[Im[z]>=0,z,-z];(*Defines function that makes all imaginary parts
   positive, fixes branch problem*)
f[z0_,z_]:=z0+flip[Sqrt[(z-z0)^2-4*T/n]];(*Conformal map: This is the solution to
    the upward L.E. with constant driving function equal to z0*)
drivingfunction=Table[N[c*Sqrt[T-S[[i]]]],{i,1,n+1,1}];
dfplotdata=Transpose@{time,drivingfunction};
data=Reverse[drivingfunction];
zvals={data[[1]]};
For[i=1, i<= n, i++,zvals=Prepend[Map[Function[z,f[data[[i]],z]],zvals],data[[i
   +1]]]];(*Runs L.E. on samples*)
```

Output Graphs

```
Subscript[p, 1]=ListPlot[Sdata,PlotLabel-> "Time Change"];
Subscript[p, 2]=ListPlot[Tadata,PlotLabel-> "Subordinator"];
Subscript[p, 3]=ListPlot[dfplotdata,PlotLabel-> "TC DF Data"];
Subscript[p, 4]=ListLinePlot[dfplotdata,PlotLabel-> "TC DF"];
Subscript[p, 5]=ListPlot[{Re[#],Im[#]} &/@ zvals,PlotLabel-> "Domain Data"];
Subscript[p, 6]=ListLinePlot[{Re[#],Im[#]} &/@ zvals,PlotLabel-> "Domain Data
   with Lines"];
pic=GraphicsGrid[{{Subscript[p, 1],Subscript[p, 3],Subscript[p, 5]},{Subscript[p,
    2],Subscript[p, 4],Subscript[p, 6]}},ImageSize-> Full,LabelStyle->Blue,
   PlotLabel-> StringForm["Time Changed L.E. with alpha=`1` and c=`2`",alpha,c]];
Export["C:\\Users\\andre\\Google Drive\\research\\simulations\\timechangele1.pdf
   ",pic,"PDF"];
Show[pic]
```

D Mathematica Code for Bounding Candidate Space-filling Hull

```
(*This code was written with help from Charles Kee*)
Clear["Global‘*"];
c=N[3Sqrt[2]]; (*Scaling constant*)
k=5;
point=N[c/2];
(*Pick upper or lower bound. Set to 0 for lower and 1 for upper.*)
bound=0;
(*Generates data for lower and upper bound functions*)
data={0,0,0,0.5};
For[i=2,i<=k,i++,
temp=0.5*data;
data=Table[0,{j,1,4^i}];
data=Join[temp,(-1)*temp+0.5-N[1/2^i],temp,temp+0.5]];
temp=Join[c*data,{c}];
data=temp;
low=data;
high=data+(c/2^(k));
If[bound==0,data=low,data=high];
time=Table[i/256,{i,0,256,1}];
list=Table[0,{i,0,256,1}];
temp=point;
list[[1]]=temp;
time1=1/4^k;
time4=4*time1;
n=Length[data]-1;
j=4^(k-4);
m=2;
For[i=1,i<=n,i++,
```

```
star=temp-data[[i]];
temp=Sqrt[star*star+time4]+data[[i]];
j=j-1;
If[j==0,
list[[m]]=temp;
j=4^(k-4);
m=m+1]];
list[[257]]>c
True
smalldata=Table[data[[i]],{i,0,Length[data],4^(k-4)}];
pdata=Transpose[{time,list}];
qdata=Transpose[{time,smalldata}];
Export["C:\\Users\\andre\\Desktop\\plot0.pdf",ListLinePlot[{pdata,qdata,{{3/4,3c
   /4}},{{1,c}}},PlotStyle-> {Blue,Black,Red,Red},ImageSize-> Full],"PDF"];
Export["C:\\Users\\andre\\Desktop\\lowerlambda1.pdf",a1,"PDF"];
ToExpression["c=4.01; \\text{driven by lower bound}",TeXForm,HoldForm]
c==4.01;driven by lower bound
Export["C:\\Users\\andre\\Desktop\\plot1.pdf",Labeled[ListLinePlot[{pdata,qdata
   ,{{3/4,3c/4}},{{1,c}}},PlotStyle-> {Blue,Black,Red,Red},ImageSize-> Full],
   Style[ToExpression["c=4.01;\\text{driven by lower bound; 12th iteration};g_
   {3/4}(c/2)>\\frac{3c}{4};g_1(c/2)>c",TeXForm,HoldForm],"Graphics"]],"PDF"];
```

Vita

The author received his B.S. in Mathematics in 2011 from Tennessee Technological University and enrolled in the Ph.D. program at the University of Tennessee in the fall of 2011. He received his Master of Science in Mathematics in May 2015. He received his Ph.D. in Mathematics and Master of Science in Statistics in May 2018.